COUNTERMEASURES TO PROTECT BRIDGE PIERS FROM SCOUR

REFERENCE DOCUMENT

Prepared for

National Cooperative Highway Research Program
Transportation Research Board
National Research Council

P.F. Lagasse, P.E. Clopper, L.W. Zevenbergen, and L.G. Girard

Ayres Associates Inc
3665 John F. Kennedy Parkway
Building 2, Suite 200
Fort Collins, Colorado 80525

December 2006

COUNTERMEASURES TO PROTECT BRIDGE PIERS FROM SCOUR

REFERENCE DOCUMENT

Prepared for

National Cooperative Highway Research Program
Transportation Research Board
National Research Council

AYRES ASSOCIATES
P.O. Box 270460
Fort Collins, Colorado 80527
(970) 223-5556, FAX (970) 223-5578

Ayres Project No. 32-0430.00
2407-REF.DOC

December 2006

TABLE OF CONTENTS

PART 1

DETAILED DESCRIPTION OF THE NCHRP 24-07(2) LABORATORY TESTING PROGRAM

PART 2

CODE OF PRACTICE TRANSLATIONS – GERMAN FEDERAL WATERWAYS ENGINEERING AND RESEARCH INSTITUTE (BAW)

(page intentionally left blank)

LIST OF FIGURES

LIST OF TABLES

(page intentionally left blank)

FOREWORD

The Final Report for NCHRP Project 24-07(2) is presented in two volumes. The Final Report and Design Guidelines contain the findings, interpretation, and appraisal of results of testing a range of pier scour countermeasures, conclusions and recommendations, and detailed design guidelines for each countermeasure tested. This Reference Document contains the detailed description of the laboratory testing program and translations of Code of Practice documents published by the German Federal Waterways Engineering and Research Institute (BAW) relevant to the pier scour countermeasure application.

For a discussion of the results of the testing program reference to the Final Report, Chapter 3 is suggested. For more details on specific tests, reference to the Data Report prepared by Colorado State University is suggested. This Reference Document is available as a web document. The Data Report is available from the Research Agency.

(page intentionally left blank)

1. INTRODUCTION

1.1 Background

NCHRP Project 24-07(2) was initiated in April 2001 to refine the results of earlier work, test additional pier scour countermeasures, and develop selection criteria and detailed guidelines and specifications. Laboratory testing for an initial set of countermeasures (riprap, articulating concrete blocks, and indoor tests of partially grouted riprap) was conducted in the hydraulics laboratory at the Colorado State University (CSU) Engineering Research Center. Testing began in August 2003 and was completed in December 2004. Continuation funding for additional countermeasure testing (gabion mattresses, grout-filled mattresses, riprap at skewed piers, mounded riprap, and prototype-scale tests of geotextile bags and partially grouted riprap) was authorized in December 2004 and testing of these countermeasures was completed in December 2005.

1.2 Testing Program Summary

Items identified as gaps in the current state of the practice were reviewed and a specific test, or series of tests, was designed to address each deficiency. Merits and deficiencies of each countermeasure were considered in developing the testing program, including:

- Selection criteria
- Design specifications and guidelines
- Construction specifications and guidelines
- Maintenance and inspection guidelines
- Performance evaluation guidelines

Dominant-process design models that accurately reflect the mode of failure associated with the particular countermeasure were reviewed in order to size the armor elements for the laboratory conditions. Typically, these models included local hydraulic conditions characterized by a combination of velocity and shear stress. It was decided to size all countermeasure armor for a design velocity of two times the critical velocity of the 0.7 to 0.9 mm sand comprising the bed material, resulting in an approach velocity of 0.6 m/s (2 ft/sec) for countermeasure design.

The laboratory tests were not designed to replicate any particular prototype scale conditions. For example, a $2V_{crit}$ run (using a 20-cm (8 in) square pier) was not intended to represent a specific scale ratio of a prototype pier or flow condition. However, in each case, the test countermeasure was "designed" to withstand the $2V_{crit}$ hydraulic condition. For example, the riprap size was selected such that particle dislodgement or entrainment was not anticipated during the $2V_{crit}$ run. This did not mean that the riprap (or any other countermeasure) would not fail due to other factors, such as settling, edge undermining, or winnowing of substrate material. Selected runs utilizing an approach velocity greater than $2V_{crit}$ were intended to take each system to failure.

The performance of each countermeasure was compared with the benchmark performance of riprap. Criteria for rating performance was consistent between countermeasures, but was not necessarily identical for all countermeasures. A countermeasure was considered to have failed if the countermeasure (or its component particles) was dislodged, lifted, or undermined. Relative performance was gauged by whether the countermeasure functioned as intended. Specifically, if settling along the countermeasure edge was expected, actual

settlement was not considered poor performance. Maximum scour anywhere within the limits of the countermeasure or along the edge of the countermeasure was documented.

The testing program also addressed stability and performance issues associated with the extent of the countermeasure placement around the pier, and the termination details at the pier and around the periphery of the installation. Lastly, various filter types and extents were investigated by varying this aspect for selected test runs.

2. TESTING FACILITIES AND PROTOCOLS

Laboratory testing of countermeasures to protect bridge piers from scour was conducted at the Hydraulics Laboratory at Colorado State University (CSU). An 8-foot wide, recirculating flume was utilized for all indoor bridge pier scour countermeasure performance testing. Prototype testing of partially grouted riprap was performed in a 20-foot wide outdoor facility. Critical velocity and shear stress for the articulated concrete blocks used in testing were determined in a 2-foot wide flume prior to testing in the 8-foot flume.

2.1 Indoor Flumes

2.1.1 Eight-Foot Flume

A recirculating flume, 2.4 m (8 ft) wide and 61 m (200 ft) in length with a mobile sand bed was used for all indoor pier scour countermeasure tests. Water was supplied with the use of two 125 horsepower pumps, which could operate separately or in tandem to achieve a given discharge. Maximum capacity of the flume was 1.56 m^3/s (55 cfs). For all countermeasure tests, the slope of the flume was kept constant at 0.3%. A flow straightening assembly was placed at the entrance to the flume to break down large-scale circulation and condition the flow field prior to entering the test section.

Three, 20 cm (8 in) square piers were placed in the flume along the centerline. The piers were identical, constructed of Plexiglas, and painted white for photographic purposes. Piers were secured to the flume floor and extended approximately 38 cm (15 in) above the sand bed. The sand bed itself was approximately 1 m (40 in) deep. A level bed surface was produced by a screed board attached to a cart that was drawn across the surface of the bed. The 8-foot flume before installation of the piers is shown in **Figure 2.1.** A schematic of the flume after pier installation is shown in **Figure 2.2.**

Figure 2.1. Eight foot flume before pier installation.

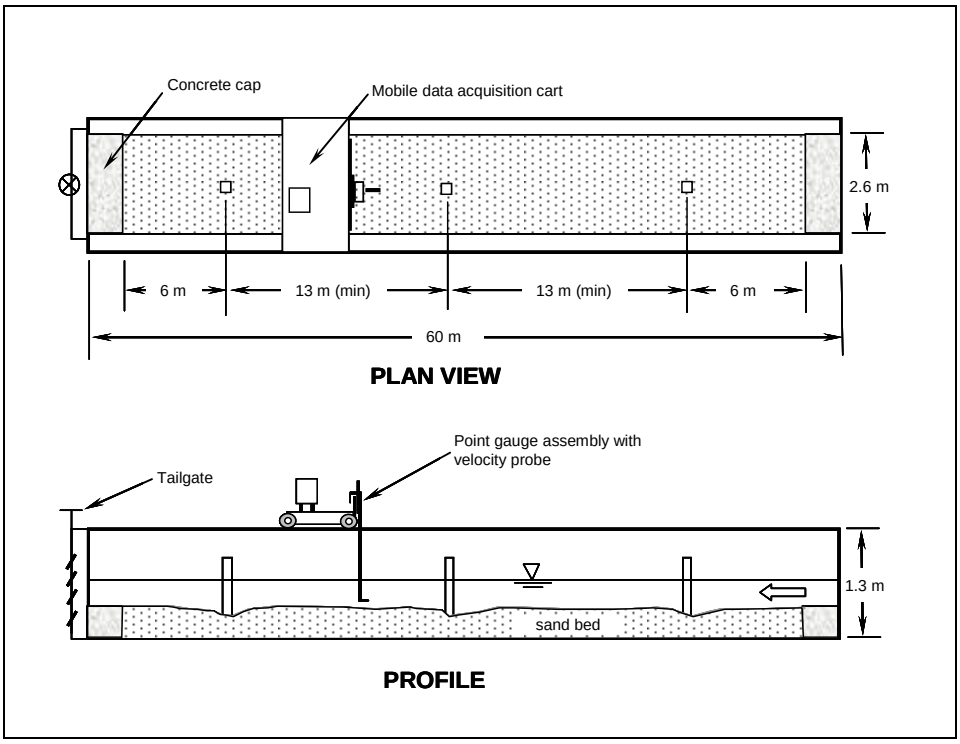

Figure 2.2. Schematic diagram of 8-foot flume.

2.1.2 Test Procedure and Data Acquisition

A matrix of flume tests was developed for the research program and approved by the NCHRP research panel prior to initiating the tests. A typical test consisted of a series of two discharges. Discharge rates were predetermined to correspond to flow velocities of V_{crit} and $2V_{crit}$ where V_{crit} is the calculated critical velocity of the sediment utilized throughout the testing program (0.3 m/s (1 ft/sec)) . The V_{crit} and $2V_{crit}$ runs were performed without sediment recirculation. Separate runs on selected countermeasure configurations were performed at velocities greater than $2V_{crit}$ with sediment recirculation; therefore, both clear-water and live-bed conditions were examined.

Prior to each test, the tailgate was closed and the flume slowly filled with water until the target flow depth of 30.5 cm (1 ft) was established. Flow was introduced very slowly to ensure no local scour occurred during start-up. During the slow filling process, air was allowed to escape from the sand bed. **Figure 2.3** shows Pier C as flow was introduced to the testing flume.

With the flume full of water, discharge was slowly increased to the target discharge, while simultaneously opening the tailgate until steady flow at the target depth of 30.5 cm (1 ft) relative to the initial bed surface was obtained. This process ensured a gradual acceleration of flow until the target velocity was achieved and maintained.

Each run then proceeded for a duration of approximately 2.5 hours while velocity and water surface data was collected at each pier, and at designated locations between piers. For tests utilizing live-bed conditions with sediment feed, the duration was increased to 8 hours per run. After each test, the discharge was gradually decreased and the tailgate adjusted to ensure that no additional scour occurred during the drain-out period. Typically, the flume was allowed to drain out overnight, and the sand bed around each pier was mapped the next day.

Figure 2.3. Flow being introduced to the flume (looking downstream).

Velocity and water surface elevation were monitored periodically at predetermined locations during each test to ensure target hydraulic conditions were maintained. A motorized cart traversed the flume along a track attached to the top of the flume and served as a platform to mount data acquisition equipment. Water surface elevations and velocity profiles were documented at designated locations along the flume. Water surface elevations were measured utilizing a point gage assembly mounted to the mobile data acquisition cart. Accuracy of the point gage was ± 1.5 mm (0.005 ft.) Velocity acquisition equipment was mounted to the cart via the same point gage. Measurements were recorded adjacent to each pier and between each pier to quantify the water surface elevation and the velocity profile.

Velocity data was collected and recorded with a SonTek Acoustic Doppler Velocimeter (ADV). Three main components made up the ADV: the probe head, conditioning module and data recorder. The probe head, a three-pronged apparatus that was submerged to a predetermined depth was attached to the point gauge assembly. Velocities were measured in a three-space coordinate system at a sampling volume located approximately 5 cm (1.2 in) below the probe head. The data-conditioning module served as the link between the probe head and data recorder. Digital processing, necessary to interpret the Doppler signal from the probe head, was performed by the conditioning module. A personal computer was used as a data recorder. A schematic of the point gage assembly is shown in **Figure 2.4.**

Along the centerline of the flume, point velocities were recorded at 60% of the flow depth every 1.8 m (6 ft), and also at locations immediately adjacent to each pier. Also, point velocity at 60% flow depth was recorded one half of the distance from pier face to the flume wall. Lastly, 1.8 m (6 ft) upstream of each pier, point velocity data was recorded at 20, 40, 60, 80, and 90% of flow depth so as to obtain a detailed vertical velocity profile of the approach flow. **Figure 2.5** shows a map of the data acquisition locations to illustrate the type and location of data recorded during each test.

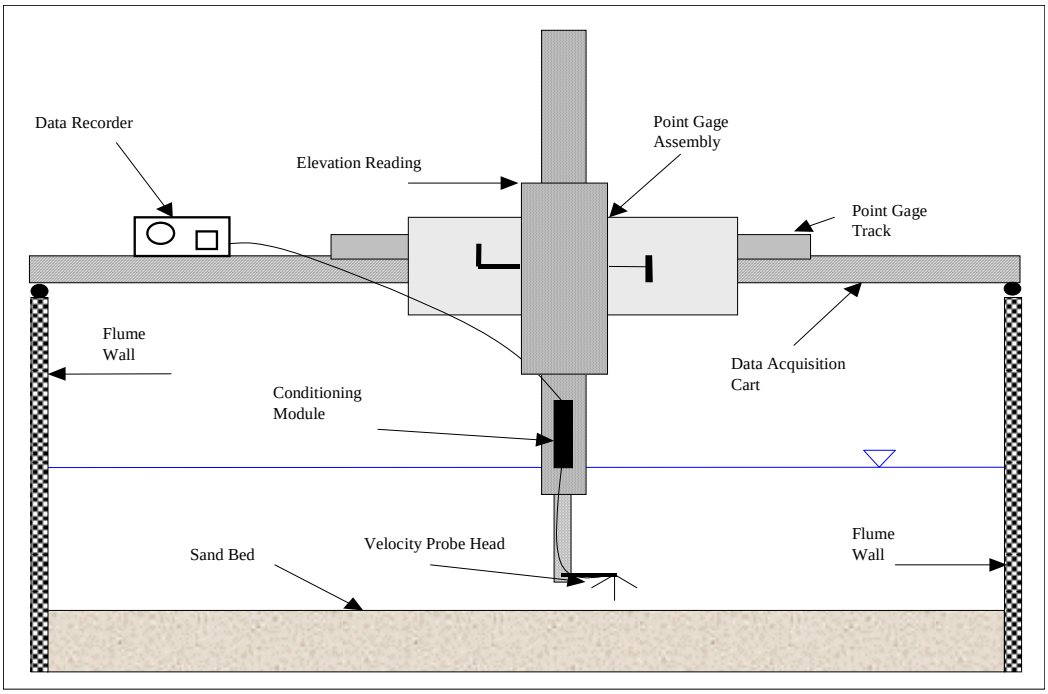

Figure 2.4. Data acquisition setup.

After each run, the water was drained out slowly so as not to induce any additional scour. Bed elevation data was collected every 1.8 m (6 ft) along the centerline of the flume except in areas surrounding the three piers. Typically, in the vicinity of each pier, the elevation of the countermeasure and any peripheral scour was measured on a grid. Assuming symmetry, this grid arrangement was used from the centerline extending to the right side of the flume. If asymmetry was observed, additional points were measured on the left side as well.

All elevations were referenced to a relative benchmark established in the laboratory. The measurements themselves were made with a point gauge mounted on the movable data collection cart. The cart itself was surveyed with an electronic distance measuring (EDM) total station referenced to the lab benchmark. Accuracy of the bed elevation measurements was within ± 1.5 mm (0.005 ft). **Figure 2.6** shows a schematic of a typical scour hole and the data collection points associated with bed elevation measurements.

2.2 Two-Foot Flume

Preliminary tests of the articulating concrete blocks (ACBs) and gabion mattresses were conducted in a 0.61-meter (2-foot) wide, 18.3-meter (60-foot) long, recirculating flume to determine the critical values of velocity and shear stress for subsequent design of tests in the 8-foot flume. Bed slope during the testing program ranged from 1.1 to 8.2 percent for the gabion mattresses, and 0.4 to 1.2 percent for the ACBs. Discharges were regulated by a 75 horsepower variable speed pump with a maximum discharge capacity of approximately 0.3 m^3/s (11 cfs). **Figure 2.7** shows a photograph of the 2-foot flume prior to modification required for the testing program.

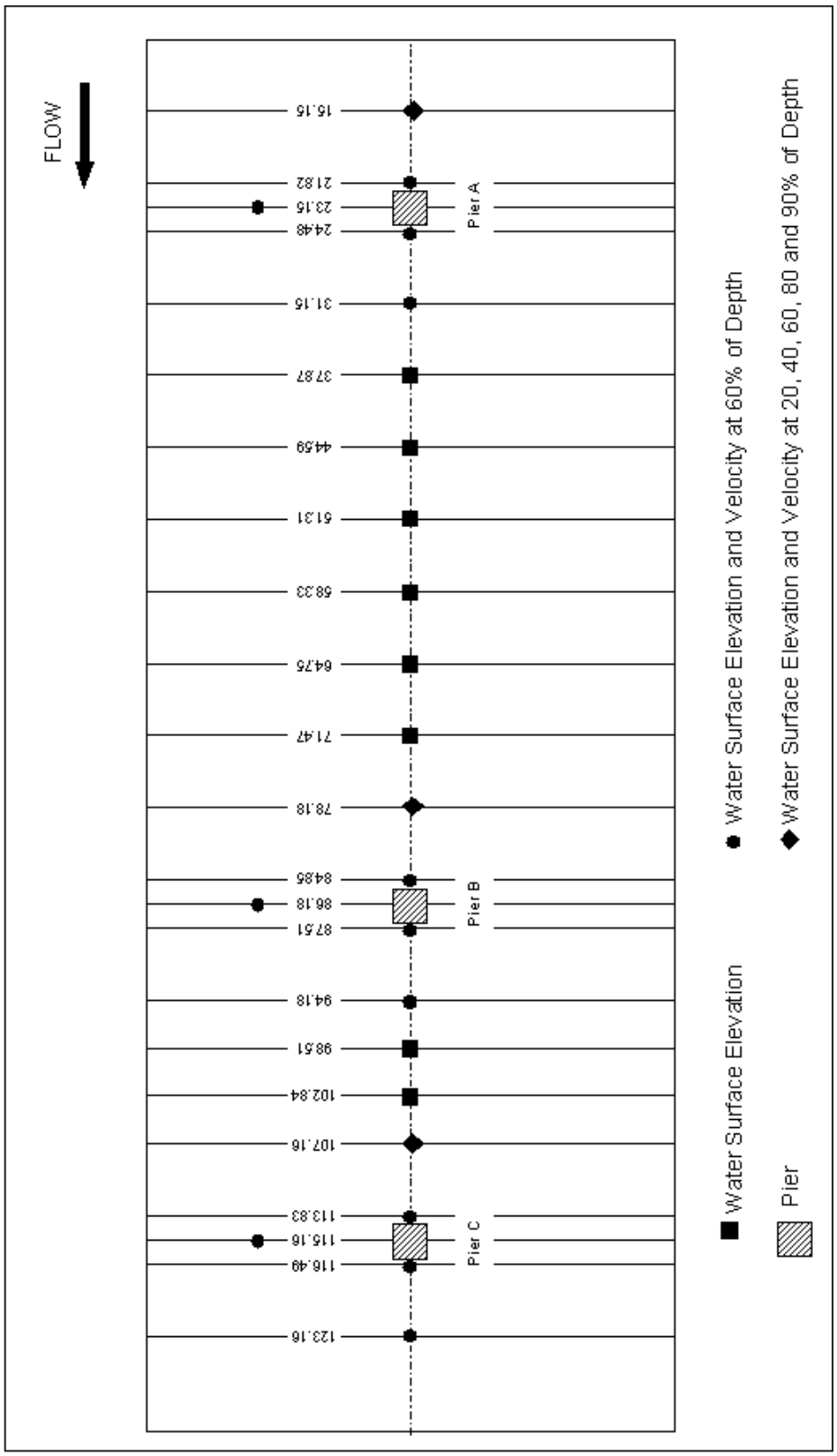

Figure 2.5. Data acquisition locations.

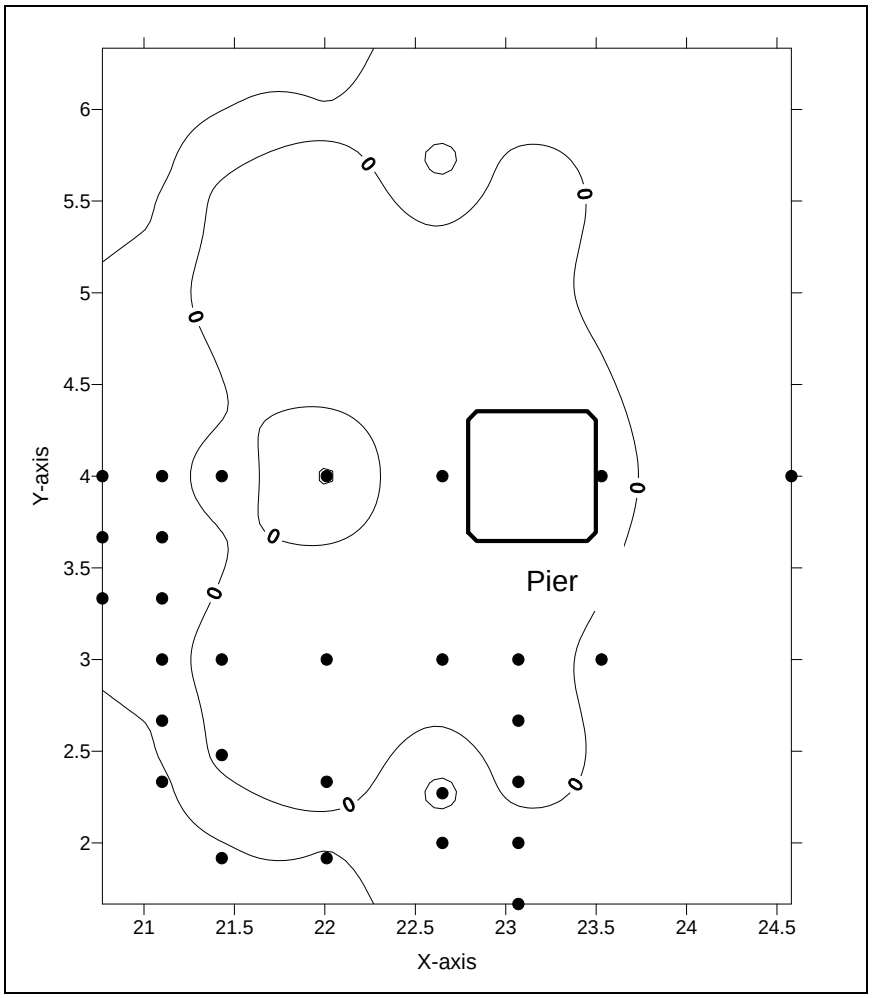

Figure 2.6. Typical scour hole map showing data collection locations.

Figure 2.7. Two foot flume prior to modification.

2.2.1 Flume Modifications

Several alterations to the 2-foot flume were required for ACB testing. First, two ramps spanning the width of the flume were installed to raise the bed elevation to accommodate a sand bed and ACB installation. A 3.7-meter (12-foot) wall was installed 19 cm (0.62 ft) from the left flume wall to create the testing channel. On both the downstream and upstream ramps, a wall with a 1V:4H slope was installed to create a smooth transition from the 61 cm (2 ft) channel to the 19 cm (0.62 ft) testing channel. Sand was placed and compacted to the level of the ramp between the 3.7-meter (12-foot) wall and the left flume wall. A nonwoven geotextile filter was installed on top of the sand and attached to the sidewalls. ACBs were installed on top of the geotextile filter layer. Aluminum flashing was installed along the sidewalls over the edge blocks to prevent water from channeling down between the flume wall and the block system. **Figure 2.8** shows the 2-foot flume after ACB modifications.

Adaptations to the 2-foot flume were required for gabion mattress testing. First, two ramps spanning the width of the flume were installed to raise the bed elevation to accommodate a sand bed and gabion mattresses installation. A 1.8 meter (6 feet) wall was installed 20.3 cm (8 in) from the left flume wall to create the test channel. On both the upstream and downstream ramps, a wall with a 1V:4H slope was installed to create a smooth transition from the 2-foot flume width to the 8-inch wide test section. Sand was placed and compacted to 1.3 cm (0.5 in) below the level of the ramp between the 6-foot wall and the left flume wall. A nonwoven geotextile filter was installed on top of the sand and attached to the sidewalls. Gabions mattresses were installed on top of the geotextile filter layer. Aluminum flashing was installed along the sidewalls over the edge of the gabion mattresses to prevent water from channeling down between the flume wall and the gabion system. **Figure 2.9** is a photograph of the 2-foot flume after the above modifications.

Figure 2.8. Two foot flume after ACB modification.

Figure 2.9. Two foot flume after modification for gabion mattresses testing.

2.2.2 Test Procedure and Data Acquisition

Data collection included pretest bed elevations, water surface elevations, post-test bed surface elevations, and documentation of hydraulic conditions at the point of incipient failure. Bed and water surface elevations were taken from a point gage assembly mounted to a mobile cart mounted on rails at the top of the flume. Accuracy of the point gage was 0.3 mm (0.001 ft). Bed elevation data was taken every 30.5 cm (1 ft) on the sides and center of the testing channel. **Figure 2.10** is a schematic of the point gage assembly utilized to collect data in the 2-foot flume.

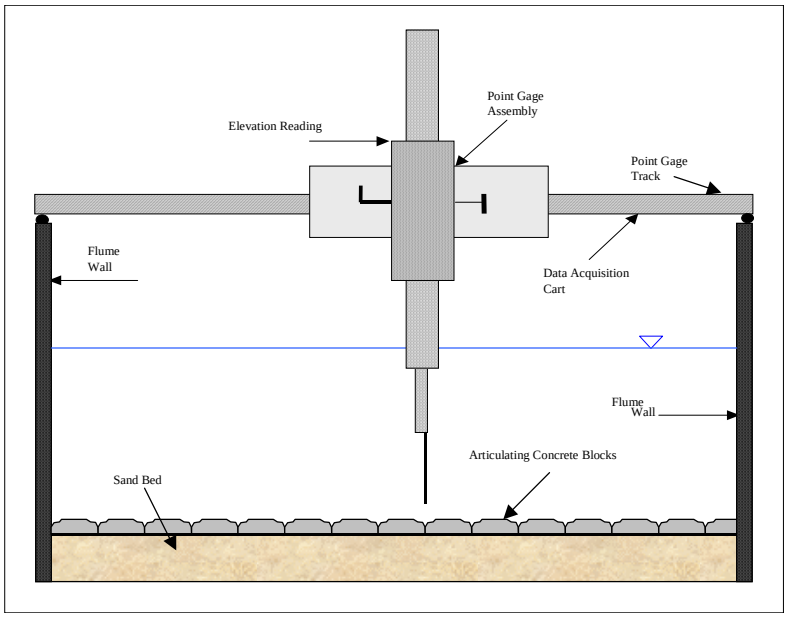

Figure 2.10. Two foot flume data acquisition system.

3. UNPROTECTED PIERS

3.1 Bed Material and Incipient Motion

The sand comprising the bed material in the indoor 8-foot flume was characterized by a d_{50} grain size that ranged from approximately 0.7 to 0.9 mm, depending on variations in the locally available supply. The coefficient of uniformity, C_u, defined as d_{60}/d_{10}, ranged from 4.1 to 5.2. A representative grain size distribution graph is shown in **Figure 3.1**.

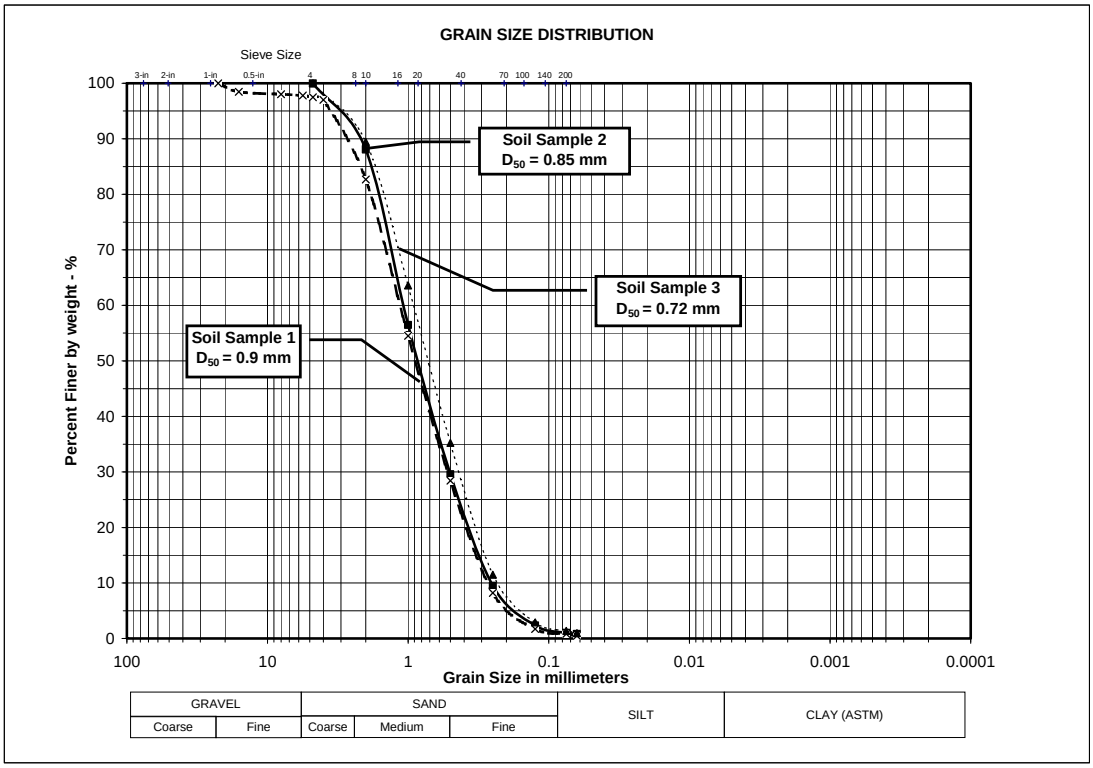

Figure 3.1. Grain size distribution of bed material.

Critical velocity, V_c, for the bed material was estimated using the following method. This estimate includes an assumed Shields parameter of 0.047 for the initiation of movement, and a Manning's n value of 0.018 based on previous work with this material. In addition, the hydraulic conductivity of the bed material was estimated to be approximately 0.04 cm/s based on the grain size distribution.

Bed shear stress can be calculated from the Manning equation as

$$\tau_o = \frac{\gamma}{y^{1/3}}\left(\frac{nV}{K_u}\right)^2 \qquad (3.1)$$

where:

K_u = Units conversion factor equal to 1.0 for SI units, and 1.486 for English units

From testing protocols, flow depth was held constant at 0.3048 m (1 ft). Solving Equation 3.1 for conditions at incipient motion by substituting critical shear stress, τ_c, and critical velocity, V_c, gives:

$$\tau_c = 2.14\ V_c \tag{3.2}$$

For noncohesive bed materials, the critical shear stress can be defined using Shields relationship:

$$\frac{\tau_c}{(\gamma_s - \gamma)d_{50}} = K_s \tag{3.3}$$

where:

τ_c = Critical shear stress at incipient motion (N/m^2, lb/ft^2)
γ = Unit weight of water (9800 N/m^3, lb/ft^3)
γ_s = Unit weight of the sediment (N/m^3, lb/ft^3)
K_s = Shields coefficient

A typical value of Shields coefficient (K_s) for sand with a d_{50} ranging from 0.065 mm to 2.0 mm is K_s = 0.047 (HEC-18, 3rd Edition (Richardson and Davis 2001)). Using K_s = 0.047, the minimum and maximum values of mean bed material, d_{50} = 0.72 mm and d_{50} = 0.90 mm, the resulting range of critical velocity for the bed material was estimated to be 0.33 m/s to 0.37 m/s (1.08 ft/s to 1.21 ft/s).

A conservative value of 0.305 m/s (1.0 ft/s) was adopted for establishing the target approach velocities. The intent was to create a condition for the initial run of each countermeasure type that resulted in true clear-water conditions, with no movement of the bed material except for local scour in the immediate vicinity of the piers. Tests confirm that an approach velocity of 1.0 ft/s resulted in no bed material movement except for local scour; runs performed at 2.0 ft/s or greater resulted in live-bed conditions and the formation of dunes throughout the entire length of the flume.

3.2 Predicted Scour

Local scour at the pier for both live-bed and clear-water conditions was estimated using an equation based on the CSU equation HEC-18 (Richardson and Davis 2001). The equation is:

$$\frac{y_s}{a} = 2.0K_1K_2K_3K_4\left(\frac{y_1}{a}\right)^{0.35} Fr_1^{0.43} \tag{3.4}$$

where:

y_s = Depth of scour (m, ft)
y_1 = Flow depth directly upstream of the pier (m, ft)
K_1 = Correction factor for pier nose shape
K_2 = Correction factor for angle of attack of flow
K_3 = Correction factor for bed condition
K_4 = Correction factor for armoring by bed material size

a = Pier width (m, ft)
Fr_1 = Froude number directly upstream of the pier
V_1 = Mean velocity of flow directly upstream of the pier (m/s, ft/s)
g = Acceleration of gravity (m/s^2, ft/s^2)

For a square nose pier, $K_1 = 1$, for an angle of attack equal to zero $K_2 = 1$, for angle of attack equal to 15° $K_2 = 2.19$, and for an angle of attack equal to 30° $K_2 = 3.0$. For plane bed clear-water scour $K_3 = 1.1$, and for no armoring of the bed material $K_4 = 1.0$. Flow depth directly upstream of the pier was assumed equal to 0.305 m (1 ft), width of the square piers was 20.3 cm (8 in) and width of the rectangular piers was 4.5 cm (1.75 in). The Froude number of the approach flow was determined by:

$$Fr_1 = \frac{V}{\sqrt{gy_1}} \tag{3.5}$$

Froude number was determined using a design velocity of (1.2) ($2V_c$) = 0.7 m/s (2.4 ft/s). In this equation, the coefficient 1.2 is a multiplier applied to the section average velocity, and accounts for the location of the pier on the centerline of the flume. The computed Froude number was 0.423. The computed values of local scour at an unprotected pier under the conditions described above are presented in **Table 3.1.**

Table 3.1. Computed Local Scour.

Pier	Depth of Local Scour
Square piers	38.1 cm (15 in)
Pier A, skew = 15°	29 cm (11.4 in)
Pier B, skew = 0°	13.3 cm (5.2 in)
Pier A, skew = 30°	39.8 cm (15.7 in)

A modified version of Laursen's equation, as presented in HEC-18 (3rd Edition), was used to determine depth of scour in a contracted section under clear-water conditions.

$$y_2 = \left[\frac{K_u Q^2}{d_m^{2/3} W^2} \right]^{3/7} \tag{3.6}$$

$y_s = y_2 - y_o$ = average contraction scour depth, (m, ft)

where:

y_2 = Average equilibrium depth in the contracted section after contraction scour (m, ft)
Q = Flow discharge through the contracted section (m^3/s, ft^3/s)
d_m = Diameter of the smallest non-transportable particle in the bed material in the contracted section computed from d_m (m) = (1.25 * d_{50})
W = Bottom width of the contracted section less pier widths (m, ft)
K_u = Equal to 0.025 SI units (0.0077 English units)
y_o = Existing depth in the contracted section before scour (m, ft)

For the square piers, using Q = 0.45 m^3/s (16 ft^3/s), determined from continuity with a design velocity equal to $2V_c$, W = 2.23 m (7.33 ft), and d_{50} = 0.75 mm (0.0025 ft), the computed average equilibrium depth in the contracted section was 0.41 m (1.34 ft) and the resulting estimate of contraction scour at the pier was 10.4 cm (4.1 in). For the rectangular piers, using Q = 0.45 m^3/s (16 ft^3/s), determined from continuity with a design velocity equal to $2V_c$, W = 2.4 m (7.85 ft), and d_{50} = 0.75 mm (0.0025 ft), the computed average equilibrium depth in the contracted section was 0.41 m (1.34 ft) and the resulting estimate of contraction scour at the piers in Test C10 was 7.8 cm (3.1 in).

3.3 Testing

Tests 1 and 2 provided data for an unprotected square pier, under clear-water and live-bed conditions, respectively. Test 1 was a control test and had no protection around the piers, allowing for determination of scour under both clear-water and live-bed conditions. **Figure 3.2** shows Pier A after completion of Test 1b. Test 2 was a control test and had no protection around the piers, allowing for determination of scour under sediment feed conditions. Test 2 was run for a sufficient duration (8 hours) to permit bed forms to migrate through the system.

During the continuation funding portion of the testing program, three rectangular piers measuring 4.5 cm (1.75 in) by 41 cm (16 in) were installed in the 8-foot flume in place of the 20 cm (8 in) square piers for Tests C10, C12, and C14. Test C10 was a control and had no protection around the piers, allowing for determination of scour under both clear-water and live-bed conditions. Pier A was skewed 15° to the flow, Pier B was parallel to the flow, and Pier C was skewed 30° to the flow, (**Figure 3.3**). **Figures 3.4 and 3.5** present photographs of Piers A and B, respectively, after Test C10a. **Figure 3.6** shows Pier C after Test C10b. Specific conditions associated with each test run are provided in **Table 3.2**.

Figure 3.2. Looking upstream at Pier A after completion of Test 1b.

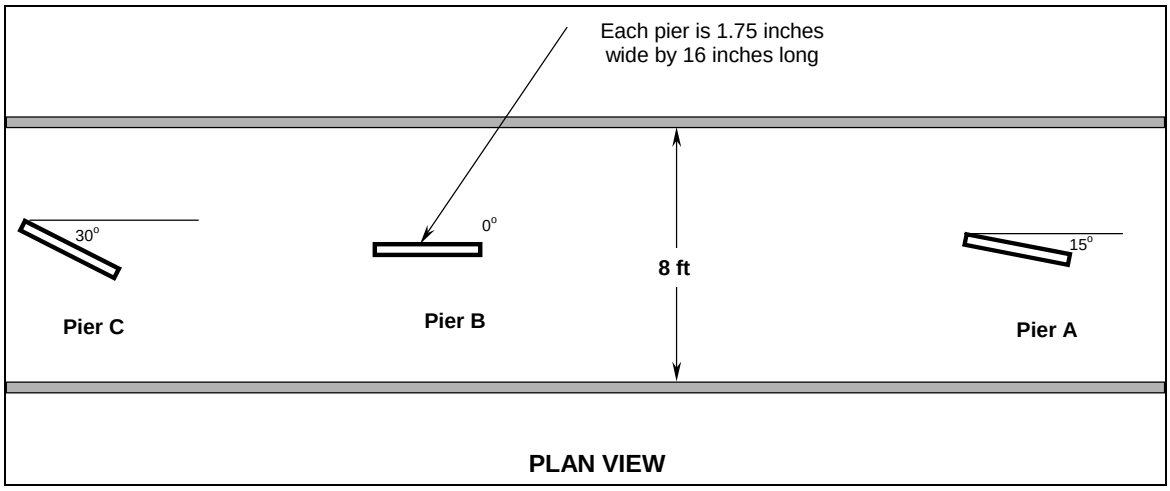

Figure 3.3. Schematic of the skewed piers installed in the 8-foot flume.

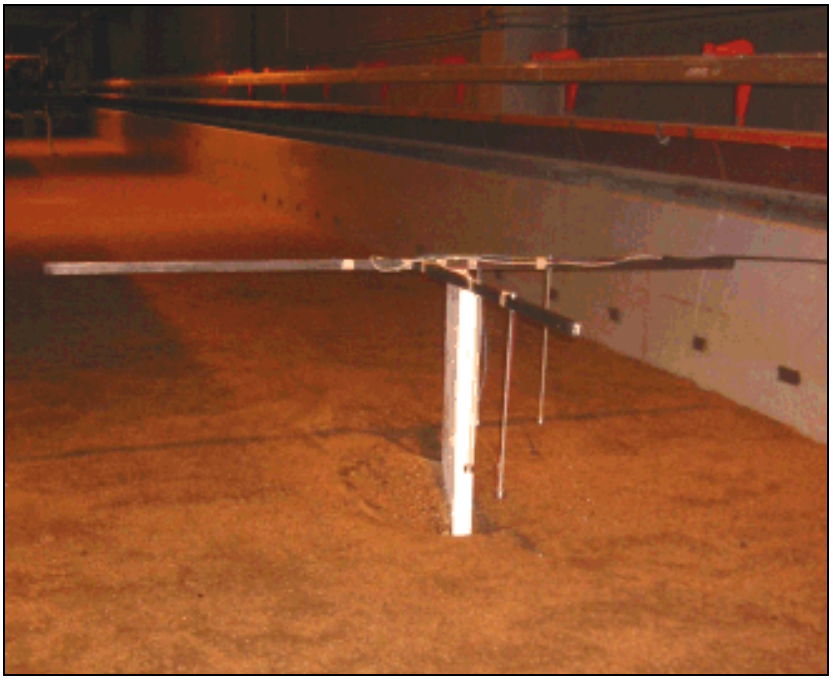

Figure 3.4. Pier A after completion of Test C10a at $1V_{crit}$, looking downstream.

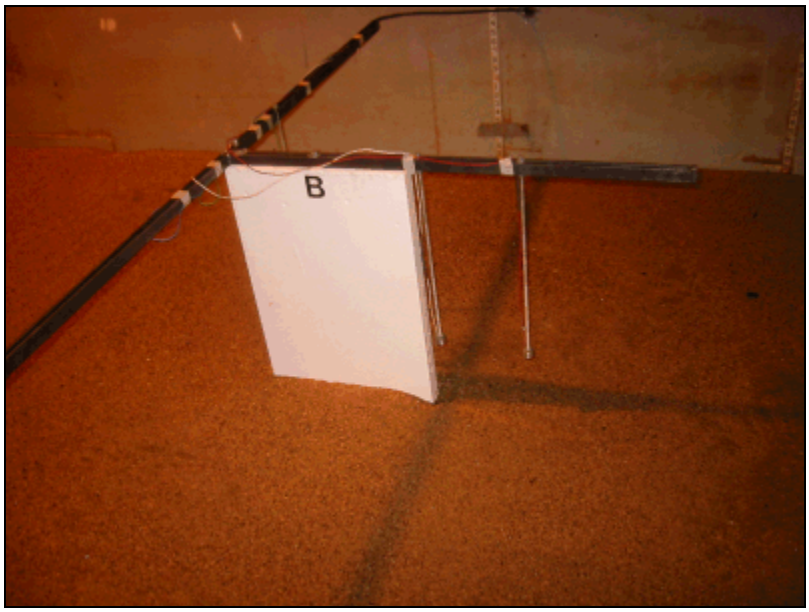

Figure 3.5. Pier B after completion of Test C10a at $1V_{crit}$, flow is from right to left.

Figure 3.6. Pier C after completion of Test C10b at $2V_{crit}$, looking upstream.

Table 3.2. Tests with No Protection at Pier.										
Test Number	Pier A		Pier B		Pier C		Duration (hr)	V/Vc	Sediment Feed	Bedforms
	Description	Filter	Description	Filter	Description	Filter				
1a	Unprotected	None	Unprotected	None	Unprotected	None	2	1	No	Clear-water; plane bed
1b	Unprotected	None	Unprotected	None	Unprotected	None	2	2	No	Mobile; dunes
2a	Unprotected	None	Unprotected	None	Unprotected	None	8	2.5	Yes	Mobile; dunes
C10a	Skewed 15° Unprotected	None	Unprotected	None	Skewed 30° Unprotected	None	2	1	No	Clear-water; plane bed
C10b	Skewed 15° Unprotected	None	Unprotected	None	Skewed 30° Unprotected	None	2	2	No	Mobile; dunes

(page intentionally left blank)

4. RIPRAP

4.1 Materials

4.1.1 Armor Stone

Riprap, which is the most commonly used pier scour countermeasure, often consists of large stones placed around a pier to armor the bed. This armoring prevents the strong vortex flow at the front of the pier from entraining bed sediment and forming a scour hole. The ability of the riprap layer to provide scour protection is, in part, a function of stone size, which is a critical factor in terms of shear failure (Lagasse et al. 2006a).

Riprap used for testing in the indoor flume was sized for stability at an approach velocity of $2V_c$ in accordance with the procedures outlined in HEC-23 (Lagasse et al. 2001). The method is essentially that of Parola and Jones (1989), with the section average approach velocity multiplied by 1.2 to account for flow distribution across the flume. This yielded a design velocity of (1.2) ($2V_c$) or 0.73 m/s (2.4 ft/s) for the riprap sizing calculations.

Riprap d_{50} was determined using the standard Isbash formula for sizing riprap on a channel bed.

$$d_{50} = \frac{0.692(KV)^2}{(S_s - 1)2g} \tag{4.1}$$

where:

d_{50} = Riprap size (m)
V = Design velocity (m/s)
K = Coefficient for pier shape
S_s = Specific gravity of the riprap
g = Acceleration of gravity (9.81 m/s^2)

Using V = (1.2) *($2V_c$) = 0.73 m/s (2.4 ft/s), K = 1.7 for a square nose pier, and S_s = 2.65, the required d_{50} was 33 mm (1.3 in). Two limiting gradation curves were developed given the riprap d_{50} of 33 mm, per guidelines presented in HEC-11 (Brown and Clyde 1989). Riprap gradation limits are presented in **Table 4.1**.

Table 4.1. Riprap Gradation Limits.

Percent of Gradation Smaller Than	Stone Size Range	Diameter (mm)
100	1.5 d_{50} to 1.7 d_{50}	50 to 56
85	1.2 d_{50} to 1.4 d_{50}	40 to 46
50	1.0 d_{50} to 1.15 d_{50}	33 to 38
15	0.4 d_{50} to 0.6 d_{50}	13 to 20

CSU created a unique combination of stone sizes to fit, as closely as practicable, the specified grain size gradation limits established by the guidelines in Table 4.1. The resulting d_{50} was 30 mm (1.2 in). **Figure 4.1** shows the grain size distribution of riprap utilized in the testing program.

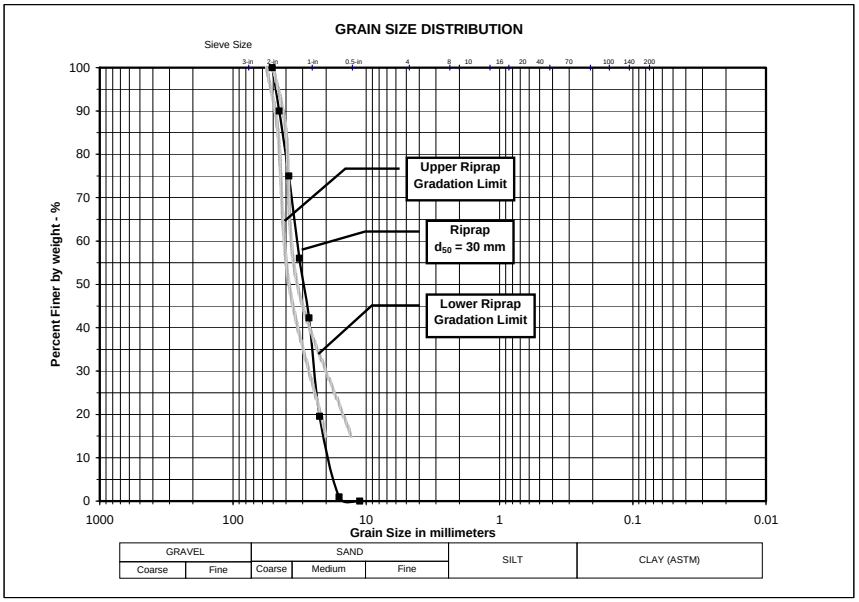

Figure 4.1. Riprap grain size distribution.

The riprap size was selected such that particle dislodgement or entrainment was not anticipated during the $2V_{crit}$ run. This did not mean that the riprap would not fail due to other factors, such as settling, edge undermining, or winnowing of substrate material. Riprap runs utilized approach velocities of $1V_{crit}$, $2V_{crit}$, and $2.5V_{crit}$. Runs utilizing an approach velocity of $2.5V_{crit}$ were intended to take each system to failure by particle dislodgement.

4.1.2 Filters

Geotextile Filter

Geotextile selection for filter fabric was made using the method outlined in Koerner (1998), "Designing with Geosynthetics." The method establishes a maximum allowable aperture size and minimum allowable permeability to achieve compatibility with the bed material.

According to this method, the geotextile for this application should exhibit a permeability that is more than 4 times greater than that of the bed material, i.e., $K_g/K_s > 4.0$. For particle retention, the effective aperture size of a geotextile filter, in this application, must be less than the d_{90} of the bed material (approximately 2.0 mm). This method places more emphasis on permeability and less emphasis on particle retention compared to other procedures, such as HEC-11 or AASHTO M-288. **Table 4.2** summarizes the hydraulic and physical properties of the geotextile filters used in this study.

The areal extent of filter placement around the pier was identified as a parameter to be investigated under this testing program. For geotextile filters, both "full" and "partial" coverage were examined. The term "full coverage" indicated that the geotextile extended beneath the riprap all the way to the periphery of the installation, whereas "partial" indicated that the geotextile extended only two-thirds the distance from the pier face to the periphery of the riprap. The two-thirds filter coverage corresponds to recommendations developed in NCHRP 24-07(1) (Parker et al. 1998) and confirmed in NCHRP 24-07(2) (Lagasse et al. 2006b).

Table 4.2. Hydraulic and Physical Characteristics of Geotextile FIlters.							
Filter Name	Geotextile Type	Mass/Unit Area	AOS	Permeability	Trade Name	Manufacturer	K_g/K_s
W1	Woven	205 g/m^2	0.850 mm	0.20 cm/s	Geotex® 117F	SI Geosolutions (Propex)	5.0
NW1	Nonwoven	163 g/m^2	0.212 mm	0.21 cm/s	Mirafi® 140 N	Mirafi Construction Products	5.25
NW2	Nonwoven	250 g/m^2	~ 0.10 mm	0.4 cm/s	HaTe® B 250 K4	Huesker Synthetic GmbH	10.0
NW3	Nonwoven	278 g/m^2	0.18 mm	0.21 cm/s	Mirafi® 180 N	Mirafi Construction Products	5.25

Granular Filter

Granular filter requirements were developed using the criteria specified in HEC-11. The initial step establishes the compatibility of the filter with the sand bed material in terms of both particle retention and permeability by defining upper and lower limits of d_{15} for the filter. This determines the largest size allowable to maintain particle retention and smallest size allowable to ensure the filter has greater permeability than the sand. The requirements for filter to soil relationship are:

$$\frac{d_{15}\text{filter}}{d_{85}\text{soil}} < 5 \qquad (4.2)$$

and

$$5 < \frac{d_{15}\text{filter}}{d_{15}\text{soil}} < 40 \qquad (4.3)$$

Using d_{15} soil = 0.3 mm, d_{85} soil = 2.0 mm, the resulting filter-to-soil requirements are:

d_{15} filter < 5 x 2.0 mm, as a result d_{15} filter should be < 10 mm
d_{15} filter < 5 x 0.3 mm, as a result d_{15} filter should be > 1.5 mm
d_{15} filter < 40 x 0.3 mm, as a result d_{15} filter should be < 12 mm
Therefore, 10 mm> $d_{15\ \text{filter}}$ >1.5 mm

The d_{85} of the filter must be large enough so that the filter does not pass through the riprap. The requirements for filter to riprap relationship are:

$$\frac{d_{15}\text{riprap}}{d_{85}\text{filter}} < 5 \qquad (4.4)$$

Using d_{15} riprap = 20 mm, the resulting riprap-to-filter requirement is:

d_{85} filter > 20.0 mm/5, therefore d_{85} filter should be > 4.0 mm

The material selected for use was a nominal 10 mm (3/8 in) crushed rock from a local source. A grain size distribution graph for the granular filter layer is presented in **Figure 4.2**; grain size distribution curves for the riprap stone and the bed sand are included for comparison.

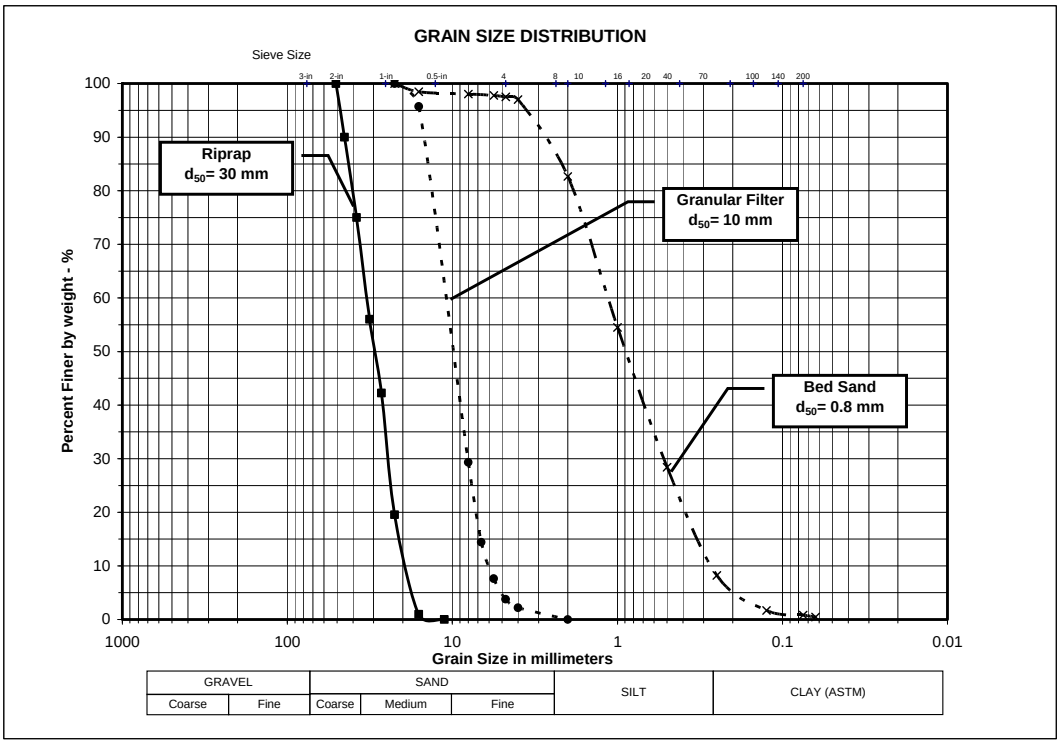

Figure 4.2. Granular filter, riprap stone, and bed sand grain size distributions.

Figure 4.3 shows the woven geotextile "W1" as well as the granular filter (referred to as G1) used in the testing program. Sand bed material and the 30 mm (1.2 in) riprap are also shown in the photograph for comparison.

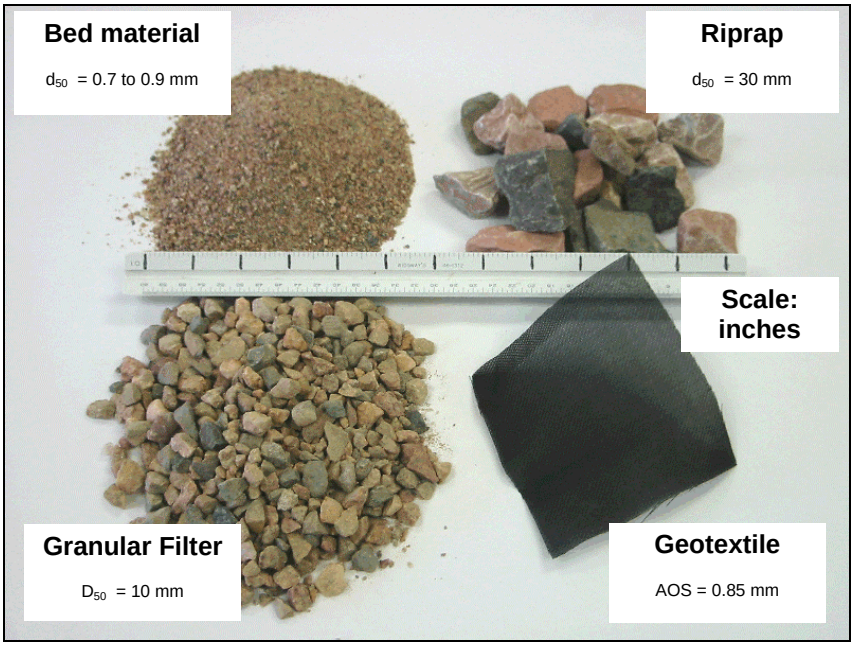

Figure 4.3. Various materials used in the riprap testing program.

4.2 Riprap Tests

4.2.1 Overview

Tests conducted to quantify the design and performance of riprap as a pier scour countermeasure are presented in **Table 4.3** and summarized in the following sections. Tests 3 (clear-water and live-bed) and 4 (live-bed with sediment feed) provided data on riprap performance using current layout guidelines. Tests 5 (clear-water) and 6 (live-bed) were conducted in an effort to compare filter types and areal coverage of the filter layer as presented in NCHRP 24-07(1) (Parker et al. 1998). Test 6 incorporated the best performing combinations from the previous tests with a live-bed condition. Test 7 examined the sensitivity of system performance to areal coverage of the riprap layer. Test 8 was used to examine the effect of various edge treatments on performance. Test 9 was conducted to examine the effect of extended duration with live-bed condition on the baseline riprap layout from Test 6.

One pier in Test 11 (third installation) was dedicated to examining areal coverage of the filter layer as presented in NCHRP 24-07(1). One pier in Test 12 reexamined a previously tested countermeasure design based on HEC-23 guidelines. The sediment feed tests (Tests 4, 6, and 9) were each run for a duration of 8 hours to permit bedforms to migrate through the system.

Three tests were performed to quantify the design and performance of mounded riprap (no prior excavation) as a pier scour countermeasure. One pier in Test 13 was dedicated to a preliminary examination of the effect of mounding of riprap on system performance. Test C16 provided data on system performance as a function of the height of mounding around a pier.

Two tests were performed to quantify the design and performance of riprap as a pier scour countermeasure surrounding a pier skewed to the flow. Test C12 provided data on system performance using the design parameters established for rock riprap protection in HEC-23. Test C14 provided data on system performance for rock riprap protection where the extent was determined based on the unprotected scour zone observed in Test C10.

4.2.2 Test 3

Test 3 involved examination of the relative performance provided by guidance found in HEC-18 (3rd Edition) and HEC-23 compared to when the riprap is placed to the full extent of the unprotected scour hole that develops under conditions corresponding to the design approach velocity (i.e., $2V_c$). Median diameter of the riprap on all three piers in Test 3 was 30 mm (1.2 in).

Pier A was designed per HEC-23 guidelines; riprap extended horizontally 40.6 cm (16 in) from each side of the pier in a 10 cm (4 in) deep square.

Pier B was designed per HEC-18 (3rd Edition) guidelines, resulting in a riprap layer 10 cm (4 in) deep, extending level with the ambient bed surface 46 cm (18 in) on all sides of the pier. The base sidewalls of the riprap on Pier B were at an inverted 1.5H:1V slope. A geotextile filter extended the full distance from the pier face to the perimeter of the riprap.

Table 4.3. Riprap Tests.											
Test Number	Duration (hrs)	Pier A		Pier B		Pier C		Duration (hr)	V/Vc	Sediment Feed	Bedforms
		Description	Filter	Description	Filter	Description	Filter				
3a	2	Riprap	None	Riprap	W1	Riprap	None	2	1	No	Clear-water; plane bed
3b	2	Riprap	None	Riprap	W1	Riprap	None	2	2	No	Mobile; dunes
4a	8	Unprotected	None	Riprap	NW2	Riprap	NW2	8	2.5	Yes	Mobile; dunes
4b	8	Unprotected	None	Riprap	NW2	Riprap	NW2	8	3	Yes	Mobile; dunes
4c	8	Unprotected	None	Riprap	NW2	Riprap	G1	8	2.5	Yes	Mobile; dunes
5a	2	Riprap	W1	Riprap	W1	Riprap	G1	2	1	No	Clear-water; plane bed
5b	2	Riprap	W1	Riprap	W1	Riprap	G1	2	2	No	Mobile; dunes
5c	2	Riprap	W1	Riprap	W1	Riprap	G1	2	2.5	No	Mobile; dunes
5d	2	Riprap	W1	Riprap	W1	Riprap	G1	2	3	No	Mobile; dunes
6a	8	Unprotected	None	Riprap	G1	Riprap	None	8	2.5	Yes	Mobile; dunes
7a	2	Riprap	W1	Riprap	W1	Riprap	W1	2	1	No	Clear-water; plane bed
7b	2	Riprap	W1	Riprap	W1	Riprap	W1	2	2	No	Mobile; dunes
8a	2	Riprap	W1	Riprap	W1	Riprap	W1	2	1	No	Clear-water; plane bed
8b	2	Riprap	W1	Riprap	W1	Riprap	W1	2	2	No	Mobile; dunes
9a	8	Unprotected	None	Riprap	G1	Riprap	None	8	2.5	Yes	Mobile; dunes
11a3	2	Unprotected	None	N/A	N/A	Riprap	NW1	2	1	No	Clear-water; plane bed
11b3	2	Unprotected	None	N/A	N/A	Riprap	NW1	2	2	No	Mobile; dunes
11b3 extended	5	Unprotected	None	N/A	N/A	Riprap	NW1	5	2	No	Mobile; dunes
12a	2	N/A	N/A	N/A	N/A	Riprap	None	2	1	No	Clear-water; plane bed
12 b	2	N/A	N/A	N/A	N/A	Riprap	None	2	2	No	Mobile; dunes
13a	2	Riprap, ACB	NW1	N/A	N/A	Mounded Riprap	None	2	1	No	Clear-water; plane bed
13b	2	Riprap, ACB	NW1	N/A	N/A	Mounded Riprap	None	2	2	No	Mobile; dunes
C12a	2	Skewed 15° Riprap	NW2	Riprap	NW2	Skewed 30° Riprap	NW2	2	1	No	Clear-water; plane bed
C12b	2	Skewed 15° Riprap	NW2	Riprap	NW2	Skewed 30° Riprap	NW2	2	2	No	Mobile; dunes
C14a	2	Skewed 15° Riprap	NW2	Riprap	NW2	Skewed 30° Riprap	NW2	2	1	No	Clear-water; plane bed
C14b	2	Skewed 15° Riprap	NW2	Riprap	NW2	Skewed 30° Riprap	NW2	2	2	No	Mobile; dunes
C16a	2	Mounded Riprap	None	Mounded Riprap	None	Riprap	NW2	2	1	No	Clear-water; plane bed
C16b	2	Mounded Riprap	None	Mounded Riprap	None	Riprap	NW2	2	2	No	Mobile; dunes
C16b-2	2	Mounded Riprap	None	Mounded Riprap	NW2	Mounded Riprap	NW2	2	2	No	Mobile; dunes

Pier C installation consisted of an ellipse-like form specific to the scour hole shape that resulted from Test 1. Riprap installed on the left and right sides was 65 cm (2.125 ft) from the pier face. The extent of the riprap upstream was 40 cm (1.32 ft) from the front of the pier face and the downstream extent of the riprap was 65 cm (2.125 ft) from the pier face. Riprap was installed 10-cm (4 in) deep. **Figure 4.4** shows Pier C after installation, prior to flow initialization. **Figure 4.5** shows Pier C after completion of Test 3b.

Figure 4.4. Pier C after riprap installation.

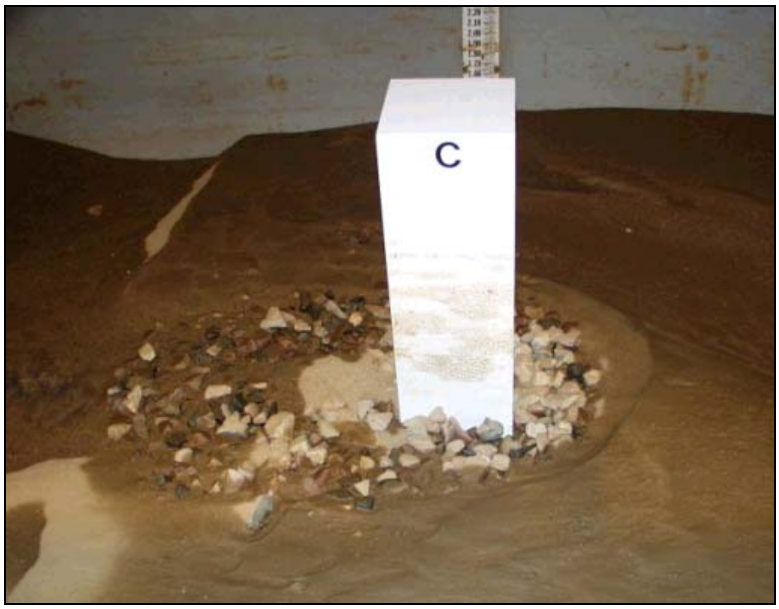

Figure 4.5. Pier C after Test 3b (flow from right to left in photo).

4.2.3 Test 4

In Test 4a and Test 4b, the pier scour countermeasure designs were identical, though velocity was varied between the tests. Velocity for Test 4a was $2.5V_c$; velocity for Test 4b was $3.0V_c$. Mean diameter of the riprap was 30 mm (1.2 in) on both piers for each test. For riprap installation design for Test 4a and Test 4b, Pier B was similar to the design for Test 3, Pier A. On Pier B, the design per HEC-23 was installed with 10.2 cm (4 in) vertical sidewalls and a 40.6 cm (16 in) horizontal extension from the pier face was maintained, a geotextile filter was added that extended two-thirds of the distance from pier face to the edge of the riprap. Pier C for Tests 4a and 4b incorporated a variation on the HEC-23 configuration with 10.2 cm (4 in) vertical sidewalls, a horizontal riprap extension of 30.5 cm (12 in), and included the addition of a geotextile filter that extended two-thirds of the distance from pier face to the edge of the riprap. No countermeasure was installed on Pier A. **Figure 4.6** shows Pier B, after installation in preparation for Test 4a. **Figure 4.7** shows Pier B after completion of Test 4b, Pier C is visible in the background.

Test 4c examined sensitivity of the system performance on depth of the riprap layer. Riprap on Pier B extended horizontally 30.5 cm (12 in) with a depth of 15.2 cm (6 in). A geotextile filter extended two-thirds the distance from the pier face to the perimeter of the riprap. Pier C consisted of the same riprap installation design as Pier B, Tests 4a and 4b, except a granular filter layer was utilized in place of the geotextile filter material. Mean grain size diameter of the granular filter on Pier C was 9.7 mm (0.38 in). Thickness of the granular filter layer was 3.9 cm (1.53 in), or four times the mean diameter of the filter material. Horizontal extension of the granular filter layer was two-thirds the distance from the pier face to the edge of the riprap. No countermeasure was installed on Pier A. **Figure 4.8** shows Pier C after Test 4c.

Figure 4.6. Pier B prior to Test 4a.

Figure 4.7. Pier B after Test 4b (flow is from lower right to upper left).

Figure 4.8. Pier C after Test 4c looking upstream.

4.2.4 Test 5

Test 5 was conducted in an effort to compare filter types and areal coverage of the filter layer as presented in NCHRP 24-07(1). Mean diameter of the riprap on piers was 30 mm (1.2 in). The same riprap installation design used in Test 3, Pier A, was used for Test 5, Pier A. Variation on the HEC-23 configuration with 10.2 cm (4 in) vertical sidewalls and 40.6 cm (16 in) horizontal extension from the pier face included the addition of a geotextile filter that extended from the pier face to the edge of the riprap. For Test 5, Pier B the design per HEC-23 from Pier A with 10.2 cm (4 in) vertical sidewalls and 40.6 cm (16 in) horizontal extension from the pier face was maintained, though the geotextile filter extended only two-thirds of the distance from pier face to the edge of the riprap. Pier C consisted of the same riprap installation design as Piers A and B, except a granular filter layer was utilized in place of the geotextile filter material. Median grain size diameter of the granular filter utilized on Pier C was 9.7 mm (0.38 in). Thickness of the granular filter layer was 3.9 cm (1.53 in), or four times the mean diameter of the filter material. **Figure 4.9** shows Pier A after Test 5a. **Figure 4.10** shows the same pier after completion of Test 5d, where flow velocity was 3.0 V_c.

4.2.5 Test 6

Test 6 was conducted in an effort to compare filter types and areal coverage of the filter layer as presented in NCHRP 24-07(1). Mean diameter of the riprap on both piers was 30 mm (1.2 in). For Test 6, Pier B consisted of the same riprap installation design as Test 4c, Pier C, except the depth of the overlying riprap layer was increased from 10.2 cm (4 in) to 15.2 cm (6 in). Mean grain size diameter of the granular filter utilized on Pier B was 9.7 mm (0.38 in). Thickness of the granular filter layer was 3.9 cm (1.53 in), or four times the mean diameter of the filter material. Horizontal extension of the granular filter layer was two-thirds the distance from the pier face to the edge of the riprap. Pier C varied the HEC-23 design from Test 3, Pier A, by increasing the depth of the riprap to 15.2-cm (6 in). Riprap on Pier C extended 40.6 cm (16 in) on each side of the pier. No countermeasure was installed on Pier A. **Figure 4.11** is a photograph of Pier C during riprap installation.

4.2.6 Test 7

Test 7 examined the sensitivity of system performance to areal coverage of the riprap layer and a geotextile filter layer as presented in HEC-23. Mean diameter of the riprap used in Test 7 was 30 mm (1.2 in) and the depth of riprap was 10.2 cm (4 in) for all riprap layouts. A geotextile filter extended two-thirds the distance from the pier face to the perimeter of the riprap on all piers. On Pier A, the riprap extended one pier width, or 20.3 cm (8 in), on all sides of the pier. On Pier B, the riprap extended 1.5 times the pier diameter, or 30.5 cm (12 in), on all sides of the pier. On Pier C, the riprap extended two times the diameter of the pier, or 40.6 cm (16 in), on all sides of the pier. The photograph in **Figure 4.12** was taken during the installation process as riprap was being placed over the geotextile filter.

4.2.7 Test 8

Test 8 was conducted to examine the effect of various edge treatments on countermeasure performance. Median diameter of the riprap on all three piers was 30 mm (1.2 in). On Pier A, horizontal extent of the riprap was 30.5 cm (12 in). Riprap thickness flanking the pier face was 10.2 cm (4 in) and remained constant for one-third the extent of the installation, where the base of the riprap then descended with a 2H:1V slope while the top remained flush with the bed surface, resulting in a perimeter thickness of 20.3 cm (8 in). At the edge of the riprap, furthest from the pier, the riprap thickness was 20.3 cm (8 in). A geotextile filter extended to two-thirds of the riprap area.

Figure 4.9. Pier A after Test 5a (flow from left to right in photo).

Figure 4.10. Pier A after Test 5d looking downstream.

Figure 4.11. Pier C, riprap placement prior to Test 6.

Figure 4.12. Pier A, riprap installation prior to Test 7.

For Pier B, upstream extent of the riprap was two times the pier width, or 40.6 cm (16 in). A riprap layer 1.02 cm (4 in) extended 20.3 cm (8 in) from the upstream pier face before the base descended with a 2H:1V slope while the top remained flush with the bed surface, resulting in a perimeter depth of 20.3 cm (8 in). Lateral riprap thickness flanking the pier face was 10.2 cm (4 in) and remained constant for 10.2 cm (4 in), where the base of the riprap then descended with a 2H:1V slope while the top remained flush with the bed surface, resulting in a perimeter thickness of 20.3 cm (8 in). The downstream riprap horizontal extent was 20.3 cm (8 in), a 2H:1V slope extended from the pier face to a peripheral thickness of 20.3 cm (8 in). A geotextile filter extended two-thirds the length of the riprap.

On Pier C, extent of the lateral, upstream, and downstream riprap was one pier width, or 20.3 cm (8 in). Surface of the riprap was flush with the bed surface; thickness of the riprap adjacent to the pier was 10.2 cm (4 in). The riprap base extended from the pier face on a 2H:1V slope to an exterior thickness of 20.3 cm (8 in). A geotextile filter extended two-thirds the length of the riprap. **Figure 4.13** is schematic diagram of the countermeasure installation for Pier B, Test 8.

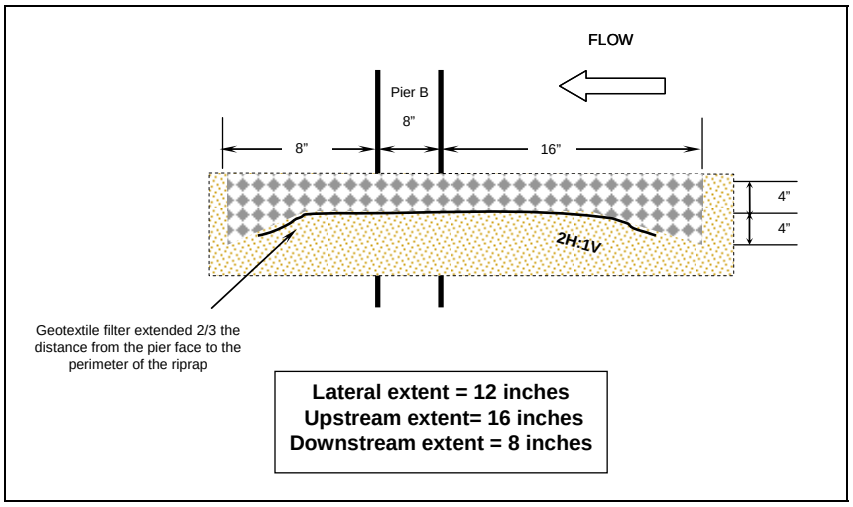

Figure 4.13. Schematic diagram of Test 8, Pier B.

4.2.8 Test 9

Test 9 was performed to quantify the effect of extended duration in a live-bed system on the riprap configurations of Test 6. After completion of Test 6a and collection of applicable data, testing of the existing bed conditions and pier scour countermeasures resumed for another eight hours. **Figure 4.14** shows Pier C after completion of Test 9.

4.2.9 Test 11

Test 11 (third installation) Pier C, re-examined the pier scour countermeasure design of Test 5, Pier B. Vertical sidewalls were 10.2 cm (4 in) and riprap extended horizontally 40.6 cm (16 in) from the pier face, a geotextile filter extended two-thirds of the distance from pier face to the edge of the riprap. Mean diameter of the riprap was 30 mm (1.2 in). Pier scour countermeasure designs for Piers A and B are described in the following section. A photograph of Pier C after the pier was exposed to $2V_c$ conditions for 5 hours during extended Test 11b-3 is presented in **Figure 4.15**.

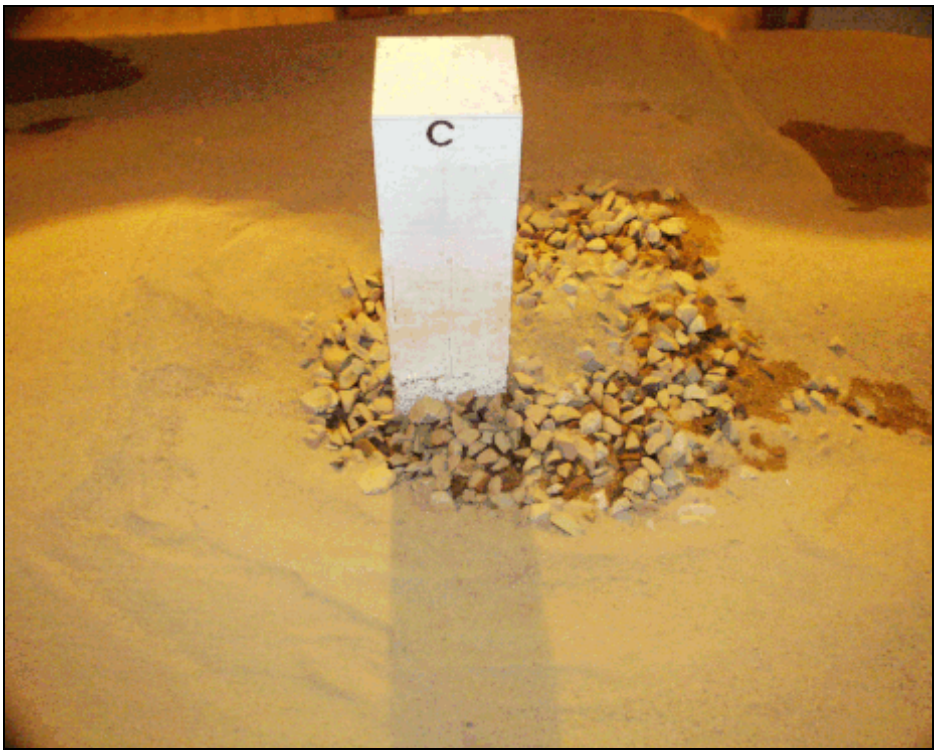

Figure 4.14. Pier C after Test 9 (flow is from left to right).

Figure 4.15. Pier C after extended run of Test 11b-3 looking upstream.

4.2.10 Test 12

Test 12, Pier C, re-examined the pier scour countermeasure design of Test 3, Pier A. Riprap extended horizontally 40.6 cm (16 in) from each side of the pier in a 10-cm (4 in) deep square. Mean diameter of the riprap was 30 mm (1.2 in). A photograph of Pier C after Test 12b is presented in **Figure 4.16**. Pier scour countermeasure designs for Piers A and B are described later, as they used materials other than loose riprap.

Figure 4.16. Pier C after Test 12b (flow from right to left in photo).

4.2.11 Test 13

For Test 13 Pier C, the bed was not excavated surrounding the pier prior to installation of the riprap. Riprap was mounded, without a filter, 10.2 cm (4 in) deep and extended horizontally 40.6 cm (16 in) from all pier faces. Mean diameter of the riprap was 30 mm (1.2 in). Pier scour countermeasure designs for Piers A and B are described in the following section. **Figure 4.17** is a schematic of Pier C, Test 13.

4.3 Mounded Riprap

4.3.1 Test C16

Test C16 documented system performance as a function of the height of mounding riprap at a pier. Riprap extent on Pier A was 41 cm (16 in) on all sides. At the pier, the riprap was stacked to a height of 4 d_{50}, or 12 cm (4.8 in) and sloped to a peripheral height of 1 d_{50}, or 30 mm (1.2 in). No filter was installed. **Figure 4.18** is the construction installation schematic for Pier A. **Figure 4.19** shows Pier A after completion of Test C16a. **Figure 4.20** shows Pier A after completion of Test C16b-2.

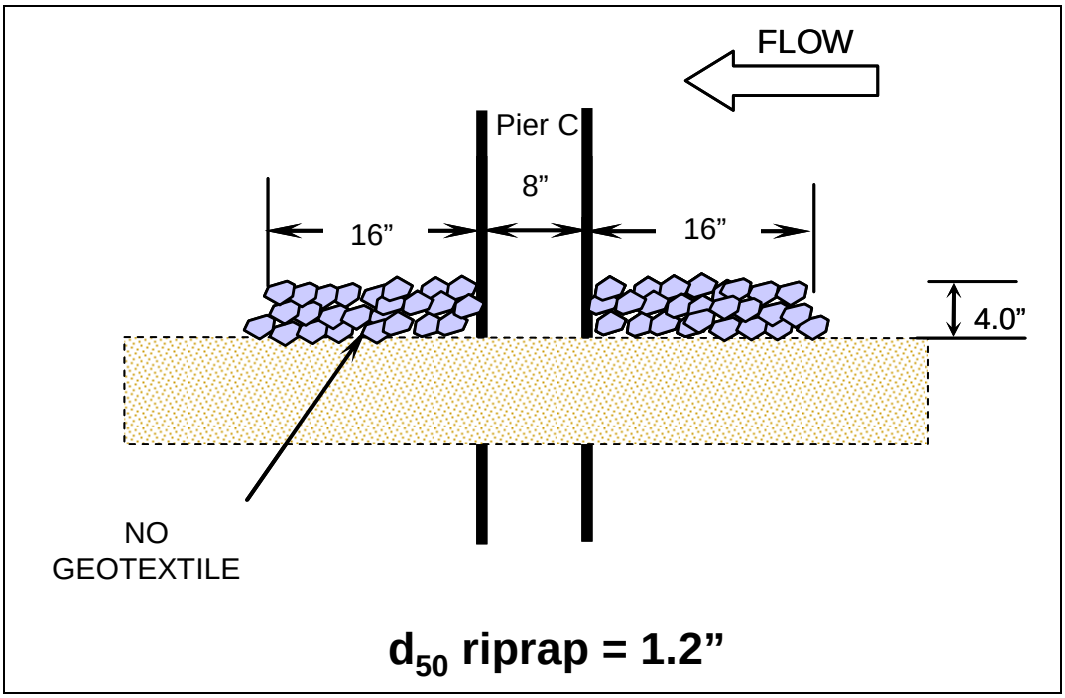

Figure 4.17. Countermeasure design for Pier C, Test 13.

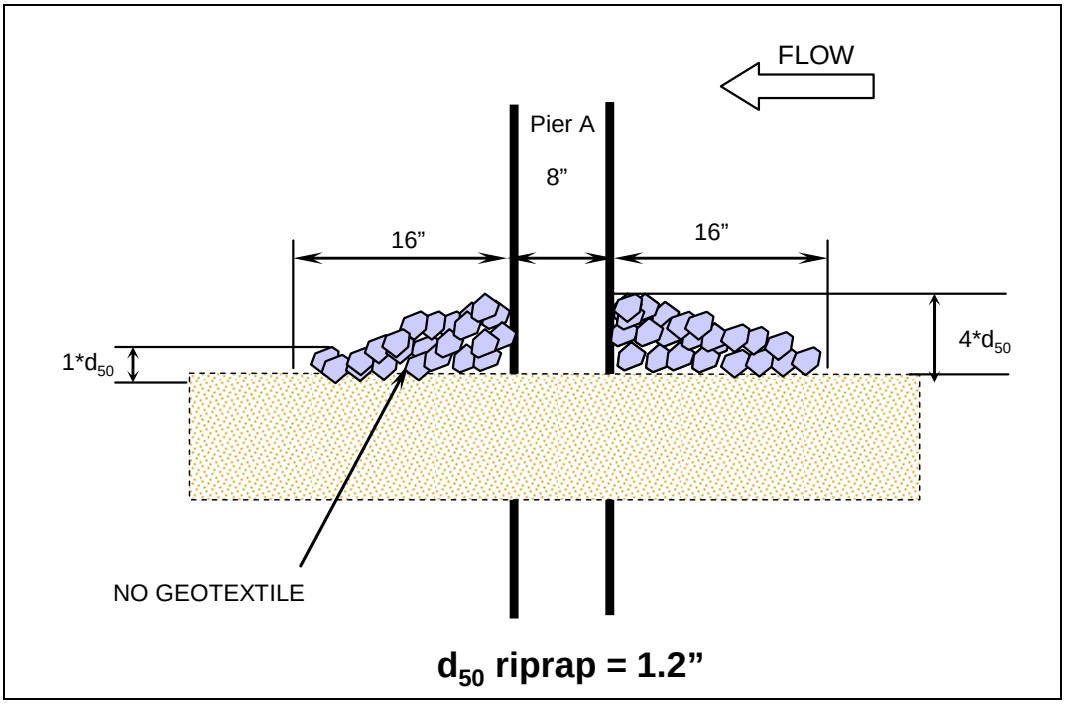

Figure 4.18. Schematic diagram of Test C16, Pier A.

Figure 4.19. Looking upstream at Pier A after Test C16a.

Figure 4.20. Pier A after Test C16b-2 (flow is from right to left).

The riprap layout on Pier B was 41 cm (16 in) on all sides and 2.5 d_{50} or 7.5 cm (3.0 in) deep across the entire installation. No filter was installed. **Figure 4.21** shows Pier B after completion of Test C16b-1.

Pier C was used as a control. The area around the pier was excavated 10 cm (4 in) deep and 30.5 cm (12 in) laterally in all directions. A geotextile filter extending two-thirds the distance from the pier face to the perimeter was installed. **Figure 4.22** shows Pier C after Test C16b-1.

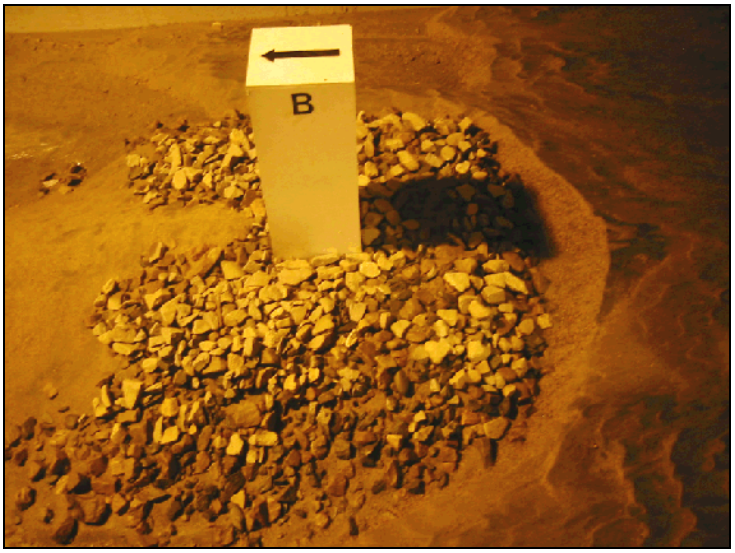

Figure 4.21. Pier B after Test C16b-1 (flow is from right to left).

Figure 4.22. Pier C after Test C16b-1 (flow is from right to left).

4.4 Skewed Piers

Tests C12 and C14 provided data for rock riprap protected rectangular, skewed piers under clear-water conditions, see Figure 3.3 for pier layout. Tests C12 and C14 involved examination of the relative performance provided by guidance found in HEC-23 compared to when the riprap is placed to the full extent of the unprotected scour hole that develops under conditions corresponding to the design approach velocity (i.e., $2V_c$). Mean diameter of the riprap on piers for both tests was 30 mm (1.2 in).

4.4.1 Test C12

Test C12 protection was designed per HEC-23 guidelines; riprap extended horizontally 10.2 cm (4 in) from each side of the pier, or two times the width of the pier. Mean diameter of the riprap used in Test C12 was 30 mm (1.2 in) and the depth of riprap was 10.2 cm (4 in) for all riprap layouts. A geotextile filter extended two-thirds the distance from the pier face to the perimeter of the riprap on all piers. A photograph of Pier B after the pier was exposed to $2V_{crit}$ conditions for 2 hours during Test C12b is presented in **Figure 4.23**. **Figure 4.24** shows Pier C after being exposed to $2V_{crit}$ conditions for 2 hours during Test C12b.

4.4.2 Test C14

Test C14 involved examination the performance of riprap placed to the full extent of the unprotected scour hole that develops under conditions corresponding to the design approach velocity. The layout for Test C14 was determined from the mapped extent of the scoured zone resulting from Test C10. Median diameter of the riprap on all three piers in Test C14 was 30 mm (1.2 in). A geotextile filter extended two-thirds the distance from the pier face to the perimeter of the riprap on all piers. **Figure 4.25** shows Pier A after Test C14a. **Figure 4.26** shows the same pier after completion of Test C14b, where flow velocity was 2.0 V_{crit}.

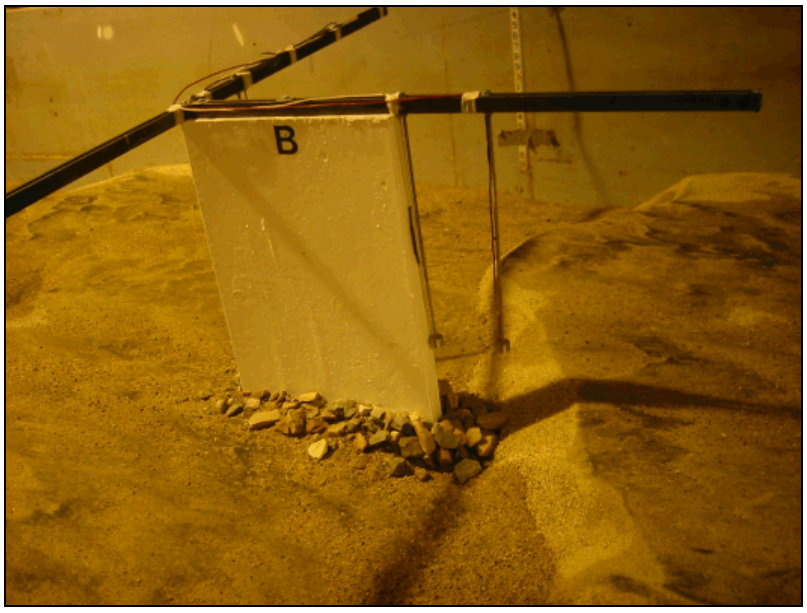

Figure 4.23. Pier B (0° skew) after Test C12b (flow is from right to left).

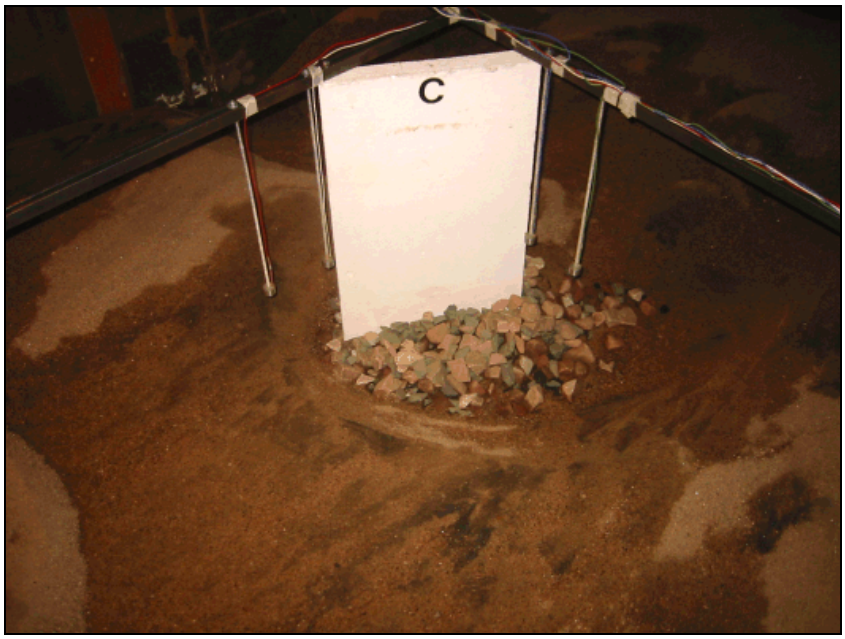

Figure 4.24. Pier C (30° skew) after Test C12b (flow is from left to right).

Figure 4.25. Pier A (15° skew) after Test C14a looking upstream.

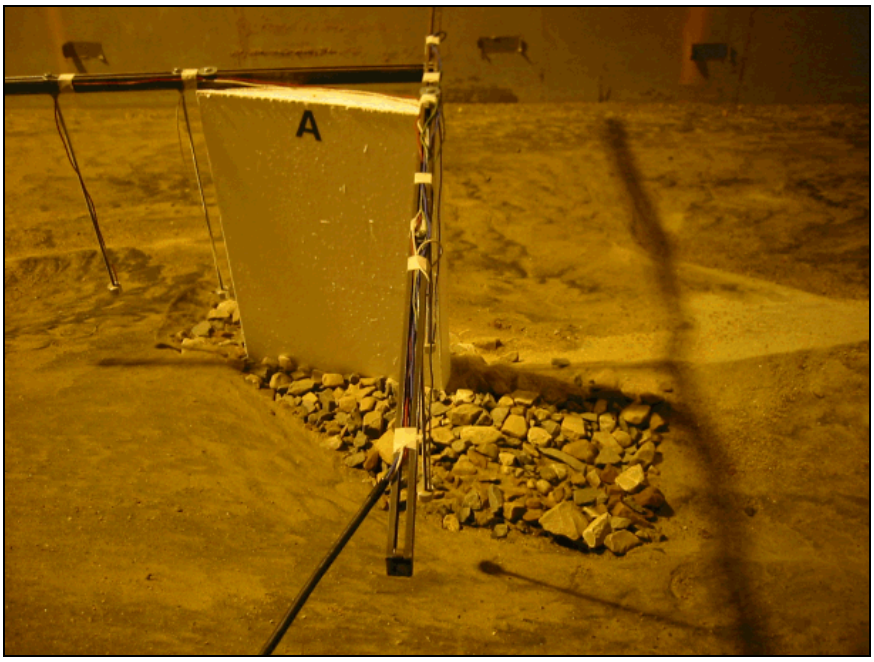

Figure 4.26. Pier A (15° skew) after Test C14b (flow is from left to right).

(page intentionally left blank)

5. ARTICULATING CONCRETE BLOCKS

5.1 Materials

Articulating concrete blocks (ACBs) were examined for their suitability as a pier scour countermeasure. Many block systems in use today are pre-cabled and installed as mattresses. Cabling is primarily a construction convenience, and while cables may prevent blocks from being lost entirely, they do not keep blocks from failing through loss of intimate contact with the subgrade, which is the criterion generally accepted for stability design. The testing procedure conducted for this ACB examination did not incorporate any simulation of cabling.

Miniature concrete blocks made of sand-cement grout were sized using the Factor-of-Safety method for hydraulic conditions representative of the CSU 8-foot flume. Results indicate that at a flow depth of 0.3 m (1.0 ft) and an approach velocity of $2V_{crit}$, a target factor of safety of 1.0 (incipient failure) was achieved under these conditions. Since the Factor-of-Safety methodology presented in HEC-23 (Lagasse et al. 2001) for ACB countermeasure design does not account for any added stability that may be afforded by cables, the testing procedure reflects HEC-23 philosophy. **Table 5.1** provides a summary of the physical and hydraulic characteristics of the miniature blocks used in this study. **Figure 5.1** shows a close-up view of the blocks and their interlocking installation pattern.

Table 5.1. Articulating Concrete Block Properties.

Property	English Units	Metric Units	Comments
Length	1 7/16 in.	3.6 cm	
Width	1 9/16 in.	4.0 cm	
Height	11/16 in.	1.7 cm	
Average weight/block	0.056 lb	25.3 g	Saturated
Average density	134 lb/ft^3	2.15 g/cm^3	Saturated
Critical shear stress	0.305 lb/ft^2	14.6 N/m^3	Tested at horizontal
Manning's n value	0.016	0.016	

5.2 Testing

5.2.1 Overview

Six tests were conducted to quantify the design and performance of articulating concrete blocks (ACBs) as a pier scour countermeasure (**Table 5.2**). Test 10 established performance criteria (i.e., critical shear stress) necessary for design per HEC-23 methods (see Section 2.2). A flume 0.61 m (2 ft) wide by 18.3 m (60 ft) long was used in the determination of the critical shear stress for the ACBs. A series of flows were conveyed through the flume until the ACBs lost intimate contact with the flume floor. The corresponding values of shear stress and flow velocity were determined and used as input to the current state of the practice design procedure (i.e., the Factor of Safety method).

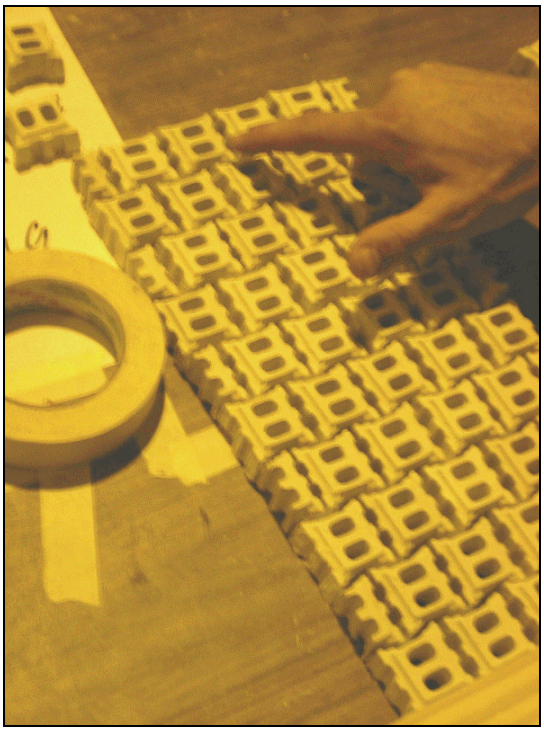

Figure 5.1. Articulating Concrete Blocks.

The three installations associated with Test 11 (clear-water and live-bed) were performed to quantify the sensitivity of an ACB system's performance as a function of areal coverage. Test 12 examined the effect of filter layer type and extent on system performance. Test 13 incorporated variations in edge turndown. Tests 14 and 18 used the best performing combination from the previous tests with a live-bed condition incorporating sediment feed. Tests 14 and 18 were run for a duration of 8 hours each, to permit bed forms to migrate through the system.

5.2.2 Test 11

The objective of Test 11 was to document and quantify the sensitivity of an ACB system's performance as a function of areal coverage. All spatial arrangements for Test 11 included a non-woven geotextile filter extending from the pier face to the perimeter of the ACBs. A sand cement grout similar to that used for the partially grouted riprap (see Section 6.1) was used to grout the interface between the blocks and the pier face on all Test 11 installations. Additionally, all installation configurations incorporated an edge turndown around the periphery of the system.

Due to a limited number of miniature blocks available, Test 11 was completed in three separate test runs. One ACB countermeasure configuration was examined at Pier B for each test run of Test 11. Test 11-first installation, Pier B, incorporated a horizontal ACB extension of 40.6 cm (16 in) from pier face to the edge of the installment, a turndown detail around the entire boundary with a radius of curvature of 25.4 cm (10 in), ending in a depth of 10.2 cm (4 in) at the perimeter. Sand was filled over the blocks to create a finished elevation flush with the initial bed level. No scour protection was installed on Piers A and C. **Figure 5.2** shows Pier B after Test 11-a1. Note the stability of the ACBs and the exposure of the edge turndowns.

Table 5.2. Articulating Concrete Block Tests.										
Test Number	Pier A		Pier B		Pier C		Duration (hr)	V/Vc	Sediment Feed	Bedforms
	Description	Filter	Description	Filter	Description	Filter				
10	ACB Shear Stress Testing in the 2-Foot Flume							Varied	No	None
11a1	Unprotected	None	ACB	NW1	Unprotected	NW1	2	1	No	Clear-water; plane bed
11b1	Unprotected	None	ACB	NW1	Unprotected	NW1	2	2	No	Mobile; dunes
11a2	Unprotected	None	ACB	NW1	Unprotected	NW1	2	1	No	Clear-water; plane bed
11b2	Unprotected	None	ACB	NW1	Unprotected	NW1	2	2	No	Mobile; dunes
11b2 extended	Unprotected	None	ACB	NW1	Unprotected	NW1	5	2	No	Mobile; dunes
11a3	Unprotected	None	ACB	NW1	N/A	N/A	2	1	No	Clear-water; plane bed
11b3	Unprotected	None	ACB	NW1	N/A	N/A	2	2	No	Mobile; dunes
11b3 extended	Unprotected	None	ACB	NW1	N/A	N/A	5	2	No	Mobile; dunes
12a	ACB	NW1	ACB	NW1	Unprotected	None	2	1	No	Clear-water; plane bed
12 b	ACB	NW1	ACB	NW1	Unprotected	None	2	2	No	Mobile; dunes
13a	ACB, Riprap	NW1	ACB	NW1	N/A	N/A	2	1	No	Clear-water; plane bed
13b	ACB, Riprap	NW1	ACB	NW1	N/A	N/A	2	2	No	Mobile; dunes
14a	Unprotected	None	ACB	NW2	N/A	N/A	8	2.5	Yes	Mobile; dunes
18a	Unprotected	None	N/A	N/A	ACB	NW2	8	2.5	Yes	Mobile; dunes

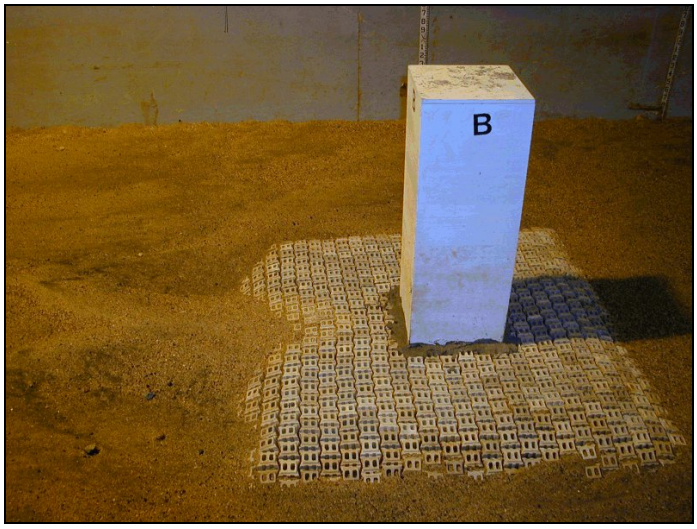

Figure 5.2. Pier B, after Test 11a1 (flow from right to left in photo).

Test 11 (second installation) Pier B, included a transverse riprap distance of 30.5 cm (12 in) from pier face to the edge of the blocks on the downstream side of the installation. The turndown detail on Test 11-second installation was continuous at a 3H:1V slope from the pier face on the upstream and sides of the pier. The turndown detail from the edge of the transverse portion in the downstream integrated a 4H:1V slope for a horizontal extension of 40.6 cm (16 in). Depth of the turndown at the perimeter of the installation was 10.2 cm (4 in). Sand was filled over the blocks to create a finished elevation flush with the initial bed level. No scour protection was installed on Piers A and C. After the Test 11-second installation, $2V_c$ run was complete and all data collected, an extended duration run was completed at $2V_c$. **Figure 5.3** shows Pier B after the extended run. Note loss of blocks upstream and on the right side of the pier.

Test 11 (third installation) Pier B, incorporated a turndown detail of a 3H:1V slope, extending from the pier face, 5.1 cm (2 in) below the ambient bed surface to a depth of 18.5 cm (7.3 in) at the perimeter. ACBs extended horizontally for 40.6 cm (16 in). Sand was filled over the blocks to create a finished elevation flush with the initial bed level. **Figure 5.4** shows Pier B before the sand be was leveled. No scour protection was installed on Pier A. Test 11, Pier C incorporated the previously mentioned riprap configuration.

Figure 5.3. Pier B after Test 11b2-extended (flow from left to right in photo).

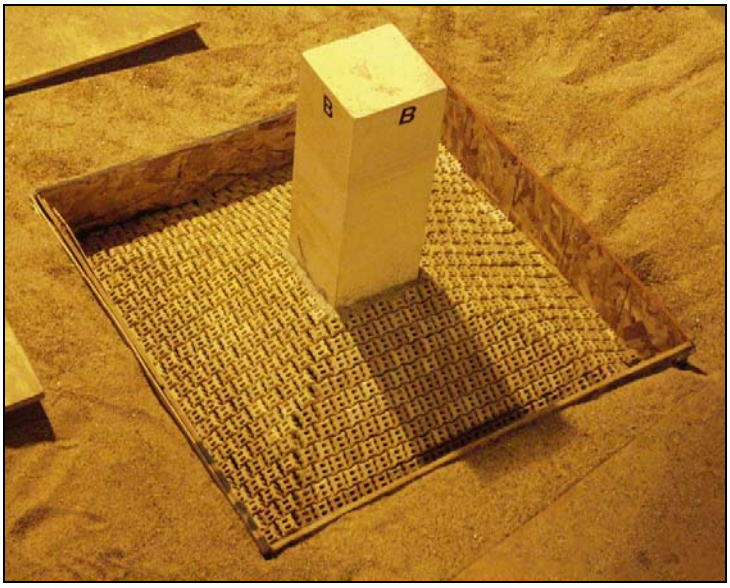

Figure 5.4. Pier B, Test 11 (third installation) before leveling the bed.

5.2.3 Test 12

Test 12 was performed to compare the performance of full versus partial geotextile filter placement with ACBs. The Pier A installation incorporated ACB turndown detail on a 2H:1V slope from the pier face extending 20.3 cm (8 in). A riprap key (d_{50} = 30 mm), flush with the initial bed, covered the blocks and extended 20.3 cm (8 in) beyond the boundary of the ACBs. The horizontal extent of the entire installation was 40.6 cm (16 in) and the depth of the installation at the perimeter was 10.2 cm (4 in). A geotextile filter extended 5.1 cm (2 in) beyond the perimeter of the blocks. The interface between the pier and blocks was grouted with sand cement grout. A schematic of the countermeasure installation for Test 12, Pier A is presented in **Figure 5.5**. Pier B incorporated a turndown detail on a 2H:1V slope extending from the pier face for a horizontal length of 40.6 cm (16 in) and a depth of 20.3 cm (8 in) at the perimeter. A non-woven geotextile filter extended the full length of the blocks. The interface between the pier and blocks was grouted with sand cement grout. Sand was filled over the blocks to create a finished elevation flush with the initial bed level. Pier C incorporated the previously described riprap design for Test 12.

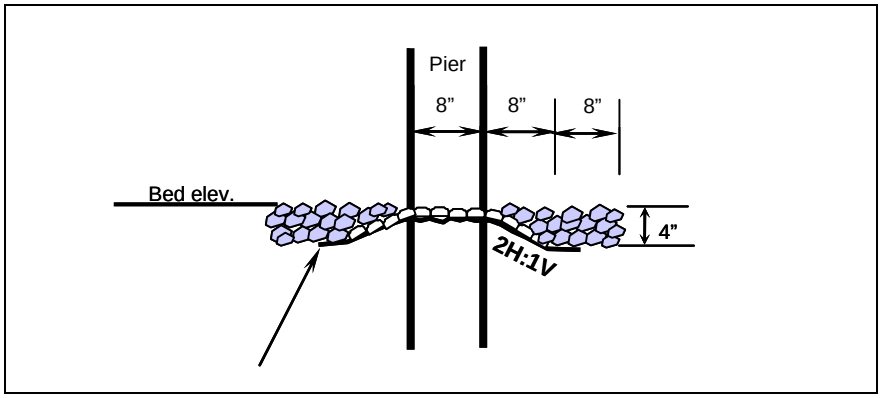

Figure 5.5. Schematic of Pier A, Test 12.

5.2.4 Test 13

Test 13 was performed to examine the benefit of edge burial in order to minimize the degradation of the system caused by undermining at the perimeter of the countermeasure. Pier A installation incorporated ACB turndown detail on a 2H:1V slope from the pier face extending 20.3 cm (8 in). A riprap (d_{50} = 30 mm) key, flush with the initial bed, covered the blocks. The riprap was on a 2H:1V slope and extended 20.3 cm (8 in) beyond the boundary of the ACBs. The horizontal extent of the entire installation was 40.6 cm (16 in) and the depth of the installation at the perimeter was 10.2 cm (4 in). A geotextile filter extended 5.1 cm (2 in) beyond the perimeter of the blocks. The interface between the pier and blocks was grouted with sand cement grout. Pier B incorporated a turndown detail on a 2H:1V slope for a horizontal length of 40.6 cm (16 in) and a depth of 20.3 cm (8 in). A non-woven geotextile filter extended the full length of the blocks. The interface between the pier and blocks was grouted with sand cement grout. A grout seam was placed along the intersection of the four planes of the ACBs. Sand was filled over the blocks to create a finished elevation flush with the initial bed level. **Figure 5.6** shows Pier B after Test 13a. Pier C incorporated the previously described riprap design.

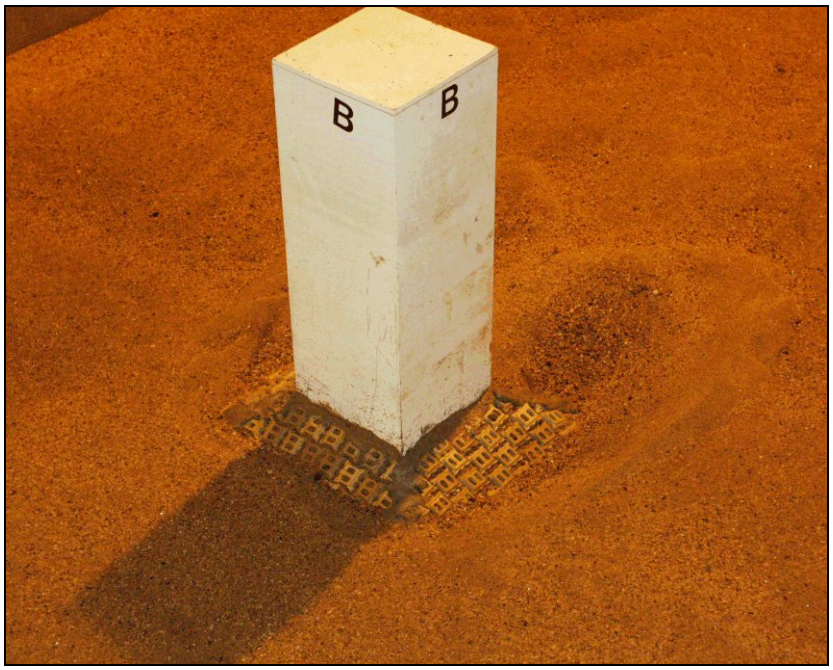

Figure 5.6. Pier B after Test 13a (flow from lower left to upper right in photo).

5.2.5 Test 14

Test 14, Pier B included a turndown detail on a 2H:1V slope. Horizontal extension was 40.6 cm (16 in); depth was level with the ambient bed surface at the pier face and 20.3 cm (8 in) at the perimeter. A non-woven geotextile filter extended from the pier face to the perimeter of the ACBs. A sand cement grout was used to grout the interface between the blocks and the pier face. A 25.4 mm (1 in) thick seam of grout was also placed along the intersection of the four planes of the ACBs. Sand was filled over the blocks to create a finished elevation flush with the initial bed level. **Figure 5.7** shows Pier B after completion of Test 14. No countermeasure was installed on Pier A. Pier C incorporated a partially grouted riprap design that is described in the next section.

5.2.6 Test 18

Installation design for Test 18, Pier C was identical to the countermeasure design for Test 14, Pier B, except depth at the pier face was 10.2 cm (4 in) below the ambient bed layer, and therefore peripheral depth of the ACBs was 30.5 cm (12 in). A schematic of the countermeasure design is presented in **Figure 5.8**. No countermeasure was installed on Pier A. Pier B incorporated a partially grouted riprap design described in the following section.

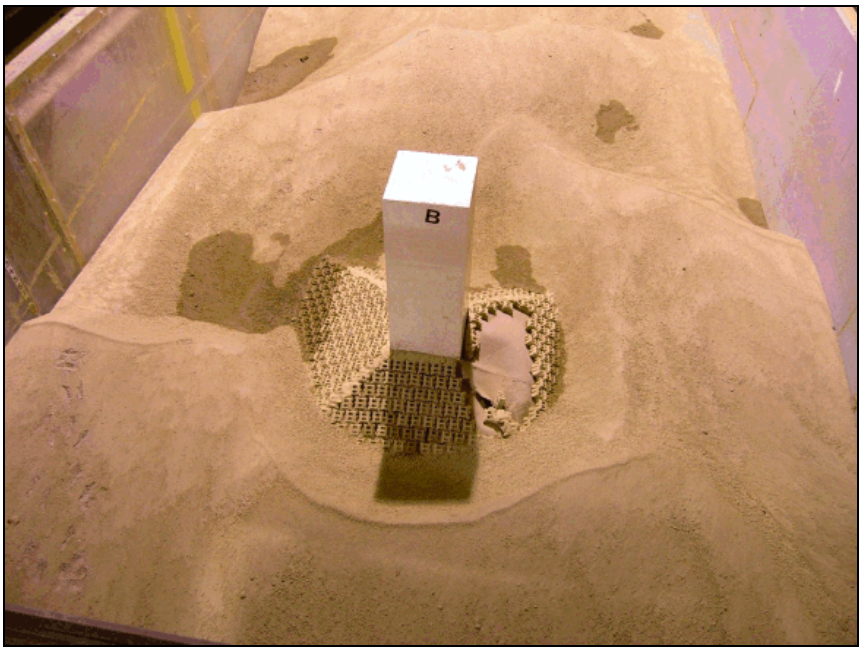

Figure 5.7. Pier B after Test 14, looking downstream.

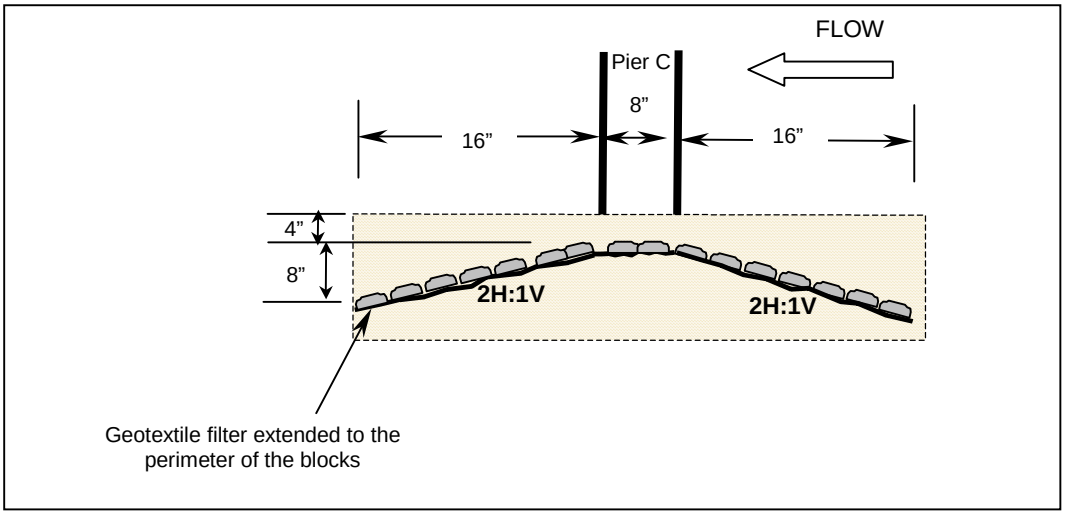

Figure 5.8. Schematic of Pier C, Test 18.

(page intentionally left blank)

6. PARTIALLY GROUTED RIPRAP

Partially grouted riprap for bridge pier protection is an adaptation of German technology investigated in detail in this study (see Lagasse et al. 2006b). Both indoor and outdoor (prototype scale) tests were conducted. For the Federal Waterway Engineering and Research institute (BAW) Code of Practice see BAW 1990 in Part 2 of this volume.

6.1 Indoor Tests

6.1.1 Materials

For the partially grouted riprap installations, various grout mix designs were developed and constructed "in the dry" using d_{50} riprap sizes of 14.7 mm (0.58 in), 25.4 mm (1 in), and 30 mm (1.2 in). Consistency of the cementitious grout mix was determined by trial and error. The initial mix design was based on pumpable fine aggregate concrete mix used in the construction of grout-filled mattresses. Test pours were performed for all three riprap sizes. **Figure 6.1** shows a test pour with the 30 mm riprap.

Figure 6.1. Test pour of grout.

Two sizes of sand for the grout mix were examined during the test pours; the first had a d_{50} of 0.7 mm and the second a d_{50} of 0.4 mm. The 0.4 mm sand produced a more fluid grout with superior flowability and was able to better penetrate into the riprap pores. Ultimately, two different mixes were needed to accommodate the different pore sizes of the three classes of riprap. The mix developed for the smaller 14.7 mm riprap contained less sand than that for the 30 mm and the 25.4 mm riprap, allowing better flow through the smaller pore spaces. The final grout mixes for the partially grouted riprap tests are presented in **Table 6.1**. Grout mix 1 was used for the 14.7 mm riprap and grout mix 2 was used for the two larger riprap sizes.

Table 6.1. Final Grout Mixes.				
	Grout Mix 1		Grout Mix 2	
	Pounds	Grams	Pounds	Grams
Portland Cement	1	453.6	1	453.6
Water	0.69	314.3	0.69	314.3
Fine Sand (0.4 mm)	1.25	567.0	1.67	755.3

For testing, riprap was installed around a pier and then a measured volume of grout was hand poured into "spots" on the riprap in a stagger patter. The target fill value of between 15 to 40% of the original void space volume was maintained for all installations tested (see BAW 1990). Conglomerate-like elements in the riprap were produced using the spot-by-spot grouting procedure. **Figure 6.2** shows the conglomerates produced during a test pour. For additional information on the partially grouted riprap concept, see Lagasse et al. 2006b.

Figure 6.2. Conglomerates produced by partial grouting of riprap.

6.1.2 Indoor Flume Testing

Five tests in the indoor flume were conducted to quantify the performance of partially grouted riprap as a pier scour countermeasure (**Table 6.2**). Test 15 provided performance results on the current state of the practice in addition to quantifying the effect of rock size (d_{50}) on performance of the system. The resulting stable d_{50} particle size for partially grouted riprap was approximately one-half the size of the rock used for the loose riprap tests.

Test 16 used the optimum performing system from Test 15 and examined the variation in system performance with layer thickness. Test 17 quantified changes in performance as a function of areal coverage of the protection system. Tests 14 and 18 incorporated the best performing configurations of the series with a live-bed condition incorporating sediment feed. Tests 14 and 18 were each run for a duration of 8 hours to permit bed forms to migrate through the system.

Table 6.2. Partially Grouted Riprap Tests.										
Test No.	Pier A		Pier B		Pier C		Duration (hr)	V/Vc	Sediment Feed	Bedforms
	Description	Filter	Description	Filter	Description	Filter				
14a	Unprotected	None	N/A	N/A	Partial Grout 25.4 mm Riprap	NW2	8	2.5	Yes	Mobile; dunes
15a	Partial Grout 14.7 mm Riprap	W1	Partial Grout 25.4 mm Riprap	W1	Partial Grout 30 mm Riprap	W1	2	1	No	Clear-water; plane bed
15b	Partial Grout 14.7 mm Riprap	W1	Partial Grout 25.4 mm Riprap	W1	Partial Grout 30 mm Riprap	W1	2	2	No	Mobile; dunes
16a	Partial Grout 14.7 mm Riprap	W1	Partial Grout 14.7 mm Riprap	W1	Partial Grout 14.7 mm Riprap	W1	2	1	No	Clear-water; plane bed
16b	Partial Grout 14.7 mm Riprap	W1	Partial Grout 14.7 mm Riprap	W1	Partial Grout 14.7 mm Riprap	W1	2	2	No	Mobile; dunes
17a	Partial Grout 14.7 mm Riprap	W1	Partial Grout 14.7 mm Riprap	W1	Partial Grout 14.7 mm Riprap	W1	2	1	No	Clear-water; plane bed
17b	Partial Grout 14.7 mm Riprap	W1	Partial Grout 14.7 mm Riprap	W1	Partial Grout 14.7 mm Riprap	W1	2	2	No	Mobile; dunes
18a	Unprotected	None	Partial Grout 25.4 mm Riprap	NW2	N/A	N/A	8	2.5	Yes	Mobile; dunes

Spot pouring of the grout preserved most of the original porosity of the riprap matrix, and resulted in considerable open space at the surface. Grout spots were staggered in a grid pattern for all installations. A geotextile filter was used with all partially grouted riprap countermeasure configurations.

The horizontal extent of riprap on Test 14, Pier C was one and a half times the pier width, or 40.6 cm (16 in), on all sides with a 10.2 cm (4 in) depth. A geotextile filter extended two-thirds the length of the riprap. D_{50} of the riprap was 25.4 mm (1 in). Approximately 80 ml of grout were poured in each spot and approximately 40 spots were poured. A photograph of Pier C after completion of Test 14 is presented in **Figure 6.3**. (No countermeasure was installed on Pier A. Pier B incorporated the previously described ACB installation.)

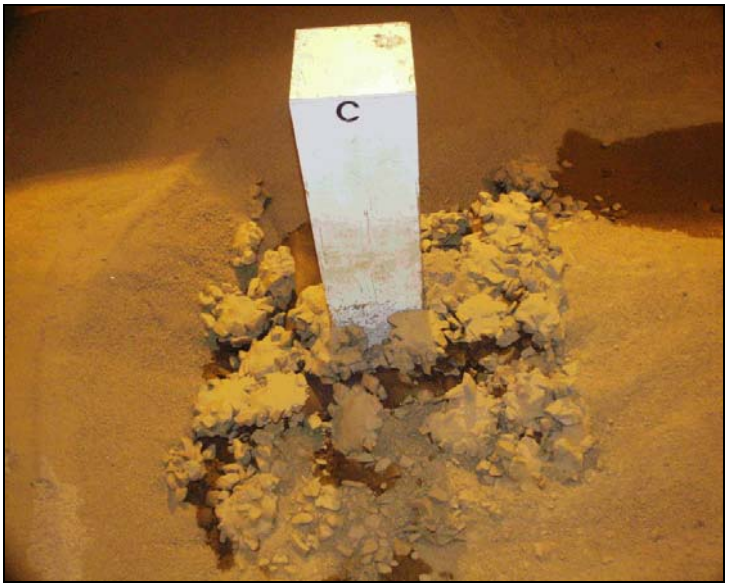

Figure 6.3. Pier C after completion of Test 14 (flow is left to right in photo).

6.1.3 Test 15

Test 15 provided performance results of the current state of practice in addition to quantifying the effect of mean rock size (d_{50}) on performance of the system. Grout spots were staggered in a 10.2 cm (4 in) by 7.6 cm (3 in) grid pattern. Approximately 200 ml of grout were poured in each spot and roughly 60-70 spots were poured on each pier configuration. The riprap configuration for each pier was the same in Test 15. Horizontal extent of riprap was two times the pier width, or 40.6 cm (16 in), on all sides with a 10.2 cm (4 in) depth at the perimeter. A geotextile filter extended two-thirds the length of the riprap. D_{50} of the riprap on Pier A was 14.7 mm (0.6 in). D_{50} of the riprap on Pier B was 25.4 mm (1 in). D_{50} of the riprap on Pier C was 30 mm (1.2 in). **Figure 6.4** shows Pier A, taken shortly after the grout spots were poured.

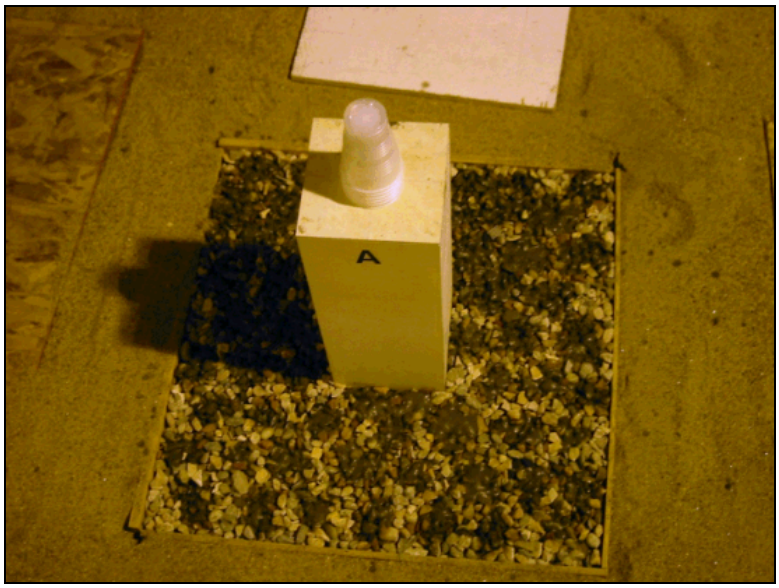

Figure 6.4. Pier A prior to Test 15, shortly after pouring grout.

6.1.4 Test 16

Test 16 was conducted to examine the variation in system performance as a function of layer thickness. Each layer was sized as a function of rock size per the guidance given in HEC-23 for standard riprap. After results of Test 15 were examined, it was determined that the smaller riprap (d_{50} = 14.7 mm) provided sufficient protection against scour and would be utilized in Test 16. Horizontal extent of the riprap on all three piers was 1.5 times the pier width, or 30.5 cm (12 in) on all sides. On all piers, the geotextile filter extended two-thirds the length of the riprap extent. The volume of grout poured per spot varied. Grout spots on Piers A and B contained 65 ml of grout and Pier C grout spots contained 100 ml of grout. The grout pattern was increased to a 12.7 cm (5 in) by 10.2 cm (4 in) stagger pattern for all installations. Depth of the riprap layer on Pier A was 5.1 cm (2 in). Depth of the installation was 10.2 cm (4 in) angled on a 4H:1V slope extending from the pier face. At Pier A, after installation of the riprap and grout spots, sand was filled in over the riprap and leveled. A schematic of the countermeasure design for Pier A is presented in **Figure 6.5**. Depth of riprap at Pier B was 5.1 cm (2 in). Depth of riprap at Pier C was 7.6 cm (3 in).

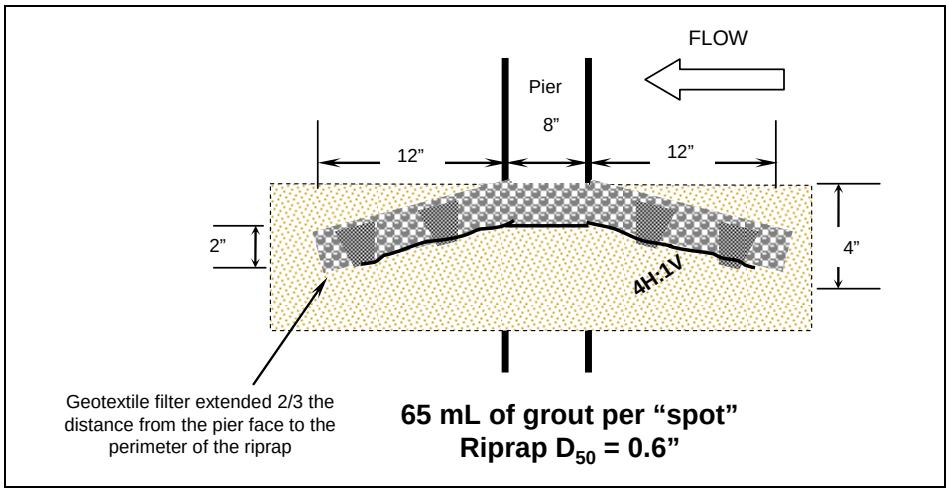

Figure 6.5. Countermeasure schematic of Pier A, Test 16.

6.1.5 Test 17

Test 17 was performed to examine reduction of the riprap layout extent due to the effect of partial grouting. All pier designs utilized riprap (d_{50} = 14.7 mm) with a layer thickness of 5.1 cm (2 in). A geotextile filter extended two-thirds the length of the riprap on all pier setups. Approximately 65 ml of grout were poured in each spot. On Pier A, the riprap extended 20.3 cm (8 in) on all sides and was level with the bed. Roughly 32 spots were poured. On Pier B, the riprap extended 20.3 cm (8 in) and was on a one 4H:1V slope. Top of the riprap at the perimeter was 5.1 cm (2 in) below the ambient bed layer. Roughly 26 spots were poured. The riprap on Pier C extended 30.5 cm (12 in) from pier face on a 4H:1V slope. Top of the riprap at the perimeter was 7.6 cm (3 in) below the ambient bed layer. Roughly 54 spots were poured. On Piers B and C, after installation of the riprap and grout spots, sand was filled in over the riprap and leveled. **Figure 6.6** shows Pier A after Test 17a was completed.

Figure 6.6. Pier A after Test 17a (flow is right to left in photo).

6.1.6 Test 18

Riprap installation for Test 18, Pier B included a turndown detail on a 2H:1V slope of a 7.6 (3 in) riprap layer. Horizontal extension of the riprap was 40.6 cm (16 in); top of the riprap was level with the ambient bed surface at the pier face and 20.3 cm (8 in) below the bed surface at the perimeter. D_{50} of the riprap was 25.4 mm (1 in). A geotextile filter extended two-thirds the length of the riprap. Grout spots were staggered in a 10.2 cm (4 in) by 10.2 cm (4 in) grid pattern. Approximately 80 ml of grout were poured in each spot and roughly 60 spots were poured. After installation of the riprap and grout spots, sand was filled in over the riprap and leveled. **Figure 6.7** shows Pier B after completion of Test 18. (No countermeasure was installed at Pier A. Pier C incorporated the previously described ACB installation).

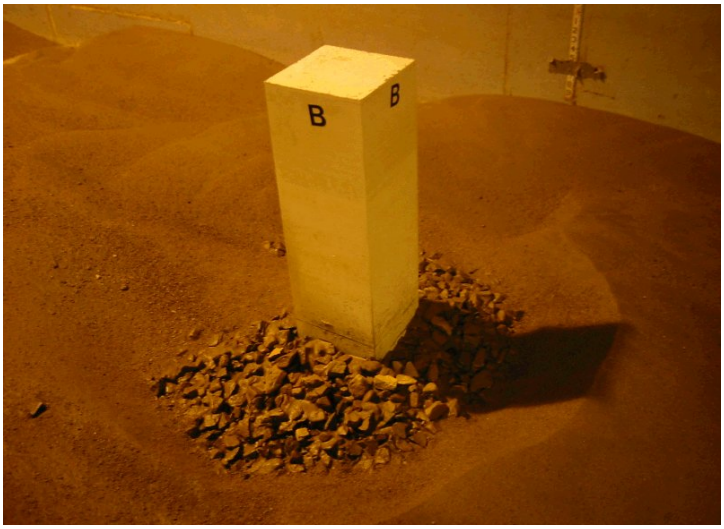

Figure 6.7. Pier B after Test 18 (flow from right to left in photo).

6.2 Prototype Scale Tests

Two tests were performed to quantify performance of partially grouted riprap at prototype scale. The tests were conducted in the outdoor facilities at Colorado State University's Engineering Research Center; specifically, the large concrete flume known as the Tarbela Flume. Installation of the countermeasure was performed at a rectangular pier measuring 0.45 m wide by 1.4 m long (1.5 ft by 4.5 ft). Test C1 examined constructability and environmental issues associated with underwater application of grout, as well as performance in high velocity conditions. Test C20 was performed to compare the stability of partially grouted riprap side-by-side with loose riprap of the same size. Partially grouted riprap tests performed as part of Task 7C continuation funding, are presented in **Table 6.3** and summarized in the following sections.

Table 6.3. Partially Grouted Riprap Tests.

Test Number	Pier	Filter	Duration (hr)	Velocity (ft/s)	Sediment Feed	Bedforms
C1	Single Pier in Tarbela Flume	Sand filled geocontainers	Varied	Varied	No	None
C20	Single Pier in Tarbela Flume	Sand filled geocontainers	Varied	Varied	No	None

6.2.1 Materials

Geocontainers. Sand filled geotextile containers were constructed using a geotextile fabric with the characteristics presented in **Table 6.4**. The geotextile containers measured 1.2 m x 0.5 m x 0.1 m (4 ft x 1.5 ft x 0.33 ft) with a typical volume of .06 m^3 (2 ft^3). Approximately 100 kg (220 lbs) of sand was placed in each bag. Commercial concrete sand meeting appropriate filter criteria was used to fill the geotextile bags. **Figure 6.8** shows the geotextile containers before being placed around the pier.

Table 6.4. Characteristics of Geotextile.

Trade Name	Mass per Unit Area	AOS	Permeability	Geotextile Type	K_g/K_s
Mirafi® 180 N	278 g/m^2	0.18 mm	0.21 cm/s	Nonwoven needle punched	5.25

Figure 6.8. Geocontainers before installation around the pier.

Bed Material. Commercial concrete sand with a d_{50} of approximately 0.7 mm was used for the sand bed in the Tarbela flume.

Armor Stone. The durable sandstone riprap used for testing in the Tarbela flume had a d_{50} of 6 inches. **Figure 6.9** shows the grain size distribution of riprap utilized in the testing program. The stone was sieved to ensure the desired gradation; stones greater than 9 inches and less than 3 inches were removed. The riprap was visually assessed, and stones appearing platy or needle-like were removed.

Grout. A grout mixture created for underwater application was used in the testing program. A proprietary admixture, Sicotan® Additive, was included in the grout to prevent dilution and dissipation of the grout into the water. **Table 6.5** presents the approximate grout component quantities.

Grout was mixed at a commercial batch plant. During the mixing process, water was added to the mixture in order to achieve the desired consistency and slump characteristics. **Figure 6.10** displays the grain size distribution curve for the coarse aggregate in the grout mix.

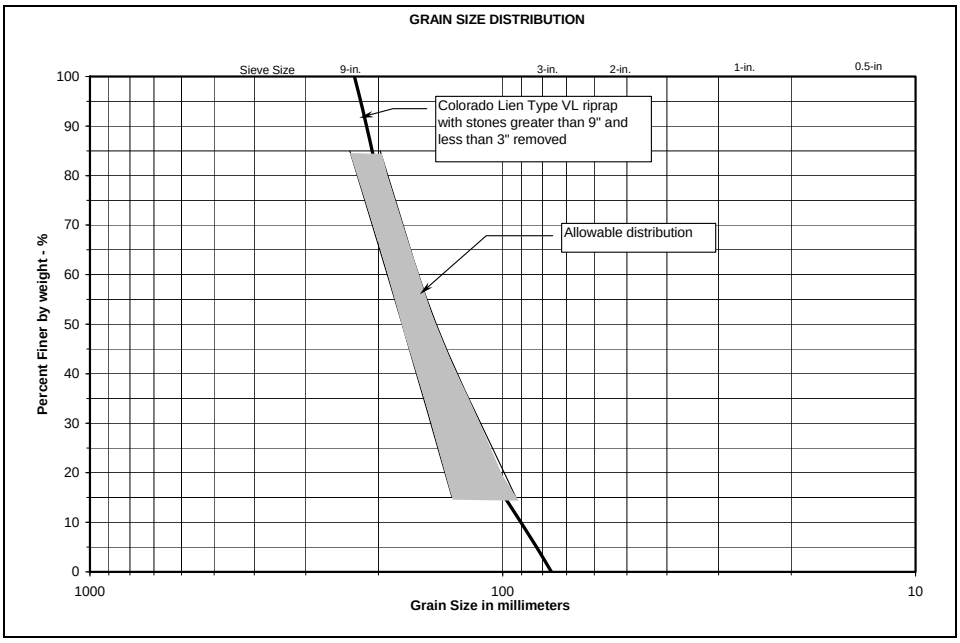

Figure 6.9. Six-inch riprap grain size distribution.

Table 6.5. Grout Mix for Outdoor Testing Program.		
	Weight (lb)	Proportion by Weight
Ordinary Portland Cement	753	0.600
Water	450	0.400
Concrete Sand (d_{50} = 0.7 mm)	1191	1.000
Coarse Aggregate (d_{50} = 3.3 mm)	1191	1.000
Sicotan® Additive	6.7	0.006

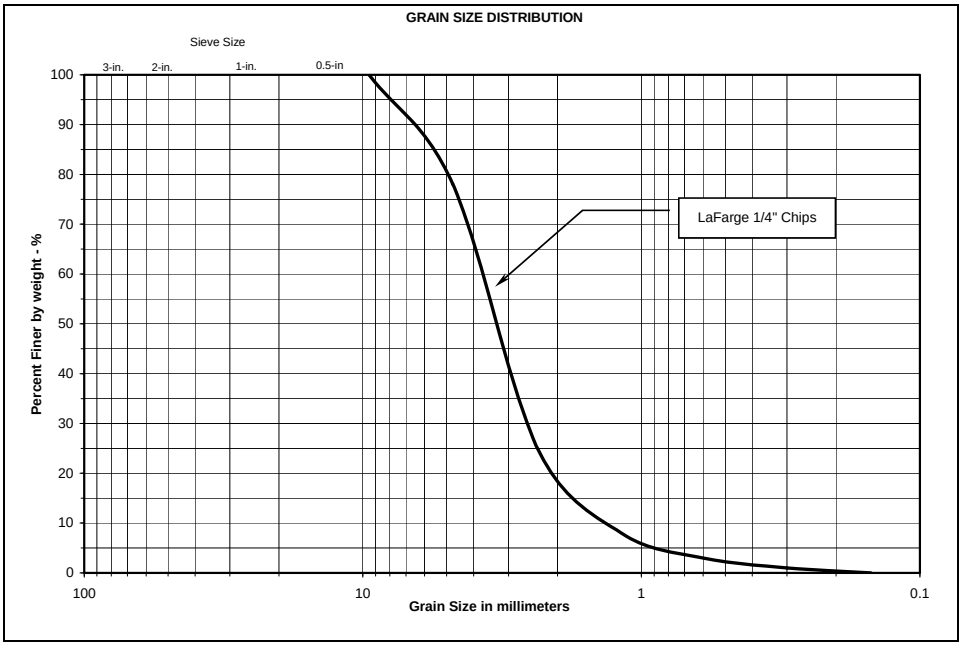

Figure 6.10. Grain size distribution for coarse aggregate in grout mix.

6.2.2 Tarbela Flume

The Tarbela flume measures 33 m (108 ft) long by 6.1 m (20 ft) wide and 2.4 m (8 ft) deep. Flow enters the flume by a 0.9 m (36 in) diameter pipe fed by a nearby reservoir. Flow entered the headbox and was discharged into the flume through a sluice gate with dimensions 1.9 m by 1.2 m (6.25 ft by 3.9 ft). A rock baffle 1.6 m (5.25 ft) tall and spanning the width of the flume was installed 4.6 m (15 ft) downstream of the headbox. The baffle was intended to uniformly distribute the flow across the width of the flume. Tail water depths were controlled by four sluice gates at the downstream end of the flume. Bed slope of the flume was 0.003 m/m (0.3%).

A test section was created 9.1 m (30 ft) downstream of the rock baffle. The test section was 9 m (30.7 ft) long and spanned the width of the flume. It was filled with 1.6 m (5.25 ft) of sand. The pier was installed in the center of the test section. Upstream and downstream of the test section the flume bed was comprised of smooth concrete floors. **Figure 6.11** is a layout diagram for Tests C1 and C20. Surrounding the pier, a scour hole measuring 3.7 m by 4.9 m (12 ft by 16 ft) was pre-formed into the sand bed to a maximum depth of 1 m (3 ft) as shown in **Figure 6.12**.

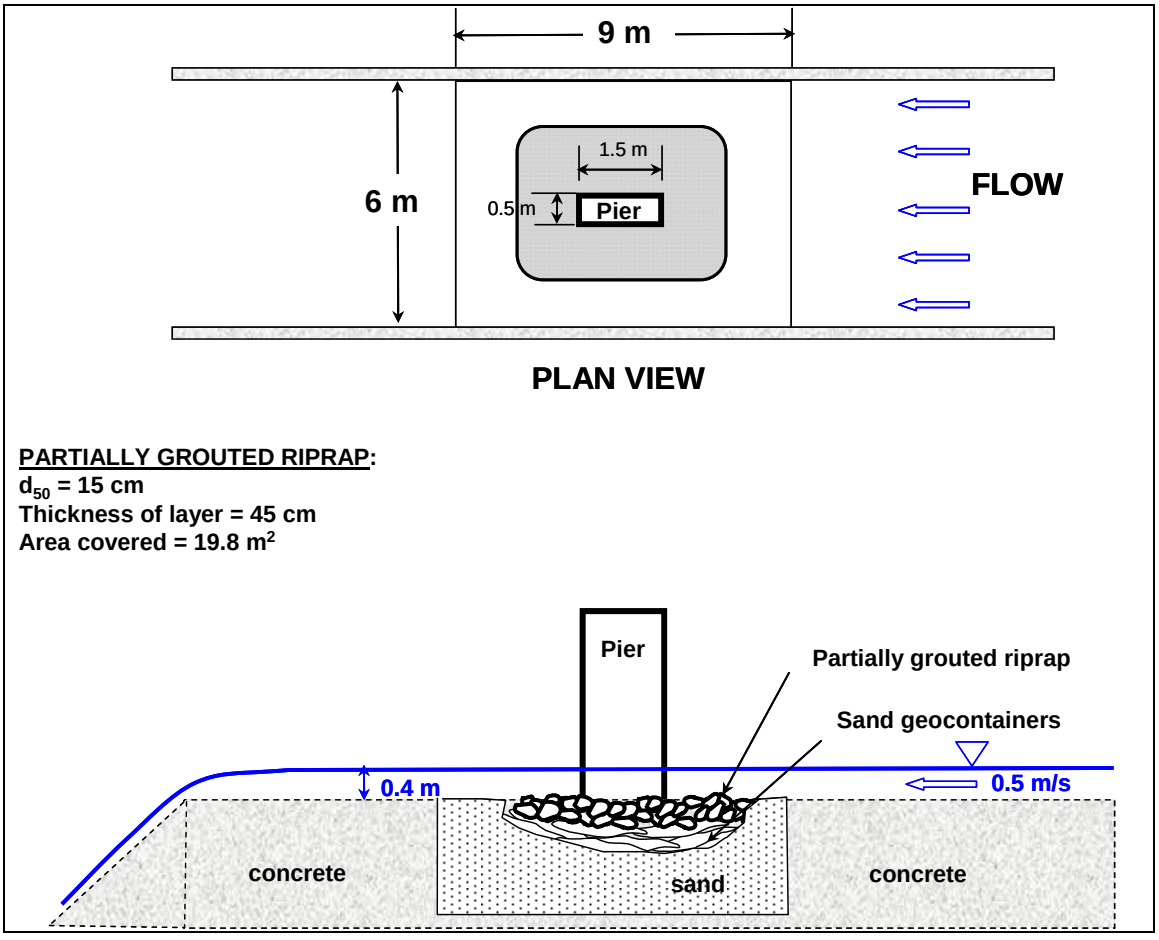

Figure 6.11. Schematic layout for Test C1 (dimensions approximate).

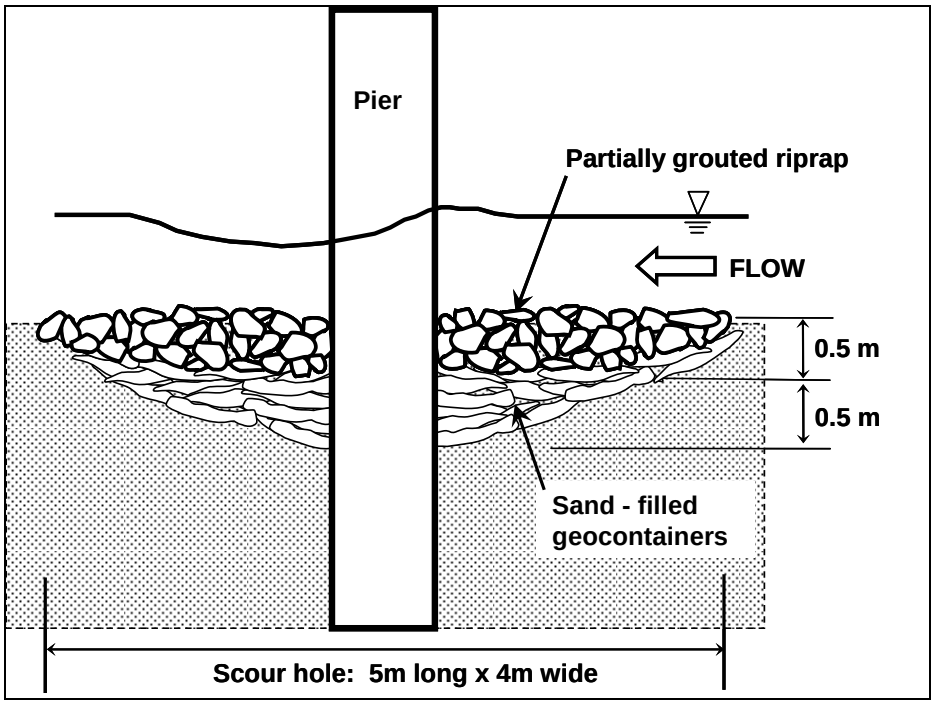

Figure 6.12. Tarbela installation, Test C1.

6.2.3 Installation

An approach flow of 0.3 m (1 ft) deep at approximately 0.5 m/s (1.5 ft/s) was established. A total of 32 geotextile containers were placed around the pier by dropping from a height of about 1.5 m (5 feet) above the water surface. Installation was facilitated by a backhoe fitted with a special grapple attached to the bucket, which enabled the backhoe to pick up the geotextile container, position around the pier to a specified location, and release the container. **Figure 6.13** is a photograph of a geotextile container being dropped near the pier; note the grapple plate attachment to the backhoe. **Figure 6.14** shows the geotextile containers after installation in approximately 0.3 m (1 foot) of flowing water.

Next, riprap was positioned on top of the geotextile containers using the backhoe with the grapple removed. **Figure 6.15** shows riprap being dropped near the pier and **Figure 6.16** shows the riprap after installation.

6.2.4 Test Procedure and Data Acquisition

Testing was initiated by slowly filling the flume with the tailgates closed and allowing the flume to fill to a depth greater than the target depth to insure target velocities were not exceeded. Once the target discharge was achieved, tailgates were slowly opened until the target depth of 0.3 to 0.5 m (1 to 1.5 ft) was established.

Velocity and water surface elevation were monitored periodically at predetermined locations, shown in **Figure 6.17**, during each test to ensure target hydraulic conditions were maintained. Water surface elevations were measured utilizing a point gage assembly mounted to railings above the flume perpendicular to the flow. Accuracy of the point gage was 3 mm (0.01 ft).

Figure 6.13. Installation of geotextile containers looking downstream, pier is on the left.

Figure 6.14. Geotextile containers after installation, flow is from upper left lower right.

Figure 6.15. Installation of riprap around pier, looking downstream.

Figure 6.16. Riprap prior to grouting, looking downstream.

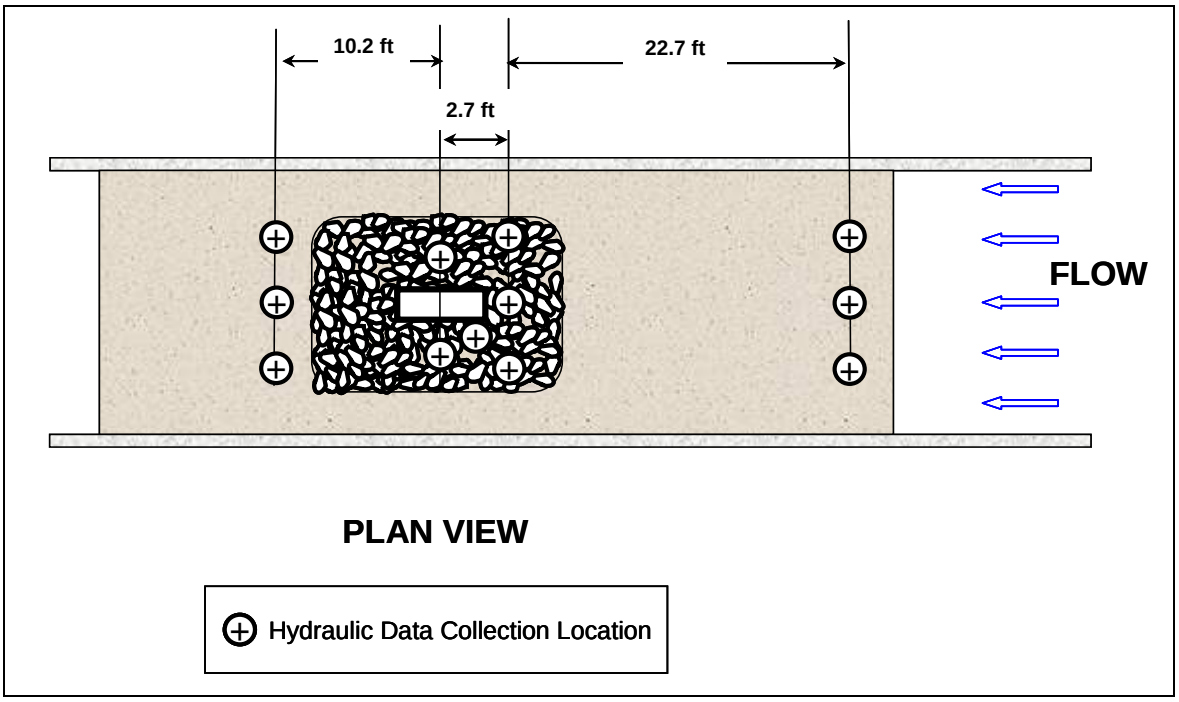

Figure 6.17. Hydraulic data collection locations.

Velocities were measured using Marsh-McBirney one-dimensional velocity meters attached to the tip of the point gage and to a wading rod. Measurements taken with the Marsh-McBirney had an accuracy of ± 3%. Point velocity data was taken at 20, 60, and 80% of flow depth at each data collection point.

6.2.5 Test C1

One test, designated C1, was performed to address constructability and environmental issues associated with partially grouted riprap installation in flowing water, along with stability performance at field scale under high velocity flow.

Constructability and Water Quality

Grouting Procedure: Prior to underwater application of the grout in the flume, a preliminary grout application was performed in the dry on a pile of riprap about 0.5 m (1.5 feet) thick. The trial application was performed to determine if the equipment could supply and control the grout pumping rate as needed for the underwater installation conditions. Grout was dispensed from a flexible hose attached to a boom on a concrete pump truck. Grout was supplied to the pump truck from a standard concrete mixer truck, as shown in **Figure 6.18**. **Figure 6.19** shows the preliminary trial grout application in the dry. **Figure 6.20** shows the surface of the riprap after partial grouting, and **Figure 6.21** shows the interior of the dry riprap pile after several exterior stones hade been removed to display penetration of the grout. Note in Figures 6.20 and 6.21 how the grout bridges between riprap stones forming larger conglomerate particles. In Figure 6.21, note that less than 50% of the total void space has been filled with grout. The preliminary application confirmed that the equipment acquired for the underwater partial grout application was satisfactory.

Figure 6.18. Concrete mixer truck and pump truck with boom.

Figure 6.19. Preliminary trial grout application in the dry.

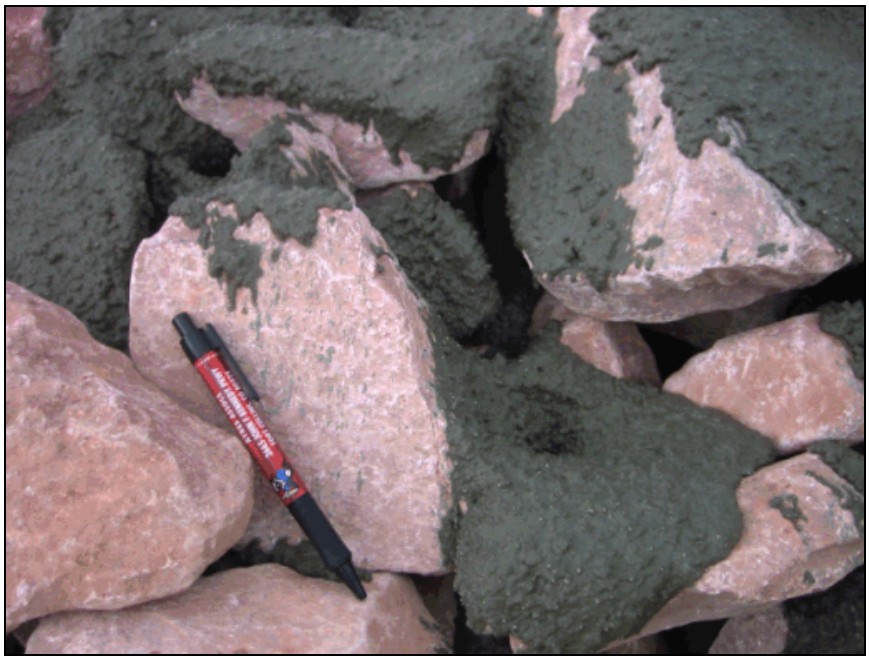

Figure 6.20. Surface of the riprap after partial grouting.

Figure 6.21. Interior of the dry riprap pile (some surface rocks removed).

Grout placement in the flume was performed by an experienced underwater grout installation specialist from Germany. The specialist was located in the flume and placed the grout directly on the riprap in 0.3 m (1 ft) of water with a velocity of 0.3 m/s (1 ft/s), as illustrated in **Figure 6.22**.

Figure 6.22. Underwater partial grouting of riprap, flow is from left to right.

Application of grout on the riprap lasted approximately 20 minutes. Approximately 1.1 m^3 (1.4 yd^3) of grout was placed, resulting in an application of 56 liters/m^2 (1.6 ft^3/yd^2). Typical grout application rates in German practice are 60 liters/m^2, so this test was representative of standard practice for this countermeasure type.

Water Quality Monitoring: Water quality was monitored before, during, and after the grout placement. Water quality parameters monitored continuously were pH, conductivity, temperature and turbidity. Based on research performed by the Virginia DOT, pH is the only water quality parameter that is expected to change significantly during grout placement (Fitch 2003). In the VDOT study, permit conditions required that pH levels remain below a value of 9.0, otherwise grouting activities were to be stopped and mitigation measures such as silt curtains were to be employed. VDOT did not monitor turbidity during their study and did not have access to the Sicotan® additive used in this study.

Water quality was monitored with a series of In-Situ Troll 9000 Profilers placed in stream at the seven locations depicted in **Figure 6.23**. The Troll 9000 Profilers continually recorded measurements of pH, conductivity, turbidity, and temperature. Baseline conditions were established prior to initiation of the grout placement 3.6 m (12 feet) upstream of the pier along the centerline of the flume (Station "A" in Figure 6.23).

During the test, the water discharge was 0.57 m^3/s (20 ft^3/s) and the average rate of grout placement was 0.0009 m^3/s (0.032 ft^3/s); therefore, the water:grout dilution ratio was 20:0.032, or 625:1. Three grab samples were selected for analysis corresponding to a baseline sample taken at Station A when testing commenced, Station C five minutes after grout application began, and Station F when grout application finished. Grab samples were collected in 250 mL polyethylene bottles that had been washed and rinsed with distilled water. Bottles were filled by dipping the bottle into the water upstream of where the sampling personnel were standing in the flume. The grab samples were analyzed by Stewart Environmental Consultants, Inc. of Fort Collins for selected inorganics and metals. The laboratory results for the samples are presented in **Table 6.6**.

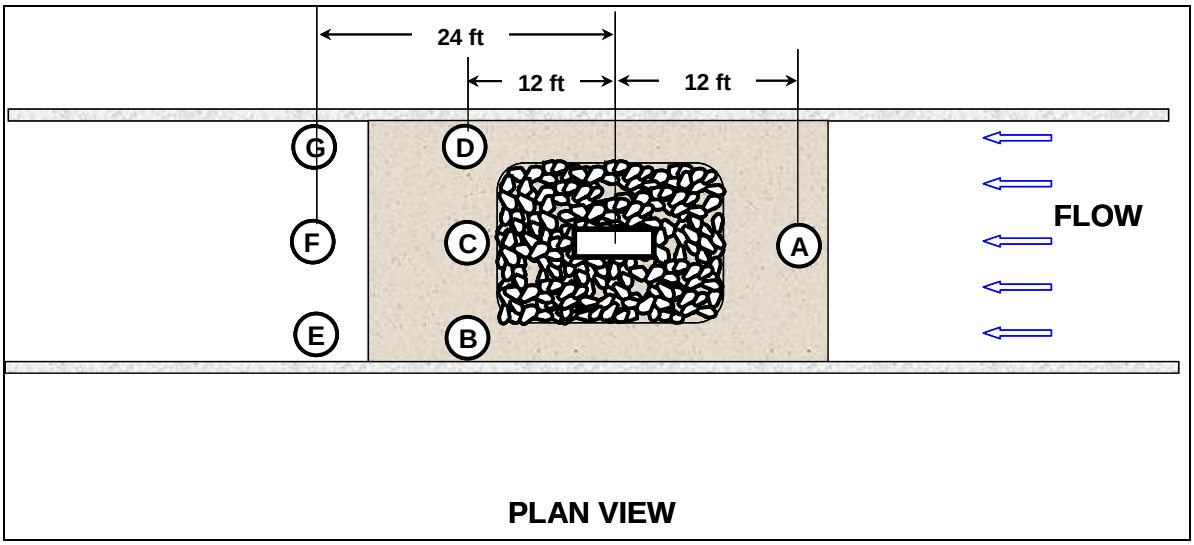

Figure 6.23. Location of water quality monitoring stations. Note Stations H, I, and J are located further downstream and are not shown in this illustration.

Table 6.6. Detailed Water Quality Analyses of Selected Grab Samples.

		STATION A 10:14 am		STATION C 10:19 am		STATION F 10:34 am	
LABORATORY VALUES		mg/l	meq/l	mg/l	meq/l	mg/l	meq/l
Sodium	Na^{+}	2.78	0.12	3.06	0.13	2.94	0.13
Potassium	K^{+}	1.00	0.03	2.40	0.06	1.60	0.04
Calcium	Ca^{2+}	9.93	0.50	23.60	1.18	16.40	0.82
Magnesium	Mg^{2+}	1.77	0.15	1.80	0.15	1.77	0.15
Carbonate	CO_3^{2-}	0.00	0.00	44.00	1.47	14.00	0.47
Bicarbonate	HCO_3^{-}	32.00	0.52	23.00	0.38	34.00	0.56
Chloride	Cl^{-}	2.00	0.06	3.00	0.08	2.00	0.06
Sulfate	SO_4^{2-}	3.30	0.07	7.80	0.16	5.40	0.11
TDS (lab ROE)		< 25		< 25		< 25	
FIELD MEASUREMENTS							
Conductivity, µmhos/cm		83		142		101	
pH, Standard Units		7.1		10.0		9.4	
Turbidity, NTU		2.6		8.4		7.1	

Continuous water quality data, collected by the Troll 9000 Profilers, was calibrated to background data collected at Station A prior to grout placement. Results from the water quality monitoring program are presented below.

pH: Background pH was 7.0 at all stations located in the flume itself. Downstream of the flume, Station J (located in the natural channel 45 m (150 ft) downstream of the flume tailgates) exhibited a background pH of 7.4.

A spike in pH was observed at the locations directly downstream of the pier during grout pumping. A maximum pH of 9.9 was recorded by the continuous monitor located 3.8 m (12 ft) directly downstream of the pier three minutes after pumping began. After grout pumping was completed, pH values dropped off quickly and typically returned to baseline conditions within 30 minutes. The one exception was the probe at Station C, which was directly in the wake of the pier and at the downstream edge of the grouted area. At this location, the pH returned to background levels after about 4 hours. Considering its location, this probe was in position to record the cumulative effect of the entire grouted area for the duration required for it to cure. At Station F, located 3.8 m (12 ft) directly downstream of Station C, a much less pronounced pH profile and more rapid decay of concentration was observed. Results of monitoring by the Troll 9000 Profilers are presented in **Table 6.7**, while **Figure 6.24** shows the pH measurements at all stations. **Figure 6.25** shows the maximum pH values at any time during the test as a function of distance from the pier.

Table 6.7. Summary of pH Measurements.

	Initial Condition	End Condition	Maximum Value	Average During Grout Placement
Station A	6.9	7.1	7.1	7.0
Station B	6.9	7.1	9.4	8.4
Station C	6.9	7.3	9.9	9.7
Station D	6.9	7.0	8.6	7.8
Station E	6.9	7.1	9.2	7.9
Station F	6.9	7.1	9.5	9.0
Station G	6.9	6.9	8.5	7.8
Station H	7.0	7.0	8.3	7.1
Station I	7.0	7.2	8.6	7.3
Station J	7.4	7.5	8.4	7.7

Note: Data at Stations A-G from continuous monitors
Data at Stations H-J from grab samples

Turbidity. Background turbidity was about 3 to 4 NTUs. Turbidity peaked at 53.9 NTUs immediately after grout application began. This peak was maintained for less than 30 seconds, after which turbidity measurements ranged from about 30-35 NTUs for approximately 5 minutes. Turbidity returned to pregrouting levels almost immediately after grout application was completed. Results of monitoring by the Troll 9000 Profilers are presented in **Table 6.8**, while **Figure 6.26** is a plot of turbidity measurements. Note in Figure 6.26 an increase in turbidity can be seen prior to grout application, corresponding to personnel walking around the test section in preparation for grout application.

Temperature. Temperature remained nearly constant, ranging from 6.9 to 7.1 degrees C (44.5 to 44.7 degrees F) throughout the testing period, indicating the grout application process did not adversely affect water temperature. Results of monitoring by the Troll 9000 Profilers are presented in **Table 6.9**, while **Figure 6.27** shows a plot of temperature measurements.

Conductivity. Background conductivity was 45 to 50 μmhos/cm prior to the test. Contrary to the findings of the VDOT study, conductivity values did appear to follow the pattern of grout installation. A notable increase in conductivity was observed at the two monitoring stations immediately downstream of the pier beginning at 10:17, three minutes after grouting application commenced. Results of monitoring by the Troll 9000 Profilers are presented in **Table 6.10**, while **Figure 6.28** is a plot of conductivity measurements.

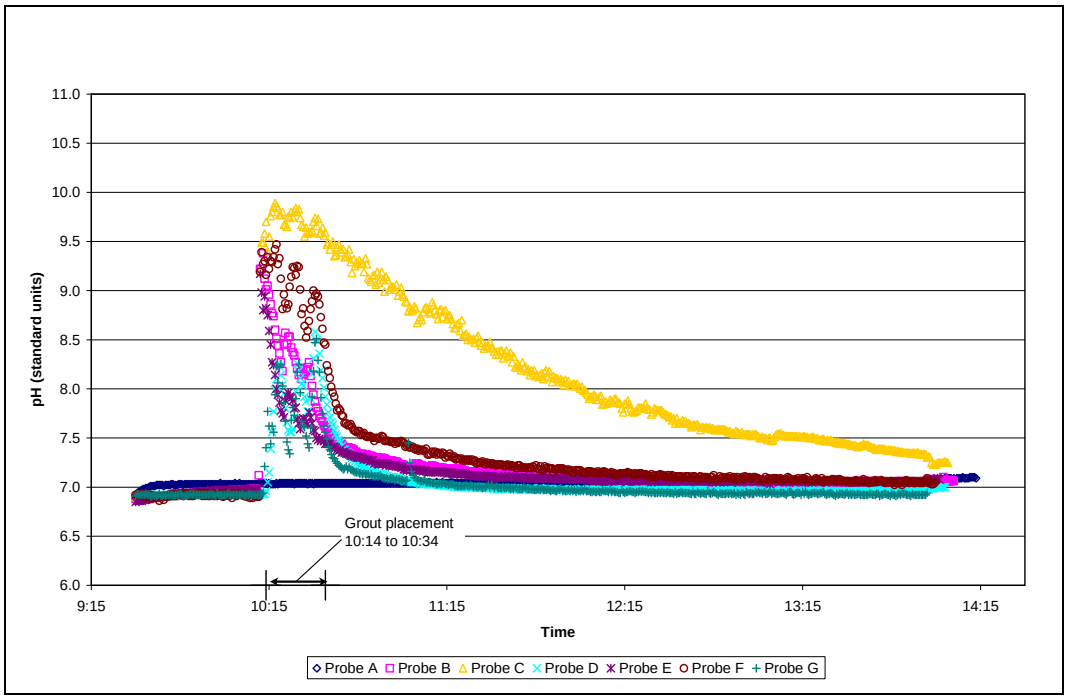

Figure 6.24. pH vs. time.

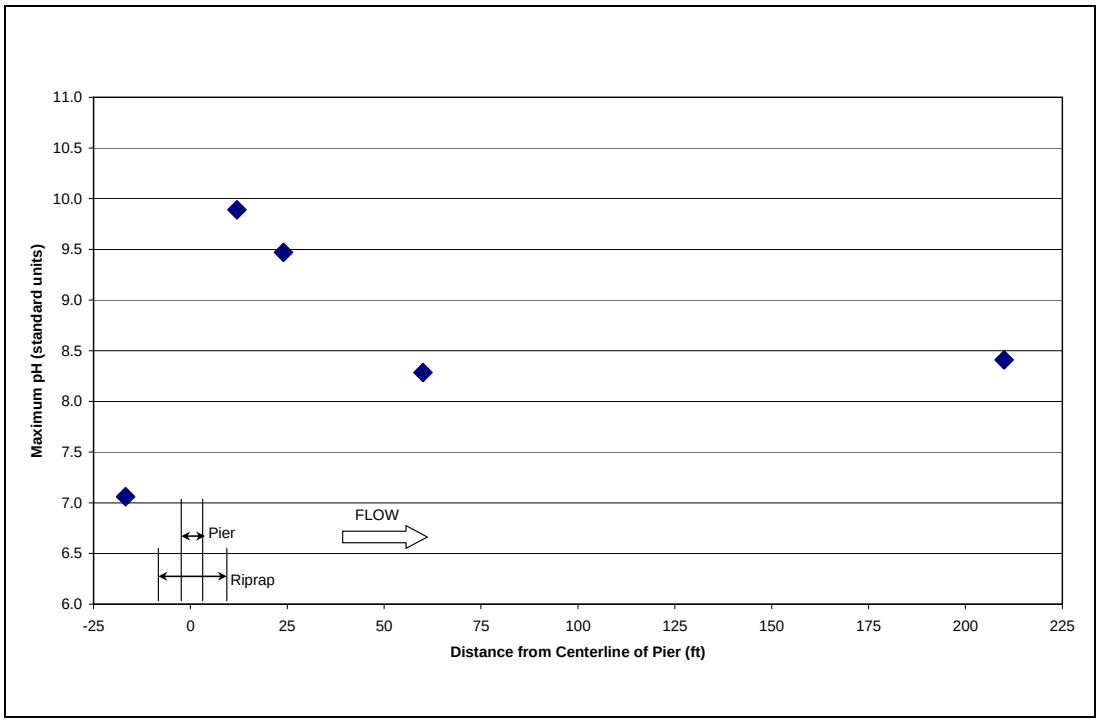

Figure 6.25. Maximum observed pH vs. distance from pier.

Table 6.8. Summary of Turbidity Measurements (NTUs).				
	Initial Condition	End Condition	Maximum value	Average during grout placement
Station A	3.6	3.3	8.3	3.7
Station B	3.6	3.6	27.9	7.1
Station C	4.0	3.7	51.3	22.7
Station D	3.8	3.4	20.6	7.1
Station E	3.1	2.9	19.1	6.1
Station F	7.1	4.0	53.9	19.5
Station G	3.7	3.7	9.1	4.9
Station H	3.2	2.6	3.2	3.3
Station I	2.5	2.6	3.0	2.7
Station J	3.3	3.4	4.6	3.6
Note: Data at Stations A-G from continuous monitors; Data at Stations H-J from grab samples				

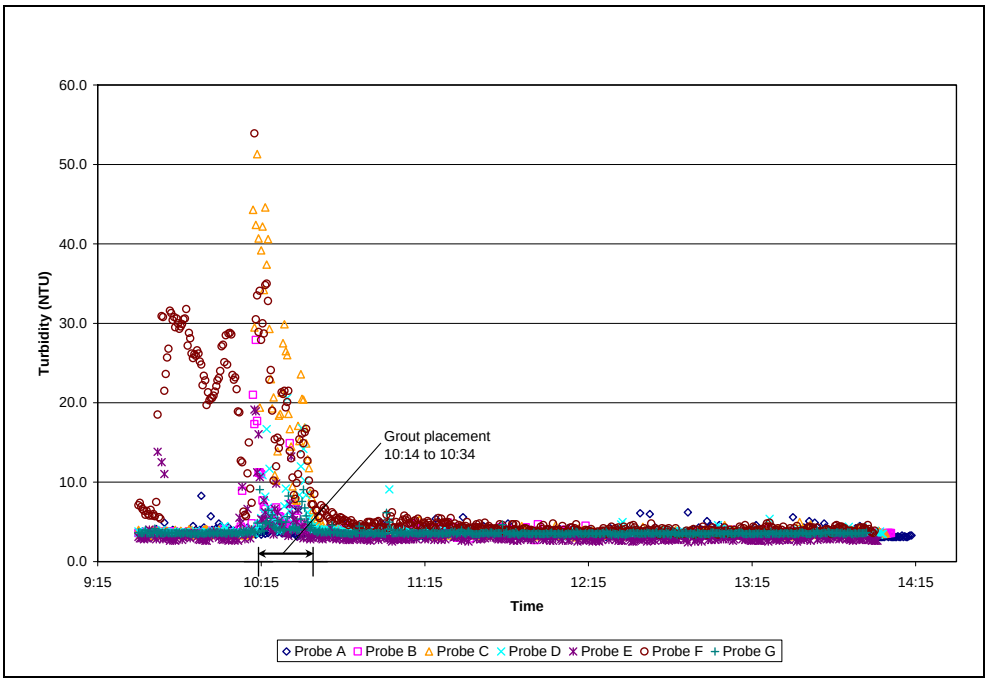

Figure 6.26. Turbidity vs. time.

Table 6.9. Summary of Temperature Measurements (°F).				
	Initial Condition	End Condition	Maximum value	Average during grout placement
Station A	44.5	44.5	44.7	44.6
Station B	44.5	44.5	44.7	44.5
Station C	44.5	44.5	44.7	44.6
Station D	44.5	44.5	44.7	44.5
Station E	44.5	44.5	44.7	44.5
Station F	44.5	44.5	44.7	44.6
Station G	44.5	44.5	44.7	44.5
Note: Data at Stations A-G from continuous monitors; No temperature data available at Stations H-J				

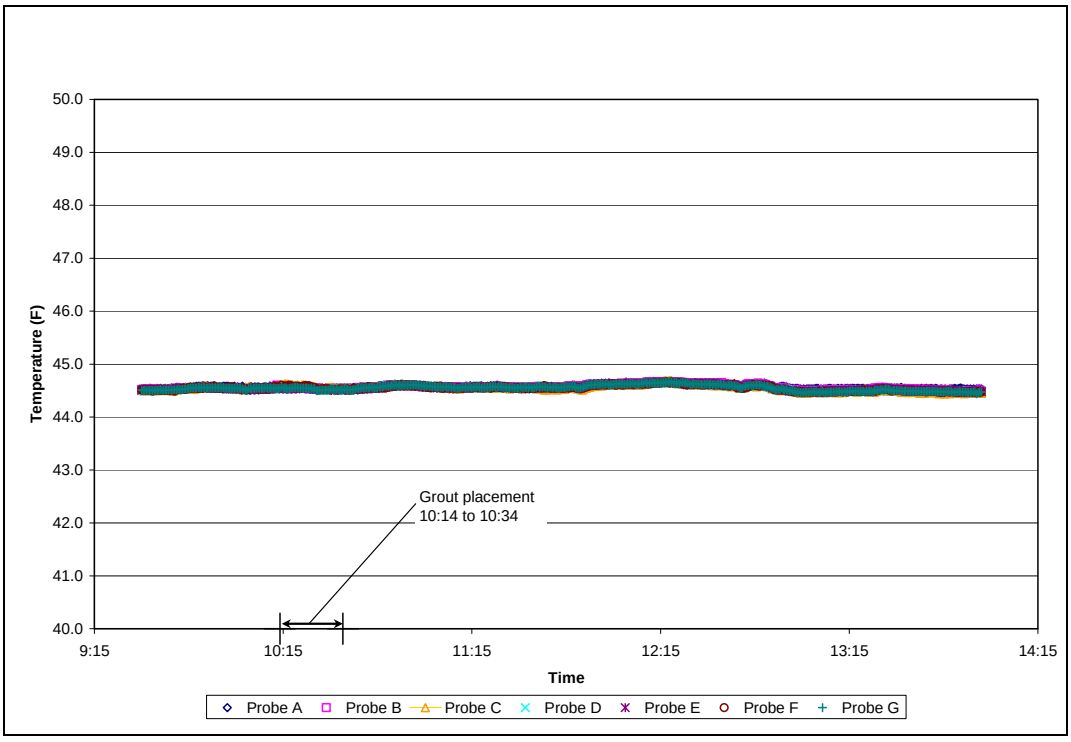

Figure 6.27. Temperature vs. time.

Table 6.10. Summary of Conductivity Measurements (μmhos/cm).				
	Initial Condition	End Condition	Maximum	Average during placement
Station A	48	48	48	48
Station B	48	48	62	51
Station C	48	49	74	61
Station D	48	49	57	50
Station E	48	48	56	50
Station F	48	49	76	62
Station G	48	48	58	50
Station H	45	44	46	44
Station I	47	44	49	47
Station J	51	43	53	49
Note: Data at Stations A-G from continuous monitors; Data at Stations H-J from grab samples				

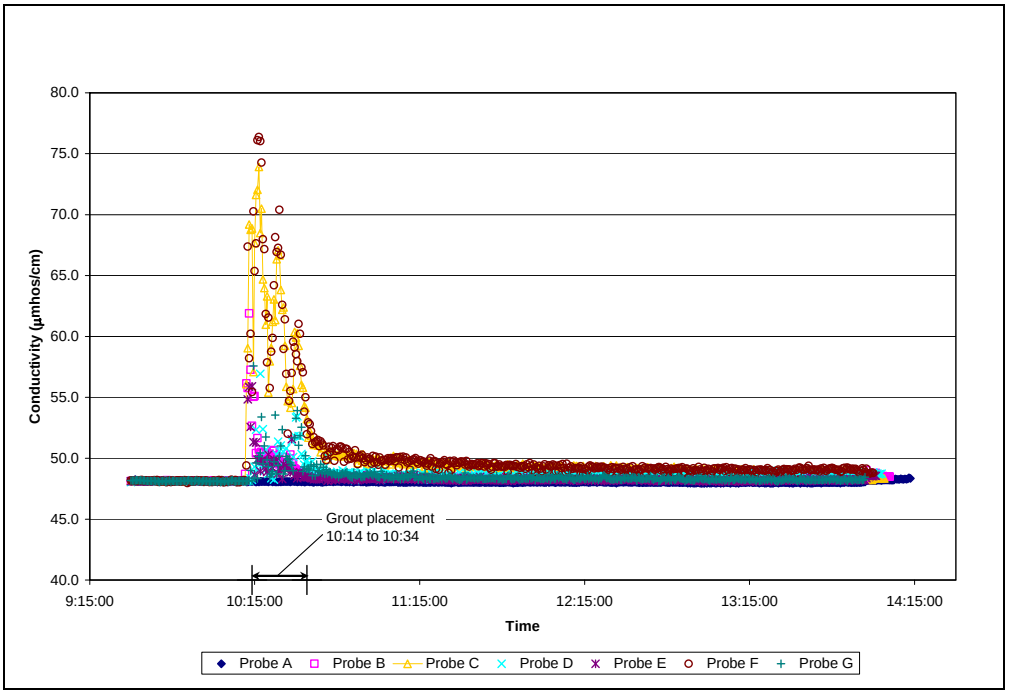

Figure 6.28. Conductivity vs. time.

After pH values returned to pre-grouting levels, as indicated by the grab sample monitoring, the tailwater control gates were shut and water was backed up in the flume. The installation remained submerged for 96 hours in order to allow the grout to cure. After 96 hours the tail gates were opened, the flume was drained and the installation was allowed to dry.

6.2.6 High Velocity Test

Loose riprap around the surface perimeter of the installation that was not firmly secured during the grouting process was removed and replaced with sand. In order to prevent degradation of the sand bed during high velocity testing, the upper 10 cm (4 in) was stabilized by tilling 4% Portland cement by dry weight (of the sand) into the sand bed. The material was compressed with a vibrating plate compactor after addition of the Portland cement.

The high velocity test ran for two hours and was terminated when the soil cement bed began to visibly fail. Approach velocities at 60% of depth during the high velocity test ranged from 1.3 to 1.7 m/s (4.2 to 5.6 ft/s). After draining the flume, several scour holes were observed in the soil cement bed, and a significant scour hole was observed downstream of the riprap installation. The soil cement in these areas had been destabilized and the underlying sand scoured to a depth of about 0.8 m (2.5 ft). The partially grouted riprap installation and underlying geotextile containers remained intact. **Figure 6.29** shows the test section after the high velocity test.

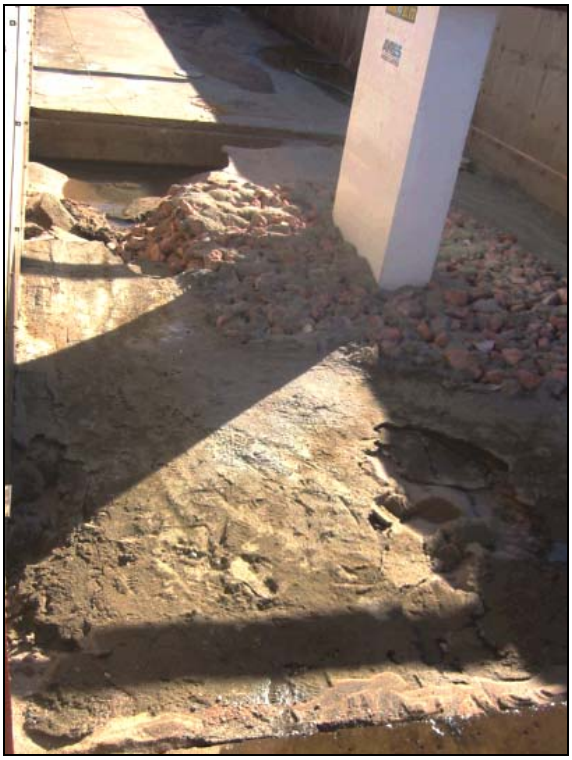

Figure 6.29. After Test C1-high velocity test looking downstream, note damage to the soil cement and scour at the downstream left corner. Partially grouted riprap remained intact.

6.2.7 Test C20

Test C20 was a comparison test between loose riprap and partially grouted riprap. To facilitate a comparison of the performance of loose riprap to partially grouted riprap, all riprap and grout were removed from the left side of the pier and replaced with loose riprap of the same gradation and d_{50} after completion of Test C1 as described in Section 6.2.5. Because the soil cement in Test C1 proved to be inadequate to stabilize the area around the partially grouted riprap, it was completely removed from the bed, exposing the underlying sand bed 10 cm (4 in) lower than the surrounding flume floor and top surface of the riprap. A geotextile fabric, with the hydraulic and physical characteristics presented in Table 6.4, was installed over the exposed sand portion of the test section. Four-inch thick articulating concrete blocks (ACBs) were installed on the geotextile fabric adjacent to the riprap. The ACBs were intended to prevent degradation of the bed in the test section as well as facilitate a smooth transition from the flume floor to the test section.

Temporary walls were installed to reduce cross sectional area of the flow and increase velocity in the test section. Walls were installed 0.46 m (1.5 feet) from the existing flume walls, transitioning the section from 6 m (20 feet) to 4.6 m (15 feet). **Figure 6.30** shows the test section after the modifications were completed.

Figure 6.30. Loose riprap, ACB, and contraction wall installation looking upstream (note loose riprap on the near side of the pier and partially grouted riprap on the far side).

The high velocity comparison test was completed in two steps. In the first step, the maximum flow rate during Test C20 was 5.6 m^3/s (198 cfs). Discharge was steadily increased until approach velocity reached a maximum of 1.8 m/s (6.0 ft/s) at full flow capacity of the flume. The test ran for 1 hour, with no movement of the loose rock. After this trial run, the flume was shut down and modifications to the inlet structure were made to achieve higher velocities at the pier. **Figure 6.31** shows the installation after the trial run.

Figure 6.31. After completion of the first step of Test C2, looking downstream.

The second step of the test ran for 2 hours, during which time the discharge was again steadily increased to the full flow capacity. At maximum discharge, the approach velocity upstream of the pier reached a maximum of 1.95 m/s (6.4 ft/s). At the higher flows, the loose riprap began to displace. **Figure 6.32** shows the loose riprap side of the installation after completion of the second half of the high velocity comparison test. Note the scour hole on the near side of the pier and the displaced riprap behind and downstream of the pier compared to the previous figure. The partially grouted side of the riprap installation can be seen in this figure, and remained essentially undisturbed. **Figure 6.33** shows the partially grouted side of the installation after the end of this test.

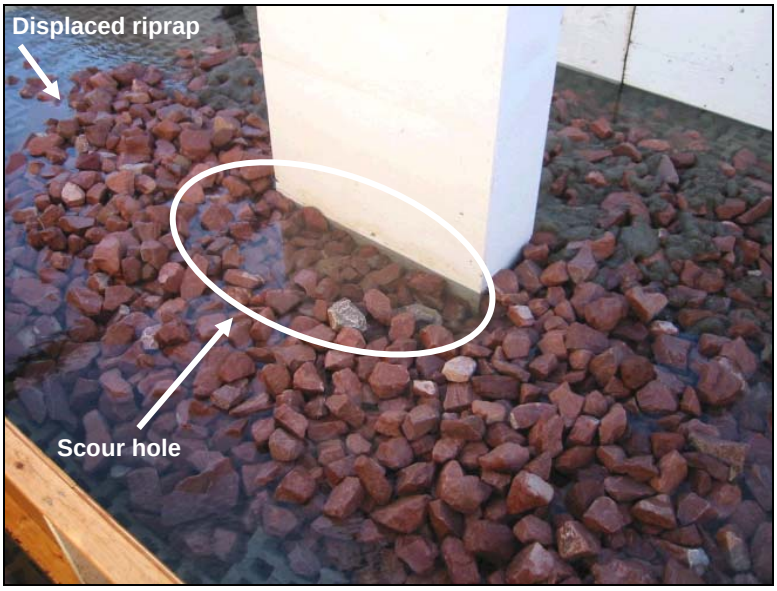

Figure 6.32. Loose riprap after completion of Test C20, flow is from right to left.

Figure 6.33. Partially grouted riprap after completion of Test C20, flow from left to right.

7. GABION MATTRESSES

7.1 Materials

Gabion mattresses consisted of a wire mesh box filled with small stones. Each gabion mattress was hand constructed with nominal dimensions of 15 cm x 10 cm x 1.25 cm (6 in x 4 in x 0.5 in). The wire mesh had a 3.2 mm (1/8 in) opening. A plastic mesh, typically used for crafts, was inserted as dividers in the gabion mattress to create three compartments.

Typically, during gabion mattress installation in the field, the units are interconnected to form a continuous monolithic structure. The testing procedure conducted for this gabion mattress testing included connected and unconnected configurations.

Gabion stone requirements were developed using the filter criteria specified in HEC-11 Brown and Clyde 1989). The initial step establishes the compatibility of the filter (gabion stone) with the sand bed material in terms of both particle retention and permeability by defining upper and lower limits of d_{15} for the filter. This determines the largest size allowable to maintain particle retention and smallest size allowable to ensure the filter has greater permeability than the sand. The requirements for filter to soil relationship are:

$$\frac{d_{15}\text{filter}}{d_{85}\text{soil}} < 5 \qquad (7.1)$$

and

$$5 < \frac{d_{15}\text{filter}}{d_{15}\text{soil}} < 40 \qquad (7.2)$$

The d_{85} of the filter must be large enough so that the filter does not pass through the riprap. The requirements for filter to riprap relationship are:

$$\frac{d_{15}\text{riprap}}{d_{85}\text{filter}} < 5 \qquad (7.3)$$

The material selected for use was a d_{50} = 5.8 mm rock from a local source. A grain size distribution graph for the gabion stone is presented in **Figure 7.1**. **Figure 7.2** shows a typical gabion mattress used in the testing program.

7.2 Testing

Four tests were performed to identify the design and performance of gabion mattresses without interconnectors as a pier scour countermeasure. The test program for gabion mattresses was similar to that designed for the ACB systems. Test C2 served as the baseline by providing performance criteria of individual units (i.e., critical shear stress) necessary for design. Test C3 was performed to provide data on system performance as a function of areal coverage. Test C4 examined termination detail and filter extent. Test C5 incorporated the best performing layouts from the previous tests with further investigation of edge turndown.

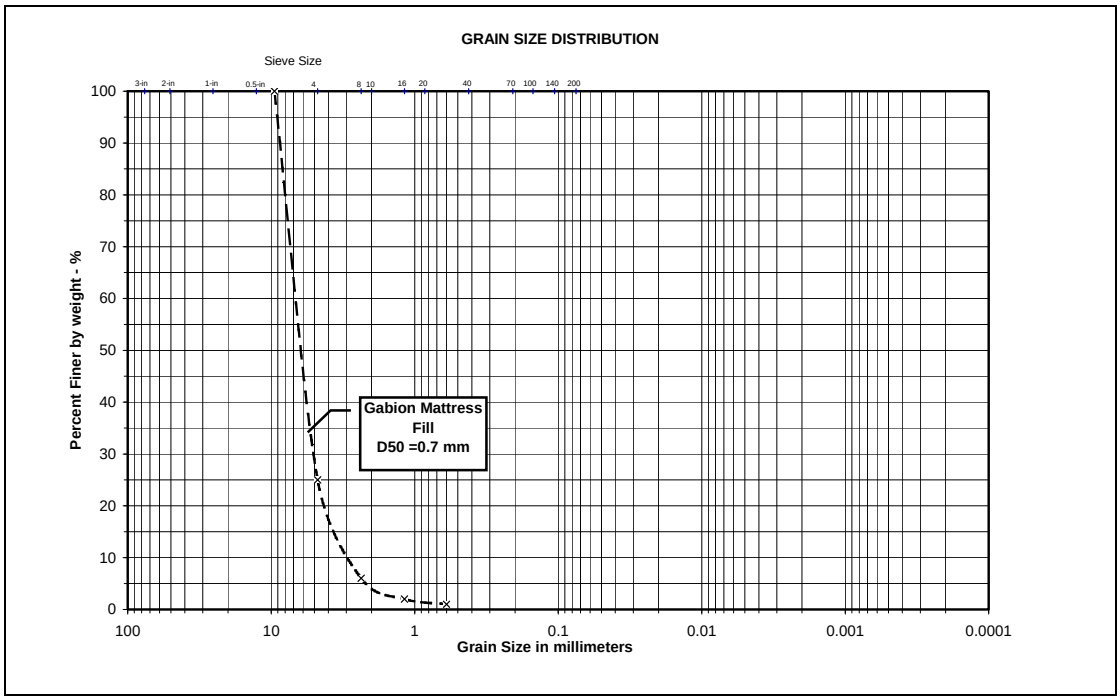

Figure 7.1. Grain size distribution for gabion mattress stone.

Figure 7.2. Typical gabion mattress with wire mesh and three compartments filled with stone.

Test C19 took the best performing combination from the previous tests with the gabion mattresses connected at the selvedges to form an interconnected unit. A summary of the gabion mattress tests is presented in **Table 7.1**.

Table 7.1. Gabion Mattress Tests.

Test Number	Pier A		Pier B		Pier C		Duration	V/Vc	Connected	Bedforms
	Description	Filter	Description	Filter	Description	Filter	(hour)			
C2	Gabion Shear Stress Testing in the 2-Foot Flume						Varied	Varied	No	None
C3a	Gabion Mattress	NW2	Gabion Mattress	NW2	Gabion Mattress	NW2	2	1	No	Clear-water; plane
C3b	Gabion Mattress	NW2	Gabion Mattress	NW2	Gabion Mattress	NW2	2	2	No	Mobile; dunes
C4a	Gabion Mattress	NW2	Gabion Mattress	NW2	Gabion Mattress	NW2	2	1	No	Clear-water; plane
C4b	Gabion Mattress	NW2	Gabion Mattress	NW2	Gabion Mattress	NW2	2	2	No	Mobile; dunes
C5a	Gabion Mattress	NW2	Gabion Mattress	NW2	Gabion Mattress	NW2	2	1	No	Clear-water; plane
C5b	Gabion Mattress	NW2	Gabion Mattress	NW2	Gabion Mattress	NW2	2	2	No	Mobile; dunes
C19a	Gabion Mattress	NW2	Gabion Mattress	NW2	Gabion Mattress	NW2	2	1	Yes	Clear-water; plane
C19b	Gabion Mattress	NW2	Gabion Mattress	NW2	Gabion Mattress	NW2	2	2	Yes	Mobile; dunes

7.3 Shear Stress Testing

Test C2 established performance criteria necessary for design per HEC-23 methods (see Section 1.2). A flume 2 ft wide by 60 ft long was used in the determination of the applied shear stress for the gabion mattresses (see Section 2.2). Bed slope during the testing program ranged from 1.1 to 8.2 percent. A series of flows were conveyed through the flume intended to result in the gabion mattresses losing intimate contact with the flume floor.

The gabions did not fail under the prescribed hydraulic conditions. Therefore, the corresponding value of applied shear stress and maximum cross-section averaged velocity were determined using the peak hydraulic conditions that occurred during testing. The equations for continuity ($Q = VA$) and applied shear stress, $\tau = \gamma y S_f$ were used to determine the maximum hydraulic conditions, where:

- Q = Flow discharge through the contracted section (m^3/s, ft^3/s)
- V = Average cross section velocity (m/s, ft/s)
- A = Cross section area (m, ft)
- τ = Shear stress (N/m^2, lb/ft^2)
- γ = Unit weight of water (N/m^3, lb/ft^3)
- y = Existing depth in the cross section (m, ft)
- S_f = Friction slope

The maximum velocity experienced by the gabion mattresses was 2.5 m/s (8.1 ft/s) and the maximum shear stress was 110 N/m^2 (2.3 lb/ft^2).

7.4 Test C3

The objective of Test C3 was to document and quantify the unconnected gabion mattresses system's performance as a function of areal coverage. All spatial arrangements for Test C3 included a geotextile filter extending from the pier face to the perimeter of the gabion mattresses. On all piers, the gabion mattresses were installed so the tops of the gabions were level with the ambient bed surface.

On Pier A, the upstream and downstream extent of the gabion mattress was 46 cm (18 in) and the lateral extent was 40 cm (16 in). **Figure 7.3** shows Pier A after completion of Test C3b. On Pier B, the upstream and downstream extent of the gabion mattresses was 31 cm (12 in) and the lateral extent was 31 cm (12 in). On Pier C, the upstream and downstream extent of the gabion mattress was 31 cm (12 in) and the lateral extent was 20 cm (8 in).

Figure 7.3. Pier A after Test C3b (flow is from left to right).

7.5 Test C4

Test C4 examined termination details and filter extent for unconnected gabion mattresses. On Pier A, the best performing spatial arrangement from Test C3 was installed minus the geotextile filter. The upstream and downstream extent on Pier A of the gabion mattress was 46 cm (18 in) and 40 cm (16 in) in the lateral extent.

Pier B incorporated a turndown detail of 4H:1V, extending from ambient bed level at the pier face to a depth of 7.6 cm (3 in) at the perimeter. Gabion mattresses extended horizontally for 30.5 cm (12 in). A geotextile filter extended the full length of the gabions. Sand was filled over the gabion mattresses to create a finished elevation flush with the initial bed level. **Figure 7.4** shows Pier B before the sand bed was leveled. **Figure 7.5** shows Pier B after Test C4b was completed.

Figure 7.4. Pier B, Test C4 before leveling of the bed.

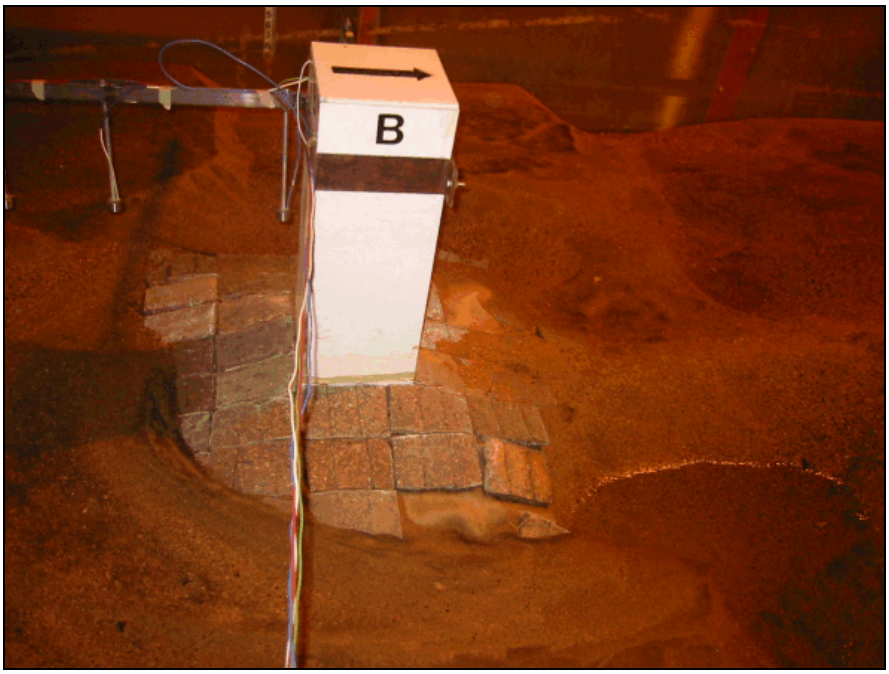

Figure 7.5. Pier B, after completion of Test C4b (flow is from left to right in photo).

Pier C incorporated a turndown detail of 2H:1V, extending from ambient bed level at the pier face to a depth of 15 cm (6 in) at the perimeter. Gabion mattresses extended horizontally for 30.5 cm (12 in). A geotextile filter extended the full length of the gabions. Sand was filled over the gabion mattresses to create a finished elevation flush with the initial bed level.

7.6 Test C5

Test C5 incorporated the best performing layouts from the previous tests with investigation of turndown detail for unconnected gabion mattresses. Pier A included a horizontal gabion mattress extension of 15 cm (6 in) with a turndown detail around the entire perimeter ending in a depth of 8 cm (3 in). A geotextile filter extended the full length of the gabions. Sand was filled over the turned down blocks to create a finished elevation flush with the initial bed level.

Pier B incorporated a turndown detail of 4H:1V, extending from ambient bed level at the pier face to a depth of 7.6 cm (3 in) at the perimeter. The Pier B installation was identical to Pier B, Test C4, except the geotextile extended only two-thirds the length of the gabions. Sand was filled over the gabion mattresses to create a finished elevation flush with the initial bed level.

Pier C incorporated a turndown detail of 2H:1V, extending from ambient bed level at the pier face to a depth of 15 cm (6 in) at the perimeter. The Pier C installation was identical to Pier C, Test C4, except the geotextile extended only two-thirds the length of the gabions. Sand was filled over the gabion mattresses to create a finished elevation flush with the initial bed level. **Figure 7.6** is a schematic of Pier C, Test C5. **Figure 7.7** shows Pier C before the sand was filled in and **Figure 7.8** shows Pier C after completion of Test C5b.

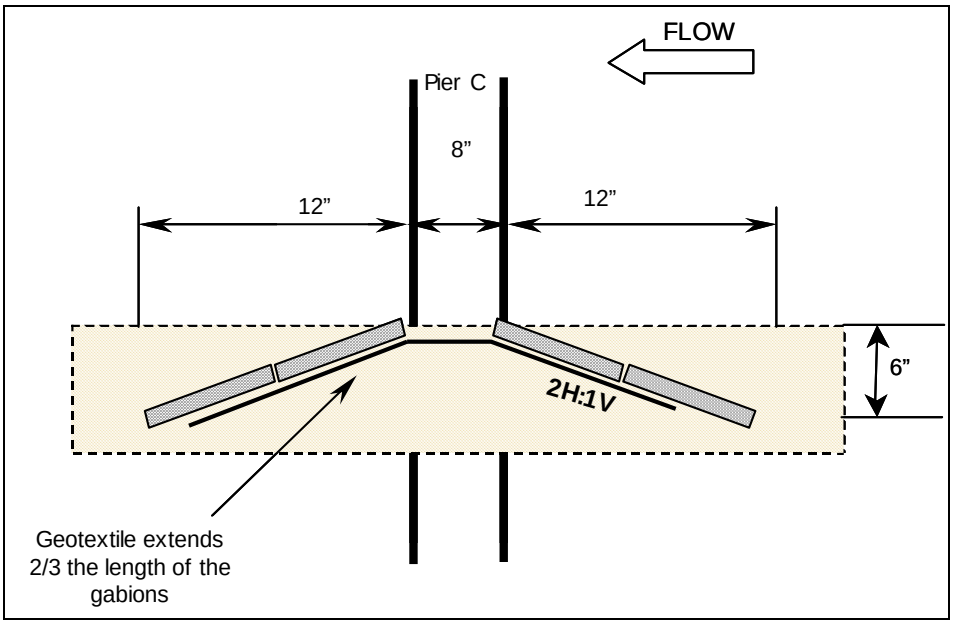

Figure 7.6. Countermeasure design for Pier A, Test C5.

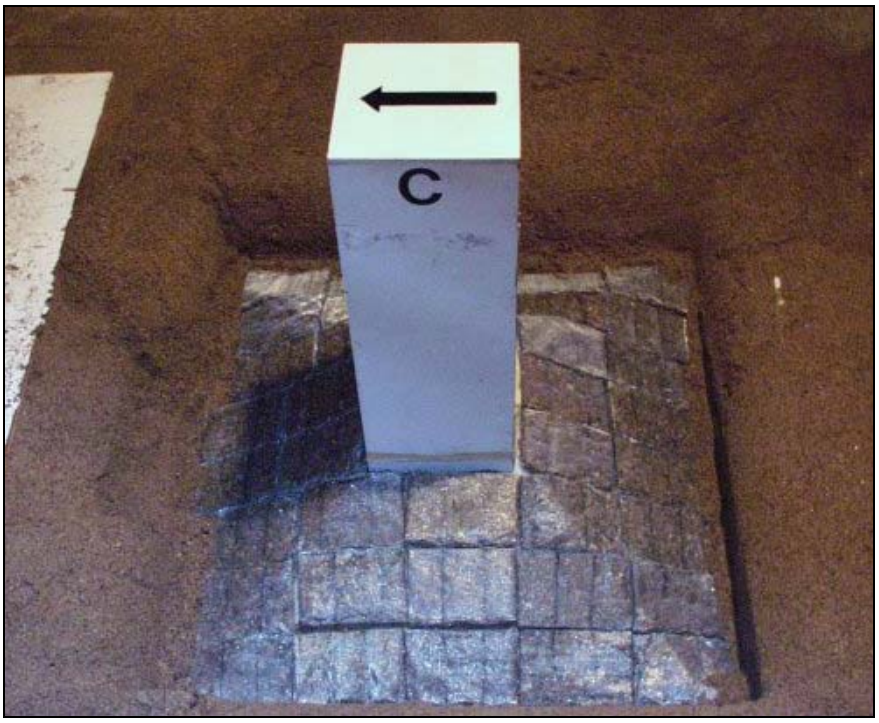

Figure 7.7. Pier C before leveling of the bed, Test C5.

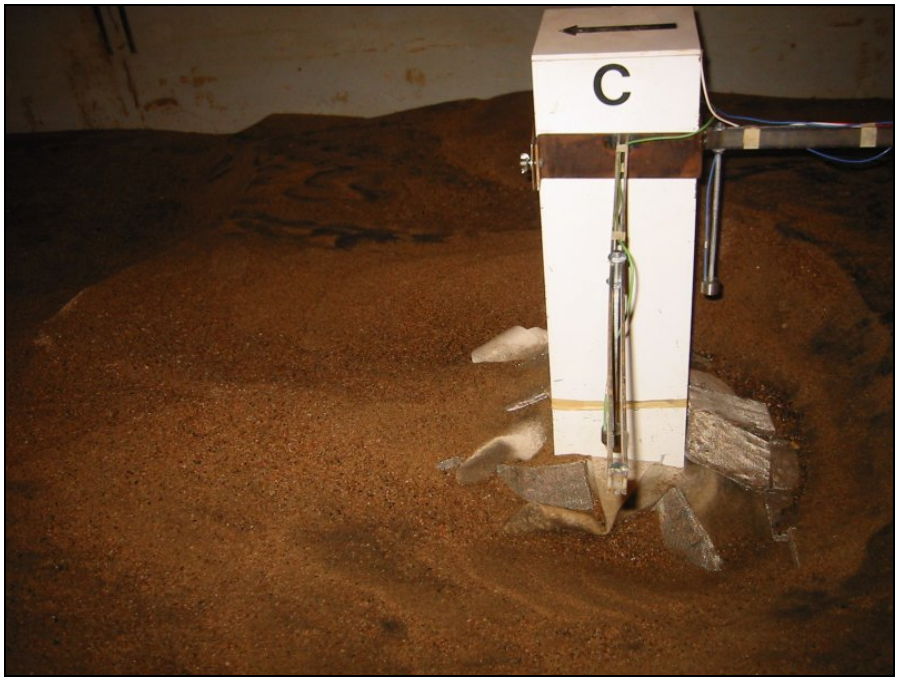

Figure 7.8. Pier C after Test C5b (flow is from right to left).

7.7 Test C19

Test C19 was performed to investigate performance of a **connected** gabion mattress system. Installations on each pier were identical to Test C5. The gabions were sewn together on the top abutting selvedges at 5 cm (2 in) intervals. Pier A included a horizontal gabion mattress extension of 15 cm (6 in) with a turndown detail around the entire perimeter ending in a depth of 8 cm (3 in). A geotextile filter extended the full length of the gabions. Sand was filled over the turned down blocks to create a finished elevation flush with the initial bed level. **Figure 7.9** shows Pier A after Test C19b. A close up of the gabion mattresses surrounding Pier A after Test C19b is shown in **Figure 7.10**; note in Figure 7.10 the shifting of the stone fill in the compartments and the strain of the wire mesh and connectors.

Pier B incorporated a turndown detail of 4H:1V, extending from ambient bed level at the pier face to a depth of 7.6 cm (3 in) at the perimeter. The geotextile extended two-thirds the length of the gabions. Sand was filled over the gabion mattresses to create a finished elevation flush with the initial bed level.

Pier C incorporated a turndown detail of 2H:1V, extending from ambient bed level at the pier face to a depth of 15 cm (6 in) at the perimeter. The geotextile extended two-thirds the length of the gabions. Sand was filled over the gabion mattresses to create a finished elevation flush with the initial bed level. **Figure 7.11** is a photograph of Pier C after completion of Test C19b.

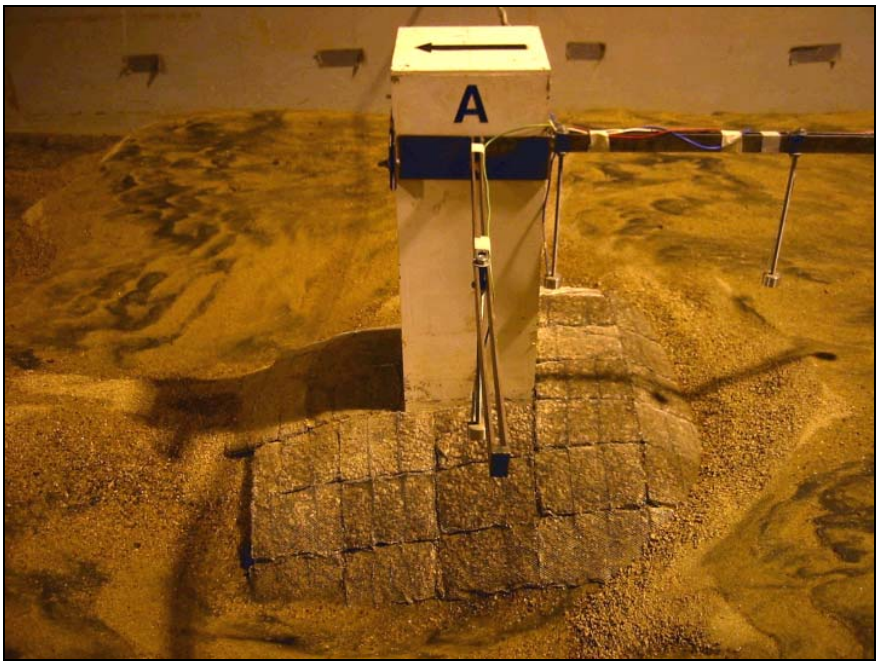

Figure 7.9. Pier A after Test C19b (flow is from right to left).

Figure 7.10. Gabion mattresses on Pier A after Text C19b.

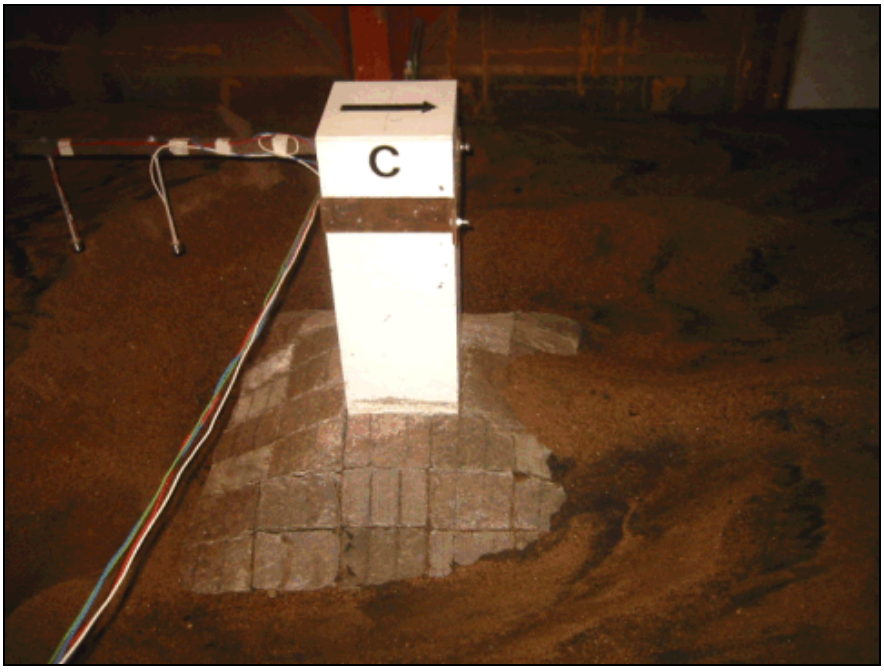

Figure 7.11. Pier C after Test C19b (flow is from left to right).

(page intentionally left blank)

8. GROUT-FILLED MATTRESSES

8.1 Materials

The performance of both rigid and flexible grout-filled mattresses was simulated by this testing program. Modeling of a rigid fabric formed concrete mattress was accomplished by soaking a synthetic batting, typically used in quilting, in a cement rich concrete grout. Mats were cut to fit the installation design; typically, a mattress was 20 by 30 cm (8 by 12 inches). The grout-filled mats were placed in the wet on top of a geotextile filter around each pier. Relief of pore water pressure from beneath the mat was allowed through weep holes cut into the center of each mat and at corners where two mats joined. **Figure 8.1** shows the grout mat batting before being filled with grout, note the weep hole cut in the center. **Figure 8.2** shows a rigid grout-filled mat being placed, with the grout still wet, around a pier.

Figure 8.1. Grout-filled mat before being filled with grout.

Figure 8.2. Placement of grout-filled mat.

The flexible grout-filled mat was modeled using sheets of 1- by 1-inch mosaic tile from Daltile®. The sheets were cut to fit each installation; abutting sheets were connected using several layers of cheesecloth, which also acted as a filter. **Figure 8.3** shows an articulating grout mat being installed at Pier A before Test C18.

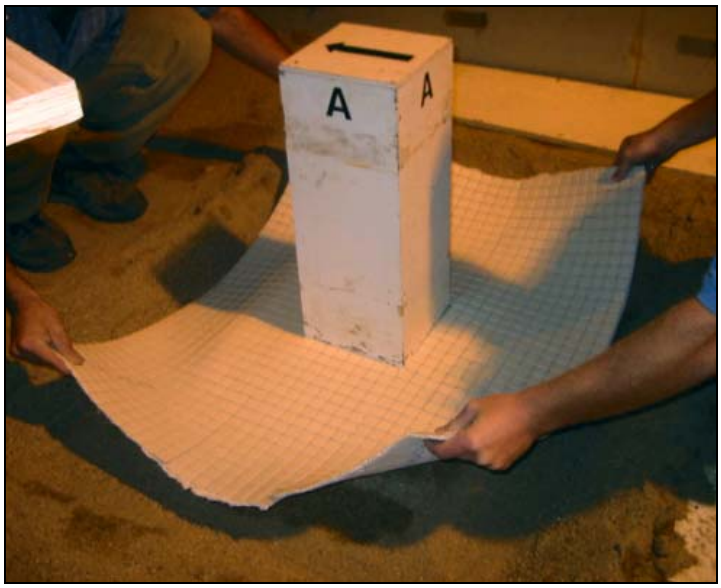

Figure 8.3. Installation of flexible grout mat.

8.2 Testing

Two tests were performed to quantify the design and performance of rigid grout-filled mats as a pier scour countermeasure, one test was performed to examine the performance of a flexible grout-filled mat. A summary of the tests is presented in **Table 8.1**. Test C7 documented system performance as a function of areal coverage. Test C8 incorporated variations in termination detail from the best performing layouts found in Test C7. Test C18 incorporated the best performing configuration from the previous tests with a flexible grout-filled mat.

Table 8.1. Grout-filled Mattress Tests.

Test Number	Pier A		Pier B		Pier C		Duration	V/Vc	Sediment Feed	Bedforms
	Description	Filter	Description	Filter	Description	Filter	(hour)			
C7a	Grout-filled Mats	NW2	Grout-filled Mats	NW2	Grout-filled Mats	NW2	2	1	No	Clear-water; plane
C7b	Grout-filled Mats	NW2	Grout-filled Mats	NW2	Grout-filled Mats	NW2	2	2	No	Mobile; dunes
C8a	Grout-filled Mats	NW2	Grout-filled Mats	NW2	Grout-filled Mats	NW2	2	1	No	Clear-water; plane
C8b	Grout-filled Mats	NW2	Grout-filled Mats	NW2	Grout-filled Mats	NW2	2	2	No	Mobile; dunes
C18a	Flexible Grout Mats	Cheesecloth	Flexible Grout Mats	Cheesecloth	Flexible Grout Mats	Cheesecloth	2	1	No	Clear-water; plane
C18b	Flexible Grout Mats	Cheesecloth	Flexible Grout Mats	Cheesecloth	Flexible Grout Mats	Cheesecloth	2	2	No	Mobile; dunes

8.2.1 Test C7

Test C7 was performed to investigate performance of a rigid grout-filled mattress system as a function of areal coverage. Installations around each pier incorporated a geotextile extending from the pier face to the periphery of the grout-filled mats. Grout-filled mats were installed so that the top of the mat was flush with the surrounding sand bed.

On Pier A, the upstream and downstream extent of the grout mats was 46 cm (18 in) and the lateral extent was 40 cm (16 in). **Figure 8.4** is a schematic of the grout-filled mattress installation on Pier A for Tests C7. **Figure 8.5** shows Pier A after completion of Test C7b. On Pier B, the upstream and downstream extent of the grout mats was 31 cm (12 in) and the lateral extent was 20 cm (16 in). On Pier C, the upstream and downstream extent of the grout mats was 31 cm (12 in) and the lateral extent was 40 cm (8 in). **Figures 8.6 and 8.7** present photographs of Pier C after completion of Test C7b.

8.2.2 Test C8

Test C8 was performed to investigate variations in termination details from the best performing layouts found in Test C7. Installations around each pier incorporated a geotextile extending from the pier face to the periphery of the grout-filled mats. The Pier A configuration from Test C7 was modified to include a 15 cm (6 in) turndown to a depth of 5 cm (2 in) around the entire periphery. The horizontal extension was flush with the initial bed elevation and was 15 cm (6 in) on the upstream and downstream sides and 25.4 cm (10 in) on the lateral sides. **Figure 8.8** shows Pier A after completion of Test C8a and **Figure 8.9** shows Pier A after Test C8b.

The installation on Pier B was a variation on the Test C7, Pier B installation. Pier B incorporated a turndown detail of 4H:1V, extending from ambient bed level at the pier face to a depth of 7.6 cm (3 in) at the perimeter. The installation on Pier C was a variation on the Test C7, Pier B installation. Pier C incorporated a turndown detail of 2H:1V, extending from ambient bed level at the pier face to a depth of 15 cm (6 in) at the perimeter.

8.2.3 Test C18

Test C18 was performed to investigate performance of a flexible grout-filled mattress system. Installations on each pier were identical to Test C8. All pier installations incorporated a geotextile extending from the pier face to the periphery of the flexible grout-filled mats.

The Pier A configuration included a 15 cm (6 in) turndown to a depth of 5 cm (2 in) around the entire periphery. The horizontal extension was flush with the initial bed elevation and was 15 cm (6 in) on the upstream and downstream sides and 25.4 cm (10 in) on the lateral sides. Pier B incorporated a turndown detail of 4H:1V, extending from ambient bed level at the pier face to a depth of 7.6 cm (3 in) at the perimeter. Pier C incorporated a turndown detail of 2H:1V, extending from ambient bed level at the pier face to a depth of 15 cm (6 in) at the perimeter. **Figure 8.10** shows Pier C after completion of Test C18a and **Figure 8.11** shows Pier C after Test C18b.

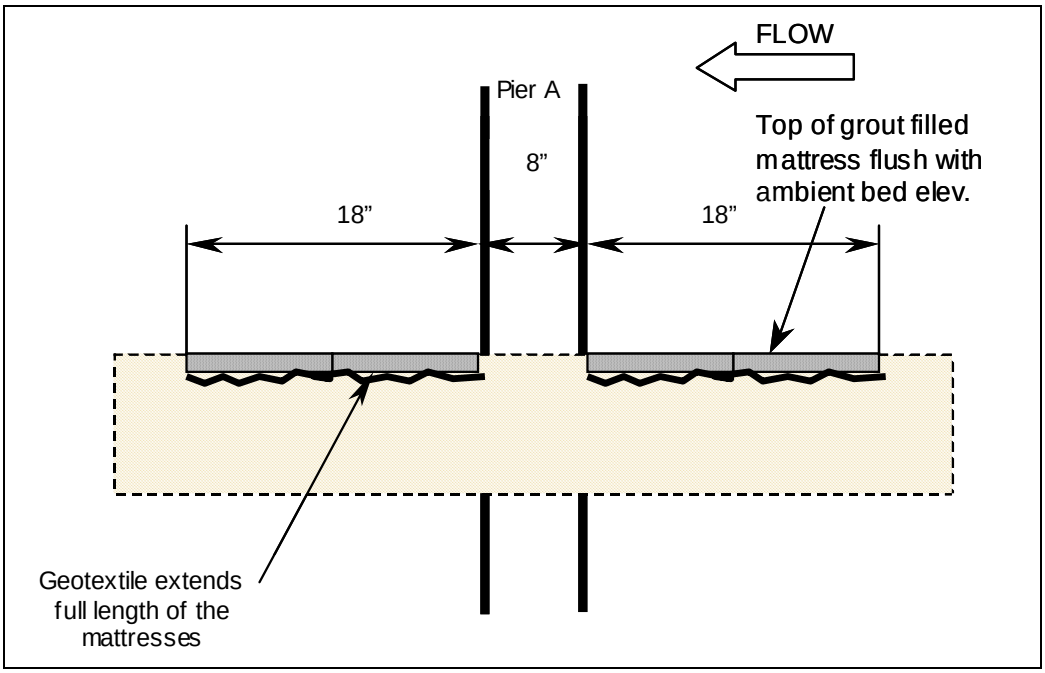

Figure 8.4. Countermeasure design for Pier A, Test C7.

Figure 8.5. Pier A after Test C7b, looking upstream.

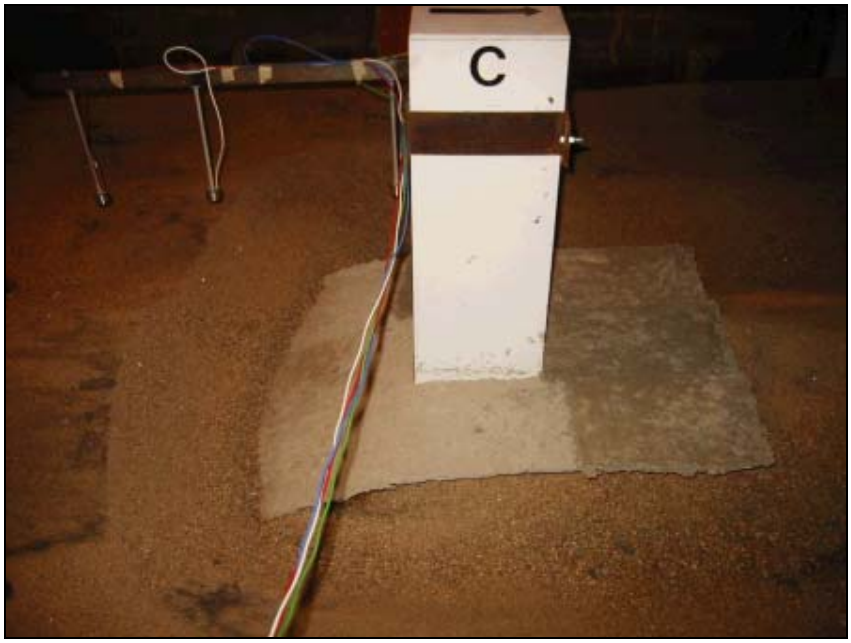

Figure 8.6. Pier C after Test C7b (flow is from left to right).

Figure 8.7. Pier C after Test C7b (flow is from right to left).

Figure 8.8. Pier A after Test C8a, looking downstream.

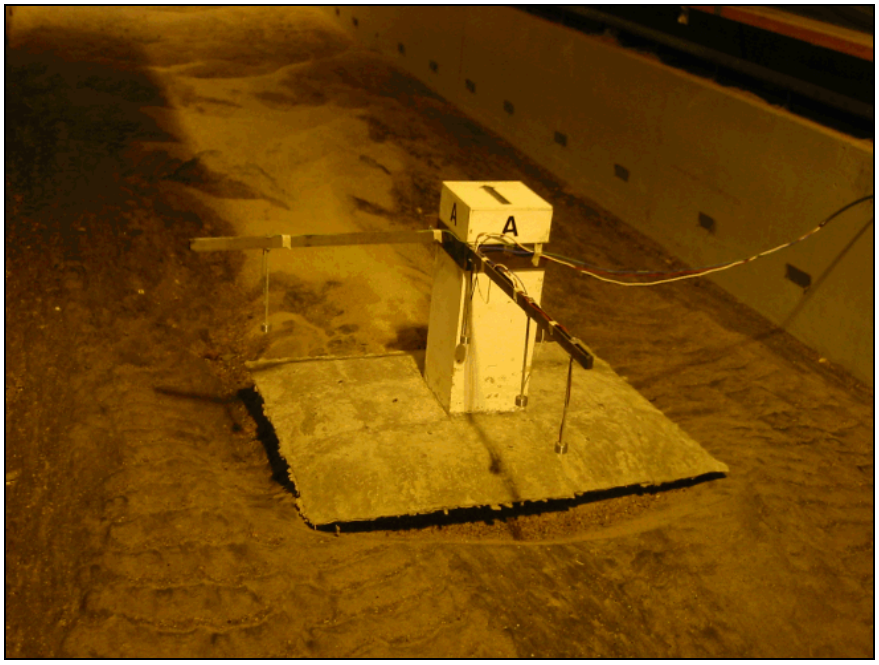

Figure 8.9. Pier A after Test C8b, looking downstream.

Figure 8.10. Pier C after Test C18a, flow is from left to right.

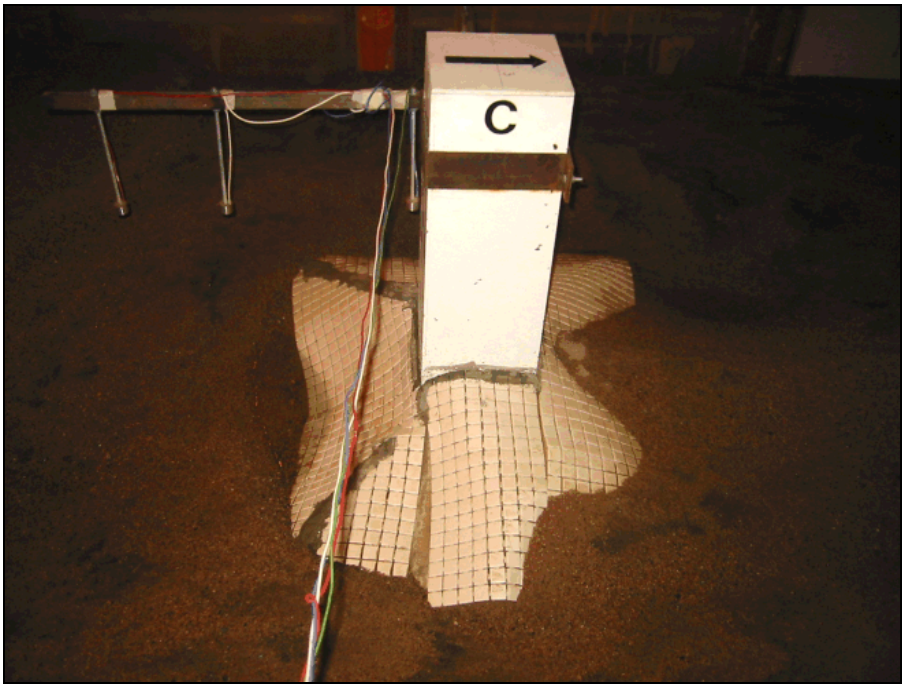

Figure 8.11. Pier C after Test C18b, flow is from left to right.

(page intentionally left blank)

9. REFERENCES

American Society of Testing and Materials (ASTM), "Annual Book of ASTM Standards," Vol. 4.08, West Conshohocken, PA (2003a).

American Society of Testing and Materials (ASTM), "Annual Book of ASTM Standards," Vol. 4.09, West Conshohocken, PA (2003b).

Brown, S.A. and Clyde, E.S. "Design of Riprap Revetment, Hydraulic Engineering Circular No. 11" (HEC-11), FHWA-IP-016, Federal Highway Administration, Washington, D.C. (1989).

Federal Waterway Engineering and Research Institute (BAW). "Code of Practice – Use of Cement Bonded and Bituminous Materials for Grouting of Armor Stones on Waterways" (MAV), BAW, Karlsruhe, Germany (1990).

Fitch, G.M. "Minimizing the Impact on Water Quality of Placing Grout Underwater to Repair Bridge Scour Damage," Final Report, VTRC 03-R16, Virginia Transportation Research Council, Charlottesville, VA (2003).

Koerner, R.M., "Designing with Geosynthetics," 4th Edition, Prentice-Hall, Inc., Englewood Cliffs, NJ, 761 p. (1998).

Lagasse, P.F., Clopper, P.E., and Zevenbergen, L.W., "Countermeasures to Protect Bridge Piers from Scour," Final Report and Design Guidelines, NCHRP Project 24-07(2), Transportation Research Board, National Research Council, Washington, D.C. (2006b).

Lagasse, P.F., Clopper, P.E., Zevenbergen, L.W., and Ruff, J.F., "Riprap Design Criteria, Recommended Specifications, and Quality Control," NCHRP Report 568, Transportation Research Board, National Research Council, Washington, D.C. (2006a).

Lagasse, P.F., Zevenbergen, L.W., Schall, J.D., and Clopper, P.E. "Bridge Scour and Stream Instability Countermeasures," Hydraulic Engineering Circular No. 23 (HEC-23, Second Edition), FHWA NHI 01-003, Federal Highway Administration, Washington, D.C. (2001).

Parker, G., Toro-Escobar, C., and Voigt, R.L. Jr. "Countermeasures to Protect Bridge Piers from Scour," Users Guide (revised 1999) and Final Report, NCHRP Project 24-7, prepared for Transportation Research Board by St. Anthony Falls Laboratory, University of Minnesota, MN, 360 pp. (1998).

Parola, A.C. and Jones, J.S., "Sizing Riprap to Protect Bridge Piers from Scour," Third Bridge Engineering Conference, Transportation Research Record No. 1290, Vol. 2, pp. 276-280 (1989).

Richardson, E.V. and Davis, S.R. "Evaluating Scour at Bridges, Hydraulic Engineering Circular No. 18" (HEC-18, Fourth Edition), FHWA NHI 01-004, Federal Highway Administration, Washington, D.C. (2001).

(page intentionally left blank)